Final Report 1998-10

research

Freeze-Thaw Durability of High-Strength Concrete

UNIVERSITY OF MINNESOTA
CENTER FOR
TRANSPORTATION
STUDIES

This research was made possible with the support and contributions from the Minnesota Prestress Association. Many of its members took a role in the fabrication and testing of the girder specimens.

Technical Report Documentation Page

1. Report No.	2.	3. Recipient's Accession No.
1998-10		

4. Title and Subtitle	5. Report Date
FREEZE-THAW DURABILITY OF HIGH-STRENGTH CONCRETE	December 1997
	6.

7. Author(s)	8. Performing Organization Report No.
Roxanne Kriesel Mark Snyder Catherine E. French	

9. Performing Organization Name and Address	10. Project/Task/Work Unit No.
Department of Civil Engineering University of Minnesota 500 Pillsbury Dr. S.E. Minneapolis, MN 55455-0220	11. Contract © or Grant (G) No. (C) 69098 TOC # 83

12. Sponsoring Organization Name and Address	13. Type of Report and Period Covered
Minnesota Department of Transportation 395 John Ireland Boulevard Mail Stop 330 St. Paul, Minnesota 55155	Final Report 1993-1997
	14. Sponsoring Agency Code

15. Supplementary Notes

This report is being published without the appendices. If you wish a copy of the appendices, write to Office of Research Services at the address in box number 12; or via e-mail at ora.research@dot.state.mn.us; or by phone at 612/282-2274.

16. Abstract (Limit: 200 words)

This report presents freeze-thaw durability results of an investigation regarding the application of high performance concrete (HPC) to prestressed bridge girders. This study included a total of 30 concrete mixes and more than 130 specimens, with the following variables: aggregate type, round river gravel, partially-crushed gravel, granite, high-absorption limestone, and low-absorption limestone; cementitious material composition, Type III portland cement only, 20 percent fly ash, 7.5 percent silica fume, and combination of 20 percent fly ash with 7.5 percent silica fume replacement by weight of cement; and curing condition heat-cured or seven-day moist-cured. No air-entraining agents were used in the study's initial phase to simulate the production of precast/prestressed bridge girders.

Results indicate that it is possible to produce portland cement concrete with high strength and freeze thaw durability without the use of air-entraining agents. Overall, the moist-cured concrete specimens exhibited better freeze-thaw durability than the heat-cured concrete specimens. The reference concrete mixes--containing only portland cement–performed better than the concrete containing pozzolan material of fly ash or silica fume. The low-absorption limestone aggregate concrete mixes exhibited the best freeze-thaw durability performance--in some cases, enduring more than 1,500 freeze-thaw cycles without failing. The study found that the moisture content of the coarse aggregate at the time of mixing had a significant impact on the concrete's freeze-thaw durability.

17. Document Analysis/Descriptors		18. Availability Statement
Freeze-thaw durability high performance concrete	curing condition non-airentrained	No restrictions. Document available from: National Technical Information Services, Springfield, Virginia 22161

19. Security Class (this report)	20. Security Class (this page)	21. No. of Pages	22. Price
Unclassified	Unclassified	210	

FREEZE-THAW DURABILITY OF HIGH-STRENGTH CONCRETE

Final Report

Prepared by

Roxanne C. Kriesel
Catherine E. French
Mark B. Snyder

Department of Civil Engineering
University of Minnesota

January 1998

Published by

Minnesota Department of Transportation
Office of Research Administration
200 Ford Building Mail Stop 330
117 University Avenue
St. Paul, Minnesota 55117

ACKNOWLEDGMENTS

This project was collectively sponsored by the Minnesota Department of Transportation, Minnesota Prestress Association, University of Minnesota Center for Transportation Studies, Prestressed/Precast Concrete Institute, and NSF Grant No. NSF/GER-9023496-02. The authors acknowledge the generous donations of materials and equipment from Lehigh Cement Company; National Minerals Corporation; J. L. Shiely Company; Edward Kraemer & Sons, Inc.; Meridian Aggregates; W. R. Grace & Co.; and Elk River Concrete Products. The views expressed herein are those of the authors and do not necessarily reflect the views of the sponsors.

TABLE OF CONTENTS

List of Tables

List of Figures

NOTATION

The following notation is used throughout the text, tables and figures.

AE	Air-entrainment
DF	Durability Factor
FA	Fly Ash
GGG	Glacial Gravel Girder concrete mix
GR	Granite aggregate
LC	Length Change
LSG	Limestone Girder concrete mix
LS-H	High-absorption Limestone aggregate
LS-L	Low-absorption Limestone aggregate
PCG	Partially-Crushed Gravel aggregate
R	Repeat concrete mix (i.e. Phase II concrete mix)
RH	Relative Humidity
RDM	Relative Dynamic Modulus
RG	Round Gravel aggregate
SF	Silica Fume
SSD	Saturated Surface Dry
TYP	Typical girder concrete mix
WC	Weight Change

EXECUTIVE SUMMARY

This report describes the freeze-thaw durability research conducted as part of the University of Minnesota investigation on the application of high performance concrete (HPC) to prestressed concrete bridge girders. The overall high performance concrete research program comprised five companion investigations. Two of the investigations focussed on the materials aspects of HPC: mechanical properties and freeze-thaw durability. The remaining three investigations focussed on tests of two long-span HPC prestressed bridge girders: instrumentation and fabrication; long term behavior and flexural strength; and shear strength.

A total of 30 concrete mixes (over 130 specimens) were selected for the freeze-thaw durability study. Variables included: aggregate type (round river gravel, partially-crushed gravel, granite, high-absorption limestone, and low-absorption limestone); cementitious composition (Type III portland cement only, 20% fly ash, 7.5% silica fume, and combination of 20% fly ash with 7.5% silica fume, replacement by weight of cement); curing condition (heat-cured or 7-day moist-cured). In all of the mixes, the total cementitious content (750 lb/yd^3 (445 kg/m^3)), water-to-cementitious materials ratio (0.30 by weight) and coarse-to-fine aggregate ratio (1.5 by weight) were held constant. No air-entraining agents were used in the initial phase (Phase I) of the study to simulate the production of precast/prestressed bridge girders.

The tests were conducted in general accordance with ASTM C666 Procedure B (rapid freezing in air and thawing in water). An exception was made to the standard test procedure to investigate the effects of curing and aging (i.e. following curing, the specimens were stored in a constant temperature and humidity environment for approximately six months before testing).

Results of this investigation indicate that it is possible to produce portland cement concrete with high strength and freeze thaw durability without air-entrainment. In general, the moist-cured specimens exhibited better freeze-thaw durability than the heat-cured specimens. Moist-curing enables continuous hydration of the cementitious materials, which creates a less permeable pore structure. The hydration in heat-curing is limited by the amount of mix water. Microcracking can also develop upon drying, weakening the strength of the transition zone between the aggregate and the cement paste, and can increase permeability.

In Phase I of the study, most of the aggregates were saturated prior to mixing. In this phase of the study, specimens from the low-absorption limestone mixes (Type III portland cement only, 7.5% silica fume, and combination of 20% fly ash with 7.5% silica fume) consistently performed the best for both types of curing, with durability factors (DF) ranging from 61 to 98 ($DF > 60$ satisfactory; $60 < DF < 40$ doubtful; $DF < 40$ unsatisfactory performance). Several of the low-absorption limestone specimens endured more than 1500 freeze-thaw cycles without failing (RDM or

dilation criterion) before they were removed from the freeze-thaw testing machine. The moist-cured high-absorption limestone and partially-crushed gravel reference concrete mixes also exhibited satisfactory performance. The round gravel and granite concrete specimens were the worst performers (DF < 15).

Visual observations indicated that there were general failure mechanisms associated with each aggregate type. The mixes containing round gravel aggregates tended to deteriorate at the aggregate/paste interface. The mixes using partially-crushed aggregates suffered similar damage, but not to the extent of the round gravel aggregate mixes. The slightly better performance may be attributed to the surface texture of the aggregate. Angular, rough-surfaced aggregates develop better bond with the cement paste, strengthening the transition zone between the cement paste and aggregate. The granite concrete specimen failures tended to be dominated by cracks in the aggregate and deterioration of the aggregate/paste interface (which may have resulted from the aggregate deterioration). The freeze-thaw specimens fabricated with limestone aggregate were subjected to orders of magnitude more freeze-thaw cycles than the other beam specimens, but there was little visual evidence of deterioration.

Large dilations were observed in some of the specimens even though they did not fail the RDM criterion. The inability of some aggregate particles to restrain the dilations of the cement paste may be critical in some applications. The low-absorption (1.5%) limestone reference mix exhibited excellent freeze-thaw durability in terms of both RDM and dilation.

In Phase II of the investigation, a number of concrete mixes tested in Phase I of the study were repeated. Differences between the concrete mixes in the two phases included the moisture content of the aggregate at the time of mixing, the time period the specimens were aged prior to freeze-thaw testing, and the resulting strength of the concrete specimens. In addition, the test procedure employed in the study (heat- or 7-day moist-curing and then aging) was compared with the results of companion specimens tested in accordance with the standard ASTM C666 procedure (14-day moist-curing).

Comparing the results of Phases I and II indicates that the round gravel aggregate performance correlated with its moisture condition at the time of mixing. The round gravel mixes performed poorly when the aggregate was saturated at the time of mixing (Phase I) compared with the results of the Phase II study with unsaturated round gravel at the time of mixing. The low absorption limestone aggregate was saturated at the time of mixing for both Phases of the project, and in both phases the limestone aggregate concrete specimens exhibited good performance. The reason for the differences in behavior between the glacial gravel and limestone specimens was attributed to the different effects of the mix water in the two cases. The excess water in the over-saturated round gravel mixes tends to cling to the smooth aggregate surface and may create a weakened transition zone between the aggregate and the paste. Using unsaturated round gravel allows some moisture absorption into the aggregate that improves the contact between the paste and the aggregate increasing the

bond strength. In the case of the limestone aggregate, the angular shape and rough texture provide better contact with the paste. The high-absorption limestone mix performed better when it was not saturated, possibly due to the ability of the aggregate to absorb cement paste and strengthen the bond between the aggregate and the paste.

Limited tests were conducted in Phase II using the standard ASTM C666 curing procedure to compare with the modified procedure used in this study. The freeze-thaw performance of the round gravel concrete specimens improved when cured according to the ASTM C666 procedure, possibly due to the additional moist-curing and strengthening of the transition zone between the aggregate and the cement mortar. The limestone concrete specimens, however, performed worse than those tested in Phase I. The limestone aggregate, saturated at the time of mixing in both phases, may have needed the time period of drying prior to exposure to freeze-thaw conditions to reduce its freezable water content. During the period of aging in Phase I, water from the saturated aggregate could have been drawn out by capillary action and used as cure water for any unhydrated cement to strengthen the transition zone between the aggregate and the paste.

In addition, an air-entraining agent was used in a round gravel concrete mix in Phase II. The results of these tests confirmed that the use of air-entraining agents can substantially improve the performance of concrete which exhibits poor durability without the use of such agents.

CHAPTER 1

INTRODUCTION

PROJECT DESCRIPTION

An extensive study was completed at the University of Minnesota to investigate the application of high-strength concrete to prestressed bridge girder production. The superior mechanical properties of high-strength concrete offer significant benefits to the prestressed and precast bridge girder industry. The rapid early strength gain associated with high-strength concrete can shorten turnover times of casting beds and reduce construction times. In addition, the use of high-strength concrete in bridge girders allows increased span length, shallower cross sections and/or increased girder spacing. Economic savings from an increase in span length can be realized by eliminating or reducing the number of piers. Increased girder spacing provides savings by reducing the required number of girders per bridge.

The analytical and experimental research program on high-strength concrete comprised three primary areas of study:

* Design implications of high-strength prestressed bridge girders
* Behavior of high-strength prestressed bridge girders
* High-strength concrete materials research

The behavior of high-strength prestressed bridge girders was investigated by fabricating and testing two girders, taking full advantage of high-strength concrete to maximize span lengths. The girders were 45-in (1140-mm) deep I-sections with 132.75-ft (40.5-m) span lengths. The girders were instrumented to determine transfer lengths, long-term prestress losses, creep, shrinkage, fatigue behavior, compressive stress distribution at ultimate, and ultimate flexure and shear strengths [1,2].

The mechanical properties of high-strength concrete were investigated in the high-strength concrete materials research. Tests performed included: compressive strength, modulus of elasticity, modulus of rupture, split cylinder tensile strength, creep, shrinkage, absorption potential and freeze-thaw durability. Also investigated were the effects of testing parameters such as mold material, mold size, specimen end condition, curing condition and age. The curing process of typical prestressed girders was simulated by heat-curing specimens in accordance with typical manufacturing procedures. Results of the heat-cured specimen tests were compared with the results of tests on companion specimens cured in saturated lime-water and in air. Material variables included:

* total cementitious material content (750, 850, 950 lb/yd^3 (445, 504, 564 kg/m^3))
* type and brand of portland cement (Types I and III)
* cementitious material composition (portland cement, 0-30 percent fly ash and 0-15 percent silica fume replacement by weight of cement)
* type of silica fume (dry-densified and slurry)
* type and brand of high-range water-reducing admixture
* type of aggregate (glacial gravel (round and partially-crushed), two limestones

(high- and low-absorption) and granite)

* coarse-to-fine aggregate ratio

* aggregate gradation (as-received and recombined standard gradation)

* maximum aggregate size (0.50 and 0.75 in (13 and 19 mm)).

Nearly 7,000 specimens were cast and tested from approximately 150 concrete laboratory mixes with 28-day compressive strengths in the range of 7,000 to 17,000 psi (48 to 117 MPa) [3].

SCOPE

This report summarizes the results of the freeze-thaw durability portion of the high-strength concrete materials investigation. The total cementitious material content (750 lb/yd^3 (445 kg/m^3)), water-to-cementitious material ratio (0.30 by weight), and coarse-to-fine aggregate ratio (1.5 by weight) were held constant for this portion of the study. Four different cementitious material combinations were investigated: a reference mix (containing portland cement only), a mix containing 20 percent fly ash, a mix containing 7.5 percent silica fume, and a mix containing a combination of 20 percent fly ash with 7.5 percent silica fume. In the concrete mixes utilizing pozzolan material, the fly ash and silica fume were incorporated as replacements for portland cement on an equal weight basis. Five different types of locally obtained coarse aggregates were used in the investigation: round gravel, partially-crushed gravel, crushed granite, a high-absorption and a low-absorption crushed limestone. From each concrete

batch, both heat- and moist-cured specimens were investigated.

In addition to the 17 laboratory concrete mixes investigated, several additional concrete specimens were included in this freeze-thaw durability study. Beam specimens were taken from each of the concrete mixes for the prestressed concrete bridge girders. Also, in order to compare the laboratory mixes with mixes currently used in industry, concrete specimens were taken from a typical girder mix at a local precasting plant.

After curing, a period of aging and a period of immersion in a constant temperature water bath, the concrete specimens were tested for freeze-thaw durability. Deterioration measurements included weight, length, and fundamental transverse frequency.

Upon completion of the freeze-thaw tests of the concrete specimens described above, several concrete mixes were repeated to further investigate the freeze-thaw durability of these mixes and the failure mechanisms in each case. In addition, selected freeze-thaw test specimens were investigated forensically using linear traverse techniques to measure the air void system of the hardened concrete and identify the failure mechanisms.

Results of this investigation on the freeze-thaw durability of non-air-entrained high-strength concrete are of practical significance to the prestressed industry, which sometimes experiences difficulty obtaining the high strength specified while providing the required air content specified for durability [4].

OBJECTIVES

The purpose of this project was to investigate the freeze-thaw durability of non-air-entrained high-strength concrete. Specific objectives of the study were to determine the effects of aggregate type, curing condition, and cementitious material composition on the freeze-thaw durability of high-strength portland cement concrete.

CHAPTER 2

LITERATURE REVIEW

This chapter presents a detailed overview of the work that has been done in the field of freeze-thaw durability of concrete related to the current study. After the freeze-thaw behavior of concrete is discussed, characteristics specific to high-strength concrete are presented. Brief discussions of the effects of high-range water-reducer, pozzolans (silica fume and fly ash), aggregate, aging and period of drying on the frost resistance of concrete are then provided. To complete the chapter, short summaries are given of several studies on freeze-thaw durability of non-air-entrained high-strength concrete. The observations discussed in this chapter provide the basis for the explanation of the results of the current study in later chapters.

FREEZE-THAW MECHANISM IN CONCRETE

Early hypotheses to explain concrete damage from freezing were based primarily on the fact that water expands 9 percent when it freezes. If the concrete capillary pores are 91.7 percent or more full of water, the concrete is said to have reached "critical saturation" and would be stressed, possibly to the point of failure, when the water freezes. Concrete below the critical saturation level would not be damaged by freezing temperatures. Deterioration was found, however, in concrete with lower degrees of saturation. Laboratory studies found critical saturation levels ranging from 80 to 95 percent [5]. Further explanation of the freezing

mechanism in concrete was needed.

Powers [6] developed the hydraulic pressure hypothesis in 1945-1949 that serves as the primary explanation for failure in rapid freeze-thaw testing. Failure of the concrete, according to his theory, is caused by the hydraulic pressure generated by the water displaced by and flowing away from an advancing freeze front. Moving over a length of material, pressure from the viscous resistance to the flow through the structure of the concrete builds and, if the stress exceeds the tensile strength of the material, damage will occur in the form of local cracking. During the thaw phase of the freeze-thaw cycle, water enters the cracks, and can be frozen again. Therefore, in repeated cycles of freezing and thawing there is progressive deterioration. The magnitude of the hydraulic pressure depends on the degree of saturation, the permeability of the cement paste, the distance to the nearest unfilled air void and the rate of freezing [6]. The rapid temperature changes of the ASTM C666 test can produce this type of concrete failure due to excessive hydraulic pressure [7].

Closely-spaced air voids in the cement paste provide a shortened water flow path length that eliminates the build-up of damaging hydraulic pressure. The critical length of flow path, below which freeze-thaw damage will not occur, was determined to be on the order of 0.01 in (0.25 mm) [6]. ACI's Guide to Durable Concrete (ACI 201.2R) recommends a spacing factor (defined on page 90) less than 0.008 inch (0.20 mm) to relieve the hydraulic pressure and accommodate the freezing water expansion [8]. To achieve the spacing factor required for durable concrete, air entrainment is generally required.

Although there is general agreement that entrained air improves concrete frost resistance, air entrainment can also significantly reduce concrete strength. Therefore, in high-strength concrete, the requirements for strength and durability are in conflict. Knowing the causes of deterioration in concrete from freezing and thawing, the hypothesis has been made that high-strength concrete may, in fact, have inherent frost resistance (without the need for air-entrainment). One example is found in Norway, where non-air-entrained, high-strength concrete (11,000 to 13,500 psi (75 to 95 MPa)) has been used for highway pavement with no reports of adverse results [9].

FREEZE-THAW CHARACTERISTICS OF HIGH-STRENGTH CONCRETE

High-strength concrete is generally characterized by very low water-to-cement ratios and high cement contents, and is typically produced with the aid of high-range water-reducers and, often, one or more mineral admixtures (e.g. silica fume and/or fly ash) [10]. Philleo wrote a review of the literature on the frost susceptibility of high-strength concrete [11]. He also completed a synthesis on the subject for the National Cooperative Highway Research Program [12]. Philleo asserted that if high-strength concrete is to be durable without entrained air, it must contain no freezable water. In the hydrated cement paste the gel pores are small enough that water will not freeze in them at normal winter weather temperatures. However, the empty spaces between the gel particles, known as capillary pores, are of a size that water will freeze in them near the normal freezing point of water. Philleo explained that, in theory, freezable water can be eliminated from concrete in three ways.

The first way is to eliminate the capillary pores by using water-to-cement ratios below 0.38 and providing moist-curing until all spaces are filled with hydration products. A cement paste with the critical water-to-cement ratio of 0.38 (at which, theoretically, no unhydrated cement is left and no capillary pores are present) will actually run out of water when 90 percent of the cement is hydrated (assuming that no water was provided from the outside). This "running out of water" is termed self-desiccation. In order to withstand the effects of self-desiccation and still produce complete hydration in absence of outside water, the water-to-cement ratio must be at least 0.42. Providing moist-curing to a concrete with a water-to-cement ratio below 0.38 will allow complete hydration and fill the capillary pores so that the concrete has no capacity for freezable water [11,12].

The second way to eliminate freezable water from concrete is to make the capillary pores too small to contain freezable water. The low water-to-cement ratio of high-strength concrete reduces the porosity of the cement paste in addition to reducing the amount of capillary water susceptible to frost action (if ambient conditions permit continuous hydration for a long period of time) [7]. It has been found that 85 to 90 percent relative humidity is required for continued hydration. Use of a pozzolan in the concrete mix helps (through filler effects and production of additional hydration products) to create pores so small that water cannot freeze in them at ordinary temperatures. A longer period of curing is required for the pozzolan reaction [11,12]. However, for one high-strength concrete mix containing 796 lb/yd^3 (472 kg/m^3) Type II portland cement, 9 percent silica fume, 0.31 water-to-cementitious material ratio and 0.375 in (10 mm) crushed diabase coarse aggregate, a 7-day moist curing period was sufficient to make the

concrete almost impervious. Additional moist-curing beyond 7 days was not necessary as the concrete had retained enough moisture for further hydration. Improvement was also seen upon air-curing. However, longer curing periods are desirable for concrete mixtures containing fly ash instead of silica fume, since fly ash reacts with products from the hydration of cement, which takes time to occur [13].

The third way Philleo described to eliminate freezable water from concrete is to produce hydrated cement pastes of such low permeabilities that, after self-desiccation has used the internal water, it is impossible for water to reenter. Since the freeze-thaw failure mechanism requires concrete to be saturated in order to be adversely affected by freezing, impermeable concrete is desirable. However, the concrete must have become self-desiccated, since low permeability will serve to harm a concrete that has freezable water present. In this latter case, movement of the water to escape areas (unfilled air voids or surface of the concrete) is more difficult [11,12].

Theoretically, concrete may be produced without freezable water using one or more of the methods described above. However, since not all of the freeze-thaw tests of non-air-entrained concrete have proven durable, many concrete producers are not comfortable with the total elimination of entrained air in high-strength concrete when freeze-thaw durability is required. Therefore, because the low water-to-cement ratio of high-strength concrete makes the paste stronger and better able to withstand the tensile stresses imposed by the hydraulic pressure, some researchers have explored the possibility that high-strength concrete may not need as much

entrained air as normal strength concrete. In other words, a larger air void spacing factor requirement may be appropriate for providing freeze-thaw durability in high-strength concrete [7].

Foy, et al. [14] performed freeze-thaw tests on six air-entrained high-strength concrete mixes with water-to-cement ratios of 0.25. Type I portland cement and dense limestone coarse aggregate were used dry in all mixes. The specimens, moist-cured 14 days, had compressive strengths from 7,700 to 8,700 psi (53 to 60 MPa) at 14 days. No deterioration was seen in any of the specimens after 300 cycles of ASTM C666 Procedure A. In fact, a small gain in pulse velocity was measured for all but one mix, presumably from continued hydration while the specimens were immersed in water during testing. With hardened air contents between 2.5 and 3.0 percent, the spacing factors of these concrete specimens were 0.02 to 0.03 inch (0.51 to 0.76 mm), much higher than the required 0.008 inch (0.20 mm) for durable normal strength concrete. The authors hypothesized that, in reducing the water-to-cement ratio to 0.25, there was probably a significant reduction in the amount of freezable water initially present in the paste, which could explain the significant increase in value of critical spacing factor.

EFFECT OF HIGH-RANGE WATER-REDUCERS

As mentioned above, the low water-to-cement ratios commonly used in high-strength concrete mixes are made possible by the addition of high-range water-reducers. Several studies have explored the effects of high-range water-reducers on the freeze-thaw durability of concrete.

Attiogbe, et al. [15] wrote a summary of the research findings concerning the freeze-thaw durability of concrete made with high-range water-reducers. Like Foy, et al. [14], they found that the majority of the concrete mixes with low water-to-cement ratios had spacing factors greater than 0.008 in (0.20 mm) but were durable. They concluded that air-entrained concrete with low water-to-cement ratios containing high-range water-reducers can have adequate frost resistance at spacing factors greater than 0.008 in (0.20 mm).

Robson [16] also looked at the durability of air-entrained and non-air-entrained high-strength concrete containing a high-range water-reducer. He concluded that the addition of a high-range water-reducer changed the air-void system of the concrete by increasing the size of the air voids. All non-air-entrained concrete, field-cured (with 28-day compressive strengths of 8,855 and 9,190 psi (61 and 63 MPa)) and tested at 14 and 28 days, were nondurable, contrary to the other studies reported above.

In another study of the effect of high-range water-reducers on the durability of non-air-entrained concrete, Dhir, et al. [17] tested six concrete mixes with water-to-cement ratios from 0.39 to 0.76 and resulting 28-day compressive strengths ranging from 2,900 to 9,425 psi (21 to 65 MPa). The concrete mixes were designed for compressive strength and a constant workability of 3 in. (75 mm) slump. The study was based on cement-reduced concrete mixes (using high-range water-reducers) and normal concrete (without high-range water-reducers), keeping the water-to-cement ratio and design compressive strength constant. The concrete was made with ordinary portland cement and dry coarse aggregate of 0.785 inch (20 mm) nominal

maximum size, and moist-cured for 28 days. The freeze-thaw tests were similar to ASTM C666 Procedure B (frozen in air and thawed in water (0 °F to 41 °F (-18 °C to 5 °C)). All concrete specimens performed well, and the authors concluded that, for a given design strength and workability, use of a high-range water-reducer may improve the freeze-thaw resistance of concrete, due to lower water content and permeability. The authors also suggested that high-range water-reducing admixtures may increase the concrete strength by improving the dispersion of cement particles through the concrete mix. This was shown by comparing two concrete mixes, one with a high-range water-reducer and one without a high-range water-reducer. The concrete with the high-strength water-reducer contained less cement but produced concrete of equal compressive strength as the latter mix.

In general, the high-range water-reducers used to produce high-strength concrete while maintaining normal workability have achieved very low water-to-cement ratios, and the consequential benefits to the freeze-thaw durability of the concrete have been seen.

EFFECT OF POZZOLANS

The best current technology for designing frost-resistant concrete, according to Ellis [18], requires the use of a pozzolan, either fly ash or silica fume. Furthermore, Tuthill [19] states that any concrete that will be exposed to occasional wetting will be improved by the use of 20 percent or more of fly ash pozzolan comprising the cementing material.

ASTM C618 defines pozzolans as "siliceous or 'siliceous and aluminous' materials which, in themselves, possess little or no cementitious value, but will, in finely divided form and in the presence of moisture, chemically react with calcium hydroxide at ordinary temperatures to form compounds possessing cementitious properties [20]."

When present in the concrete mix, fly ash and silica fume react with the calcium hydroxide liberated during the hydration of cement to produce additional hydration products which occupy capillary pore space in the cement paste. Filling the capillary pores reduces the amount of space in which water can freeze and also reduces the permeability of the concrete. With a lower permeability, the rate that water can be lost from critically saturated concrete on drying is slower than for concrete without pozzolans, which is disadvantageous for freeze-thaw performance. However, once the concrete has ceased to be critically saturated, the rate at which it can absorb water on resoaking should also be slower, which is advantageous [21].

The difference between fly ash and silica fume is in terms of fineness and percentage of reactive silica. Silica fume is 50-100 times finer than cement or fly ash, and the amount of reactive silica is in the range of 90-98 percent, compared with 50 percent or less for fly ash. Thus the pore-filling capability of silica fume is much greater than that of fly ash, since the fineness enables it to intrude more easily into the smaller capillary pores and react more efficiently to create additional hydration products [21].

Silica Fume

Silica fume is a by-product of the production of silicon metal or ferrosilicon alloys and consists of very fine spherical particles. Silica fume increases the concrete strength for a given water-to-cement ratio. In concrete without silica fume, the transition zone is porous and usually the weak link. In silica fume concrete, the fine silica fume particles and the products of the pozzolanic reaction pack efficiently at the aggregate interface and make the transition zone more dense, resulting in a stronger bond between the aggregate and paste [22].

Many studies have been done to explore the effect of silica fume on the freeze-thaw durability of air-entrained portland cement concrete. The six studies summarized below each found that the addition of silica fume either improved or had no effect on the frost resistance of portland cement concrete when a satisfactory air void system had been achieved [21, 23, 24, 25, 26, 27].

Johnston [23] performed freeze-thaw tests on air-entrained concrete containing 0 and 10 percent silica fume using ASTM C666 Procedure A. The specimens were either moist-cured or "heat-cured" (i.e. heat-cured at 150 °F (66 °C), then moist-cured 5 days). With hardened air contents of 3.0 to 4.6 percent, all spacing factors were less than 0.008 inch (0.20 mm). The control mix, containing 758 lb/yd^3 (450 kg/m^3) portland cement and 0.43 water-to-cement ratio, attained a 28-day compressive strength of 5,000 psi (34 MPa) and durability factors of 100 and 102, for the heat- and moist-cured specimens, respectively. The concrete containing 10 percent

silica fume replacement of cement (for a 506 lb/yd^3 (300 kg/m^3) total cementitious material content and 0.44 water-to-cementitious material ratio) achieved a 28-day compressive strength of 6,600 psi (46 MPa) and durability factors of 97 and 94 for the heat- and moist-cured specimens, respectively. A third mix, with 10 percent silica fume in addition to cement (for a 758 lb/yd^3 (450 kg/m^3) total cementitious material content and water-to-cementitious material ratio of 0.33), attained a 28-day strength of 8,000 psi (55 MPa) and a durability factor of 97 for the moist-cured specimen. Johnston concluded that both the control and the silica fume air-entrained concrete mixes exhibited satisfactory frost resistance.

On the basis of freezing expansion of concrete cylinders tested according to Finnish standards, Virtanen concluded that air-entrained concrete containing 7.5 percent silica fume replacement of cement had better frost resistance than an equivalent portland cement concrete. With water-to-cementitious material ratios of 0.5 to 0.6, the 28-day compressive strengths of the tested concrete ranged from 4,400 to 5,900 psi (30 to 41 MPa) [24].

Galeota, et al. [25] performed freeze-thaw tests on air-entrained and non-air-entrained concrete with 0 and 20 percent silica fume in addition to 556 lb/yd^3 (330 kg/m^3) of Type I portland cement. After a 28-day moist-cure, the specimens underwent 12-hour freeze-thaw cycles in which they were frozen in air and thawed in water (-13 °F to 41 °F (-25 °C to 5 °C)). Both silica fume concretes (with and without air-entrainment) performed poorly, dropping below 40 percent Relative Dynamic Modulus after 90 and 50 cycles, respectively. The authors attributed the poor performance of the silica fume concrete to the high air void spacing factor

in the concrete. Despite the 5 percent air content, the spacing factor of the air-entrained silica fume concrete was 0.020 inch (0.51 mm), not much improvement over the 0.026 inch (0.66 mm) spacing factor of the non-air-entrained silica fume concrete. Both of the concrete mixes without silica fume survived past 250 cycles (at which time testing ended). The spacing factors of the concrete without silica fume were 0.014 inch (0.36 mm) and 0.024 inch (0.61 mm) for the air- and non-air-entrained concrete, respectively. These spacing factors were also well above the 0.008 in (0.20 mm) recommended for durable concrete.

Johnston [21] explored 0, 5, 7.5, 10, and 15 percent silica fume replacement by weight of cement in air-entrained and non-air-entrained concrete with 28-day compressive strengths of 4,000 to 6,470 psi (28 to 45 MPa) and 4,580 to 6,020 psi (32 to 42 MPa), respectively, increasing with increasing silica fume content. The 0.5-in (13-mm) nominal maximum size gravel coarse aggregate had proven frost resistance (by previous testing of air-entrained concrete by ASTM C666 Procedure A). All non-air-entrained concrete, with water-to-cementitious material ratios of 0.64, performed poorly, with durability factors from 10 to 40, while the durability factors for all air-entrained concrete ranged between 60 and 90. Spacing factors were 0.052 to 0.075 in (1.32 to 1.91 mm) for the non-air-entrained concrete and 0.009 to 0.014 in (0.23 to 0.35 mm) for the air-entrained concrete.

Additional freeze-thaw testing by Johnston was completed on twelve air-entrained concrete mixes with 0, 5, 10, and 15 percent replacement of silica fume and water-to-cementitious material ratios of 0.55, 0.70 and 0.88. Compressive strengths at 28 days were

2,060 to 5,410 psi (14 to 37 MPa), and durability factors ranged from 85 to 96. With hardened air contents of 4.1 to 9.7, spacing factors ranged between 0.007 and 0.012 in (0.17 and 0.31 mm). Johnston concluded that replacement of cement by silica fume does not detract from freeze-thaw durability, even at water-to-cementitious material ratio of up to 0.88, as long as a satisfactory air-void spacing factor is achieved [21].

The theory that the properties of silica fume may allow the production of concrete with no freezable water and an immunity from resaturation has led many researchers to test the hypothesis that air-entrainment is not necessary for the frost resistance of portland cement concrete containing silica fume.

In a study for the Portland Cement Association (PCA), one non-air-entrained concrete mix with 13.6 percent silica fume replacement of cement and 1100 lb/yd^3 (653 kg/m^3) total cementitious material content (water-to-cementitious material ratio of 0.22), moist-cured 28 days and attaining a strength of 17,250 psi (119 MPa), exhibited excellent performance. The specimens underwent over 1800 freeze-thaw cycles without failure. Another non-air-entrained concrete mix from the PCA study, however, with 8.9 percent silica fume and 900 lb/yd^3 (534 kg/m^3) total cementitious material content (water-to-cementitious material ratio of 0.29) and a compressive strength of 13,330 psi (92 MPa), failed the ASTM C666 Procedure A freeze-thaw test at 75 cycles [28].

Hooton performed freeze-thaw tests on non-air-entrained concrete mixes containing 0,

10, 15, and 20 percent silica fume replacement of cement. The concrete had 676 lb/yd^3 (401 kg/m^3) cementitious material content, water-to-cementitious material ratios of 0.36 to 0.37 and was moist-cured for 14 days, yielding compressive strengths from 8,060 to 10,900 psi (56 to 75 MPa). While the concrete without silica fume failed at 58 cycles, all silica fume concretes had durability factors greater than 90 after 900 cycles of ASTM C666 Procedure A. Hooton attributed the excellent performance of the silica fume concrete to self-desiccation combined with low permeability, resulting in a less-than-critical saturation level. An observed increase in micro-cracking with increase in silica fume content led the authors to conclude that the lower silica fume replacement content of 10 percent was the best amount [29].

Further freeze-thaw tests by Tachibana, et al. [30] on 10 percent silica fume replacement of cement in non-air-entrained concrete with 14 days of moist-curing (ASTM C666 Procedure A) resulted in durability factors of 97 to 99. The water-to-cementitious material ratios ranged from 0.22 to 0.28, and the 28-day compressive strengths were greater than 14,500 psi (100 MPa). The authors concluded that high-strength concrete with low water-to-cementitious material ratios and without entrained air is highly durable to freezing and thawing. They also asserted that approximately 10 percent replacement of cement by silica fume may be the ideal quantity to incorporate in the concrete mix in order to obtain a compressive strength of more than 14,500 psi (100 MPa) and to improve other properties of the concrete.

In Philleo's literature review of the freeze-thaw durability of high-strength concrete he mentioned the test of a non-air-entrained high-strength concrete mix with 15 percent silica fume

(water-to-cementitious material ratio of 0.24) that was moist-cured for 28 days, attaining a 31-day strength of 16,590 psi (114 MPa) and a spacing factor of 0.013 inch (0.33 mm). Testing by ASTM C666 Procedure A resulted in a durability factor of 95. Since the concrete compressive strength increased to 18,390 psi (127 MPa) at 154 days, he concluded that the concrete was not completely free of freezable water at the time the freeze-thaw test started. Philleo postulated that the water content of the concrete was so low that the air voids were not critically saturated [12].

Hammer and Sellevold [31] studied the freeze-thaw resistance of four non-air-entrained concrete mixes with 28-day compressive strengths ranging from 11,140 to 16,730 psi (77 to 115 MPa). Water-to-cementitious material ratios ranged from 0.28 to 0.46. Silica fume was added as 0, 5 and 10 percent replacement of high strength cement. Four specimens were tested per mix, and a large amount of scatter was seen in the results. Concrete specimens without silica fume exhibited durability factors from 0 to 100. For the concrete with silica fume, durability factors ranged between 60 and 100 (satisfactory frost resistance). Specimens had been air-cured one month followed by immersion in seawater one month. The authors believed this curing procedure increased the amount of freezable water in the concrete due to desiccation and microcracking during the air curing period.

Pigeon, et al. [26] conducted a freeze-thaw study of seventeen high-strength concrete mixes (air-entrained and non-air-entrained) with 28-day compressive strengths of 8,700 to 12,900 psi (60 to 89 MPa). Types I and III portland cement were used and silica fume was used as 0

and 6 percent replacement of cement. These concretes were air-cured for 1, 3, 7 and 28 days and tested using ASTM C666 Procedure A. All specimens performed well in the test with durability factors all greater than 87, even with spacing factors as high as 0.037 inch (0.94 mm) (for the non-air-entrained portland cement concrete). Results indicated that air-entrainment was not required for good frost resistance (of silica fume or portland cement concrete) at water-to-cementitious material ratios of 0.30, even after only one day of curing.

Cohen, et al. [27] performed freeze-thaw tests on four concrete mixes (two air-entrained and two non-air-entrained) containing 0 and 9 percent silica fume replacement of cement with 9,570 to 11,240 psi (66 to 78 MPa) compressive strengths. The concrete had a total cementitious material content of approximately 660 lb/yd^3 (392 kg/m^3), a water-to-cementitious material ratio of 0.35, and was moist-cured for 7, 14, 21 and 56 days. While all air-entrained concrete (with and without silica fume) attained durability factors greater than 90, the non-air-entrained silica fume concrete performed poorly. The two non-air-entrained portland cement concrete specimens moist-cured for 21 and 56 days, however, exhibited durability factors of approximately 65 (satisfactory performance). Thus, when the concrete was properly air-entrained, silica fume neither improved nor hindered the frost resistance of the concrete. For non-air-entrained concrete, silica fume did not improve the inherent frost resistance of the concrete.

In conclusion, four of the studies summarized above reported poor frost resistance of non-air-entrained silica fume concrete [21, 25, 27, 28] while seven studies reported good freeze-

thaw performance of non-air-entrained concrete containing silica fume [12, 26, 27, 28, 29, 30, 31]. Possible reasons for the poor performances are found upon examination of the given data. One of the studies in which the silica fume concrete mix performed poorly had water-to-cement ratios of 0.64 and relatively low compressive strengths (4,580 to 6,000 psi (32 to 41 MPa)) [21]. Another silica fume concrete mix that exhibited poor frost resistance contained a high percentage of silica fume (20 percent) and a relatively low cementitious material content (560 lb/yd^3 (332 kg/m^3)). Hooton [29] and Tachibana, et al. [30] had concluded, from their studies, that using 10 percent silica fume was the best amount. Also, Philleo stated that adding silica fume at 5 to 10 percent by mass of cement was the optimum amount [12]. Generally, then, the studies have shown that portland cement concrete containing silica fume can be produced with a pore structure capable of withstanding freezing and thawing without air-entrainment.

Fly Ash

Fly ash is the finely-divided residue that results from the combustion of ground or powdered coal. ASTM C618 Class C fly ash, in addition to having pozzolanic properties, also has some cementitious properties in that it may be self-setting when mixed with water.

Most researchers have concluded that fly ash has neither a beneficial nor adverse effect on the freeze-thaw performance of air-entrained concrete. Washa and Withey [32] performed freeze-thaw tests on air-entrained and non-air-entrained normal strength concrete (4,000 to 6,000 psi (28 to 41 MPa)) containing 20 percent fly ash replacement of Type I and II portland cement

and moist-cured 28 days. One to two freeze-thaw cycles were completed per day, and test results indicated that fly ash had neither a beneficial nor adverse effect on the freeze-thaw performance of air-entrained concrete. While the non-air-entrained concrete failed in less than 100 cycles, the 4-5 percent air-entrained concrete showed little damage, even after 500 cycles.

Klieger and Gebler [33] performed freeze-thaw tests on air-entrained concrete with 0 and 25 percent Class C fly ash replacement of ASTM Type I portland cement. The concrete, tested at an age of 28 days (moist-cured 14 days, then aged 14 days), exhibited good resistance with durability factors greater than 92. The air contents ranged from 3 to 7 percent and the spacing factors were all less than 0.008 inch (0.20 mm). The authors concluded that the concrete containing Class C fly ash performed as well as the concrete without fly ash.

Johnston [21] completed a study of four air-entrained concrete mixes with 0, 16, 27 and 42 percent Class C fly ash replacement by weight of cement. The water-to-cementitious material ratio was 0.53 and the 0.5-in (13-mm) gravel had proven frost resistance (by previous ASTM C666 Procedure A testing). Durability factors were 90, 84, 84 and 70 for the 0, 16, 27 and 42 percent fly ash concrete, respectively. All spacing factors were between 0.005 and 0.007 inch (0.12 and 0.19 mm). Johnston concluded that the replacement of cement with Class C fly ash does not detract from freeze-thaw performance provided a satisfactory air-void spacing factor is achieved.

Carrasquillo [34] conducted a freeze-thaw study (ASTM C666 Procedure A) on

specimens from three air-entrained concrete mixes, incorporating 0, 20 and 35 percent Class C fly ash replacement by weight of cement. Concrete specimens were moist-cured 14 days. With water-to-cementitious material ratios of 0.34 to 0.47, 28-day compressive strengths of 5,000 to 6,000 psi (34 to 41 MPa) were achieved. All of the concrete specimens from all of the concrete mixes attained durability factors greater than 90 after 300 cycles. He concluded that the concrete with fly ash was as resistant to freeze-thaw damage as the concrete without fly ash, given equal air content.

A study by Nasser and Lai [35] involving 0, 20, 35 and 50 percent Class C fly ash, replacement by weight of cement, found a decrease in frost resistance with increased fly ash content in air-entrained concrete. With water-to-cementitious material ratios of 0.51 to 0.55, the 28- and 80-day moist-cured concrete specimens developed spacing factors of 0.005 to 0.007 inch (0.13 to 0.18 mm), all within the recommended 0.008 inch (0.20 mm). ASTM C666 Procedure A test results indicated the 0 and 20 percent fly ash concrete exhibited satisfactory performance ($DF > 60$), the specimens with 35 percent fly ash had doubtful to satisfactory performance ($60 > DF > 40$), and the specimens with 50 percent fly ash were frost susceptible ($DF < 40$). The 28-day compressive strengths of these mixes were 2,400 to 3,500 psi (17 to 24 MPa), increasing with a decrease in fly ash content.

Virtanen [24] tested air-entrained concrete with 30 percent replacement of cement by fly ash for freeze-thaw durability using freezing expansion criteria from Finnish Standards. He found that 30 percent fly ash had no major effect on the performance of the concrete to freezing

and thawing, given the same strength and air content. However, he also concluded that fly ash may have a negative effect when a major portion of the cement is replaced. The 28-day concrete compressive strengths were between 4,365 to 5,160 psi (30 to 36 MPa).

Mather [36] performed freeze-thaw tests on concrete incorporating 30, 45 and 60 percent fly ash replacement of Type II portland cement by volume. Water-to-cementitious material ratios were 0.5 and 0.8. Following either 14 or 180 days of moist-curing at 73 °F (23 °C), the specimens were subjected to testing by Procedure A of ASTM C666. For both water-to-cementitious material ratios at both ages, there was a progressive reduction of both strength and durability factor as the proportion of cement replaced by fly ash increased. With compressive strengths less than 2,200 psi (15 MPa), all concrete mixes with water-to-cementitious material ratios of 0.8 had durability factors less than 23 (frost susceptible). Reducing the water-to-cementitious material ratio to 0.5 improved the freeze-thaw performance and increased the compressive strength of the concrete up to 5,540 psi (38 MPa). The concrete mixes incorporating 30% fly ash exhibited satisfactory freeze-thaw performance (DF > 60) for both curing methods. Satisfactory performance was also seen in the 45% fly ash concrete specimens that were moist-cured for 180 days.

Whiting [37] studied the freeze-thaw durability of air-entrained and non-air-entrained concrete incorporating 10-18 percent Class C fly ash replacement of cement. Two curing methods were used. Some specimens were continuously moist-cured and tested at the age of 28 days. Other specimens were moist-cured for 7 days, air-dried for 21 days and then immersed

in water 3 days prior to testing. All of the air-entrained concrete performed well in the freeze-thaw tests, attaining durability factors of 99 or greater at nominal strengths of 6,000, 8,000 and 10,000 psi (41, 55 and 69 MPa). Only the highest strength (10,000 psi (69 MPa)) non-air-entrained concrete with 15 percent replacement of cement by fly ash, given a period of air-drying, exhibited satisfactory performance, attaining a durability factor of 70.

In conclusion, eight of the above summarized studies reported good freeze-thaw performance of air-entrained fly ash concrete [21, 24, 32, 33, 34, 35, 36, 37]. However, a clear decrease in frost resistance was seen with increasing fly ash content (greater than 20 percent).

As with silica fume, the possibility arises that air-entrainment may not be needed because of the filler effect of fly ash, eliminating the porous transition zone typical of portland cement concrete and reducing air-void sizes [22]. Freeze-thaw studies have been completed that have demonstrated the frost resistance of non-air-entrained fly ash concrete [37]. However, two studies reported poor freeze-thaw performance of non-air-entrained fly ash concrete [32, 37]. The poor performance may be associated with the relatively low compressive strength of the concrete. In the study by Washa and Withey [32], normal strength concrete (4,000 to 6,000 psi (28 to 41 MPa)) was tested. In the Whiting study [37] fly ash concrete strength was 6,000, 8,000 and 10,000 psi (41, 55 and 69 MPa) in which only the highest strength non-air-entrained fly ash concrete exhibited good performance.

Fly Ash and Silica Fume

Several studies of the freeze-thaw performance of concrete mixes incorporating both fly ash and silica fume have been reviewed. In a study by Bayasi [38], 20 percent Class C fly ash was included in concrete mixes containing 10, 15, 20, and 30 percent silica fume. Permeability tests indicated a detrimental effect of fly ash on the concrete. With 20 percent fly ash replacement of cement in silica fume concrete, an increase in the permeability of the concrete was seen. As previously discussed, for non-air-entrained high-strength concrete, low permeability is desirable for frost resistance.

Marzouk [39] studied the freeze-thaw durability of a 4 percent air-entrained high-strength concrete incorporating 12 percent fly ash and 8 percent silica fume replacement of cement. A high cementitious material content of 927 lb/yd^3 (550 kg/m^3) and a low water-to-cementitious material ratio of 0.27 produced an average concrete compressive strength of 10,350 psi (71 MPa). Freeze-thaw tests, performed according to ASTM C666 Procedure A, indicated very durable concrete up to 458 cycles (without showing any significant reduction in dynamic modulus of elasticity).

In the PCA research program [28], three non-air-entrained concrete mixes incorporating fly ash and silica fume were tested using ASTM C666 Procedure A. A concrete mix containing 10.6 percent fly ash and 4.25 percent silica fume (940 lb/yd^3 (558 kg/m^3) total cementitious material) with a water-to-cementitious material ratio of 0.29, attained a strength of 12,840 psi

(89 MPa) and endured more than 300 cycles of freezing and thawing. Specimens from a concrete mix containing 15.9 percent fly ash and 11.4 percent silica fume (1100 lb/yd^3 (653 kg/m^3)) total cementitious material) with a water-to-cementitious material ratio of 0.23 and 28-day compressive strength of 15,520 psi (107 MPa), each failed suddenly between 229 and 361 cycles of freezing and thawing. A concrete mix containing 6 percent silica fume and 19.8 percent fly ash (743 lb/yd^3 (441 kg/m^3) total cementitious material) with a water-to-cementitious material ratio of 0.32 attained a 28-day compressive strength of 10,600 psi (73 MPa), but failed at 229 cycles of freezing and thawing.

The results of the freeze-thaw tests of four concrete mixes containing fly ash and silica fume have been presented. Generally, the concrete mixes that performed well contained a high cement content with less than 20 percent pozzolan replacement of the portland cement.

EFFECT OF AGGREGATE

Aggregate constitutes 70 percent of the volume of concrete, so the freeze-thaw performance of the concrete is significantly influenced by the characteristics of the aggregate. The behavior of the aggregate when exposed to freezing and thawing depends primarily on the properties related to the pore structure within the aggregate particles. In fact, aggregate particles exhibit the same type of freezing behavior as the behavior observed when cement paste is frozen. When saturated aggregate particles are frozen, the increase in volume during the formation of ice must be accommodated either within the aggregate particle itself or be forced into the

surrounding paste. As with the case of freezing cement paste, the stress in the aggregate is produced by hydraulic pressure from water flow [6]. Therefore, the important aggregate properties for freeze-thaw durability are pore size distribution and continuity, absorption capacity and the degree of saturation of the aggregate [40].

When freezing occurs, most saturated aggregates tend to expel water. As the water is forced out of the aggregate, the hydraulic pressure increases. However, since most aggregates have a much greater tensile strength than the surrounding cement paste, they may be able to withstand a considerable amount of hydraulic pressure without fracturing. As the pressures increase, the aggregate may be able to expand elastically to accommodate the increased volume. However, even if the aggregate does not fracture, its expansion may cause distress to the surrounding paste. If the water expelled by the aggregate cannot be accommodated by the cement paste, failure will occur around the periphery of the aggregate particle [41].

The degree of saturation of the aggregate is crucial since water will not be forced from the aggregate particle unless saturation is greater than 91.7 percent. The effect of the aggregate on freeze-thaw damage depends largely upon the ability of the particle to become and stay highly saturated while enclosed in cement paste. If potentially vulnerable aggregates are dry when used and are subjected to periodic drying in service, they may never become critically saturated [40]. If aggregates are saturated at the time of mixing concrete with low water-to-cement ratio pastes, self-desiccation during hydration may decrease significantly the moisture content of the aggregate [6, 26].

The absorption capacity of the aggregate is important for several reasons. In the fresh concrete, bleeding causes water to collect underneath the aggregate particles, and water-rich layers form around the aggregate particles. If the aggregate is non-absorbent, these layers are thicker and more porous than in the case of absorbent aggregate, assuming the absorbent aggregate is not already saturated and can absorb water. Therefore, non-absorbent aggregate forms a rather weak, porous zone around the aggregate while the interfacial zones around an absorbent aggregate particle may be less porous [42]. Porous aggregate (dried before use) can achieve excellent bond since the process of absorption will improve the contact between the paste and the aggregate. This relationship between bond and absorption may account, in part, for the poor correlation between the freeze-thaw durability of the concrete and the aggregate absorption, in view of the fact that strength of bond tends to increase as aggregate absorption increases (for an unsaturated aggregate) whereas durability of concrete tends to decrease as aggregate absorption increases [43].

Aggregate absorption data are frequently used in assessing the probable durability of concrete exposed to freezing and thawing. According to Minnesota Department of Transportation specifications, the maximum allowable absorption capacity for Class B aggregates (crushed quarry or mine rock) is 1.7 percent to insure durable performance of concrete superstructures [44]. Generally, it is believed that the coarse aggregate particles with relatively high absorption values are most easily saturated and contribute to the deterioration of concrete.

Although most aggregates with low absorption are durable, many durable aggregates have a high absorption capacity. The absorption test of bulk aggregates gives only a total volume of pores; however, the structure of the pores as well as their total volume is important [40].

Measurement of absorption while the aggregate particle is immersed in a water bath does not necessarily indicate the capacity of the aggregate to attain and retain a high degree of saturation in concrete. Whether or not water will enter into or be drawn from an aggregate particle while it is enclosed in cement paste depends in considerable part upon the relative size of the pores in the aggregate particle and in the cement paste. Water moving by capillarity will not enter aggregate containing only large pores, even if the voids are interconnected and penetrable. On the other hand, small voids will be penetrated; and if these openings are smaller than those of the cement paste, the water will be preferentially drawn into them from the paste. During periods of hydration or drying, while water is being withdrawn from the cement paste, water will be drawn by capillarity from the aggregate particles containing only voids which are larger than those in the paste, but the last residuals of water remaining in even relatively dry concrete may be concentrated in aggregate voids smaller than those in the paste. Thus rocks containing exceedingly small, interconnected voids are capable of attaining and retaining a high degree of saturation in concrete, and may be susceptible to repeated freezing. Porous aggregate containing large voids, on the other hand, may easily lose water and be less likely to draw water back in when the concrete is immersed in water [43].

Many concrete investigations have been conducted specifically to look at the effect of

aggregate type on the freeze-thaw durability of concrete. In fact, each of the studies reviewed have used a different coarse aggregate. However, caution must be taken when comparing results since the aggregates were not described completely, from a petrographic standpoint. With no knowledge of the structure or composition of the aggregate, accurate comparisons cannot be made. Identification as "limestone" or "river gravel," for example, provide no basis for comparison without knowledge of the lithologic properties because of the wide variation in aggregate.

Mehta and Aitcin [10] completed a laboratory study on the influence of aggregate mineralogy on the strength and elastic properties of high-strength concrete mixtures. Four different coarse aggregates were investigated, including a natural siliceous gravel with round particles and smooth texture, a fine-grained crushed diabase, a crushed limestone and a crushed granite. The nominal maximum size was 0.55 in (14 mm) for the granite and 0.39 in (10 mm) for the other three aggregates. All concrete mixes contained 843 lb/yd^3 (500 kg/m^3) Type I portland cement, 7.75 percent silica fume replacement of cement, 0.25 water-to-cementitious material ratio, and a high-range water-reducer. The 4 x 8-in (100 x 200-mm) cylindrical specimens were moist-cured for 28 days. The concrete mixes with granite and gravel aggregate gave slightly lower strengths (12,325 and 13,340 psi (85 and 92 MPa)) and elastic moduli than concrete mixes with diabase or limestone (14,645 and 14,065 psi (101 and 97 MPa)). In the compressive strength tests, the limestone and the diabase concrete showed little evidence of aggregate-cement paste debonding (or weak transition zone) but often exhibited shear plane fracture through the aggregate and paste. The concrete with siliceous gravel showed cement

paste-aggregate bond failure, indicating strong aggregate but weak transition zone. With granite, fracture was seen, but evidence suggested that the aggregate was weak (i.e. the same shear plane did not pass through cement paste and aggregate, making it probable that the aggregate fractured earlier than cement paste).

Stress-strain curves were graphed, with the test results showing the loading and unloading hysteresis loops. The width of the hysteresis loop is related either to intrinsic elastic properties of the aggregate or to the strength of transition zone. The concrete with limestone and diabase aggregate gave modulus of elasticity curves with narrow hysteresis loops and little or no unrecoverable plastic strain on unloading, indicating aggregate that is inherently strong and capable of forming a strong transition zone. The concrete with granite or gravel showed thicker hysteresis loops and unrecoverable strain on unloading, indicative of weakness in the transition zone (gravel) and in the aggregate particles (granite) [10].

Results indicated that aggregate type can play an important role in controlling the strength of the transition zone and the degree of microcracking. A weak transition zone is vulnerable to microcracking when the concrete is subjected to stress. Microcracking in the aggregate-cement paste transition zone of high-strength concrete increases permeability and reduces durability [13].

Walker and Hsieh [45] performed freeze-thaw tests on air-entrained concrete made with eight different coarse aggregates ranging from crushed limestone and trap rock to gravel from

glacial and nonglacial sources in the United States and Canada. The coarse aggregates were graded from 1 to 0.25 inches (25 to 6 mm) and were vacuum-saturated 24 hours before mixing. Type I portland cement was used, and the specimens were cured for 14 days in lime-water. Excellent performance was seen from quartzite gravel (0.40 percent absorption, 2.64 SSD specific gravity) concrete and crushed trap rock (0.58 percent, 2.94) concrete with durability factors of 98 and 99, respectively, at 100 cycles. A crushed limestone (2.28 percent, 2.72) concrete attained a durability factor of 84 at 100 cycles. The concrete specimens containing gravel with absorptions of either 3, 4 or 7 percent air content exhibited very poor durability, with 100 cycle durability factors between 1 and 5. Results indicated that the aggregate producing frost resistant concrete had relatively low absorptions. Concrete consisting of aggregates with higher absorption exhibited worse freeze-thaw performance.

Lane and Meininger [46] performed freeze-thaw tests on air-entrained concrete made with four limestones. The 1-inch (25-mm) nominal maximum size aggregates were: dense limestone (0.31 percent absorption, 2.72 SSD specific gravity) and three porous limestones (3.21 percent, 2.50; 4.50 percent, 2.45; 7.00 percent, 2.30). The aggregates were soaked in water 24 hours prior to mixing. Type I portland cement at 564 lb/yd^3 (335 kg/m^3) and water-to-cement ratios of 0.45 to 0.48 were used. Specimens were cured in a moist room and tested at 14 days by both Procedures A and B of ASTM C666. The concrete specimens exhibited no significant deterioration through 1,000 cycles of Procedure B (durability factors of 97-103). Procedure A tests also gave satisfactory results with durability factors of 79, 95, 97 and 100 and RDM failure at 350, 500, 750 and 1000+ cycles for 4.5, 7.0, 3.2 and 0.31 percent absorption capacity

limestone, respectively. The weight measurements during the freeze-thaw test showed that specimens tested by Procedure B progressively lost moisture during the test, whereas specimens tested by Procedure A showed a progressive weight gain. The authors attribute the difference in results of the two procedures to the differing degrees of saturation of the specimens during the test. In comparing the freeze-thaw test results with absorption data for the aggregates, the highest absorption aggregate did not show the worst performance. This supports the concept that the pore structure, rather than the absorption of the aggregate, controls freeze-thaw durability.

In the freeze-thaw durability tests conducted by Pigeon, et al. [26] on non-air-entrained high-strength concrete, one of the variables studied was aggregate type. Dry limestone (0.70 percent absorption, 2.77 specific gravity) and granite (1.0 percent, 2.69) were used in the non-air-entrained concrete mixes with water-to-cementitious material ratios of 0.30. Type III portland cement and 6 percent silica fume (as replacement of the cement) comprised the cementitious material. The specimens were air-cured and tested by ASTM C666 Procedure A. Both the limestone and the granite concrete mixes exhibited excellent frost resistance, with pulse velocities at the conclusion of freeze-thaw testing that were greater than at the start.

As mentioned earlier, these test results cannot be directly compared to results of the study reported herein because of the wide variation in aggregate properties. However, general trends and aggregate behaviors upon freezing are used to explain the performance of the five different aggregate types used in this study (see Chapter 4 for discussion of results).

EFFECT OF AGING AND PERIOD OF DRYING

In Philleo's literature review of the freeze-thaw durability of high-strength concrete, he concluded that when specimens were tested in strict compliance with ASTM C666, including the 14-day moist-curing condition, the concrete needed to be air-entrained with a reasonable spacing factor to exhibit freeze-thaw durability. Non-air-entrained concrete which had proven durable in laboratory testing had benefitted either from a longer period of hydration or a period of drying before testing. Therefore, he recommended altering the age-at-test and specimen conditioning requirements to test the freeze-thaw resistance of mature specimens to more typical exposures [11]. In fact, most concrete undergoes some drying before freezing and is usually more than two weeks old before first freezing [12]. The ACI Guidelines for Durable Concrete suggest a period of air-drying prior to exposure to freeze-thaw conditions [8]. While air-drying, moisture is lost by self-desiccation of the cement paste and through evaporation. In addition, concrete containing silica fume requires a greater amount of time (more than 14 days) for the pozzolanic reaction which decreases the permeability and the amount of freezable water in the cement paste [11].

Fiorato [47] reviewed the Portland Cement Association research on the durability of high-strength concrete. He looked at the results of durability tests in terms of durability factor as a function of compressive strength for non-air-entrained concrete mixes. Results were divided into those for which there was no drying prior to freeze-thaw testing and those where there were at least 14 days of drying before testing. Where drying was permitted, the concrete generally

performed better. The author suggested that there was a reduction of potentially freezable water during hydration and drying, and attributed the good performance to the ability of low permeability concrete to resist resaturation under the conditions of freezing and thawing.

In a literature survey on frost action in concrete, Sawan [41] cited two studies with the same findings. In the first study cited, Gaynor and Meininger found that drying a coarse aggregate before mixing or allowing the concrete to dry before freezing, improved the durability of concrete. In the second study cited, Wong, Anderson, and Hilsdorf also found that drying the concrete specimens before freezing increased the durability even if it was rewetted prior to testing.

Kukko and Matala [48] studied the effect of aging on the frost resistance of non-air-entrained high-strength concrete. In their test program low-heat sulfate-resistant portland cement and a very rapid-hardening portland cement were used. Silica fume and fly ash were added as a replacement by weight of cement at 5-6 percent or 25 percent, respectively. The total cementitious material ranged from 801 to 1017 lb/yd^3 (472 to 600 kg/m^3) with water-to-cementitious material ratios of 0.28 to 0.35. Specimens were moist-cured for either 3 or 5 days (at 68 °F (20 °C) and 95 percent relative humidity (RH)). The first series of tests were started at an age of 28 days and the second series were performed after "aging" the specimens over ten months. "Aging" consisted of wet-curing for 3 or 5 days, curing at 70 °F (21 °C) until 28 days, and then eight dry/wet cycles (wet at 68 °F (20 °C) and 95 percent RH for two weeks, dry at 68 °F (20 °C) and 40 percent RH for two weeks). A ninth wet/dry cycle consisted of five weeks

at 104 °F (40 °C) and 15 percent RH, then immersion in water for three weeks prior to testing. The freeze-thaw testing was somewhat like Procedure B of ASTM C666 (frozen in air at -4 °F (-20 °C) then thawed in water at 68 °F (20 °C)).

Results indicated that the aging procedure did not adversely affect the frost resistance of high-strength concrete made with rapid-hardening portland cement, with or without fly ash or silica fume. The relative dynamic modulus remained above 90 percent for all specimens past 400 freeze-thaw cycles. (The slow hardening portland cement gave slightly poorer durability). The authors concluded that good frost resistance of high-strength concrete can be reached without air-entraining when the strength exceeds 11,600 psi (80 MPa) and the water-to-cementitious material ratio is lower than 0.30 to 0.32. The authors believed that the drying period prior to testing aided in these positive results [48].

FREEZE-THAW TESTS OF NON-AIR-ENTRAINED HIGH-STRENGTH CONCRETE

Several freeze-thaw tests have been completed on non-air-entrained high-strength concrete. Portions of these studies have been summarized in the appropriate sections above. Because of their direct relation to the study described in this report, some of the studies are summarized in this section with more detail.

Perenchio and Klieger [4] performed tests on air-entrained and non-air-entrained high-

strength concrete for the Portland Cement Association. Eighteen mixes were tested using three water-to-cement ratios and three different coarse aggregates. Type III portland cement was used at 620 to 998 lb/yd^3 (368 to 592 kg/m^3) for water-to-cement ratios of 0.30, 0.35 and 0.40. The concrete was designed for zero slump. Partially-crushed dolomitic gravel (2.22 percent absorption, 2.67 SSD specific gravity) and crushed trap rock (0.50 percent, 2.98) were used at 0.375-in (10-mm) nominal maximum size and crushed limestone (2.12 percent, 2.71) was used at 0.50-in (13-mm) nominal maximum size. The aggregates were soaked in water 30 minutes prior to mixing. The concrete specimens were moist-cured 28 days, air-dried (73 °F (23 °C) and 50 percent RH) for 14 days and then immersed in water three days prior to test. The 28-day compressive strengths ranged from 7,220 to 11,580 psi (50 to 80 MPa), increasing with decreasing water-to-cementitious material ratio. Two freeze-thaw cycles were completed per day (-10 °F to 55 °F (-23 °C to 13 °C) in water). All concrete specimens (air-entrained and non-air-entrained) exhibited excellent frost resistance, yielding durability factors greater than 97 at 300 cycles. No weight gain and only small length expansions were observed. Tests were continued to 500 cycles, and all durability factors remained above 81. The air contents of the hardened concrete, determined by linear traverse, were 3.0 to 6.5 percent for the air-entrained concrete and 3.1 to 5.1 percent for the non-air-entrained concrete. While the air-entrained concrete specimens had 3.7 to 11.1 voids per inch (1.5 to 4.4 voids per cm), the non-air-entrained concrete had 1.2 to 2.6 voids per inch (0.5 to 1.0 voids per cm), showing that the relatively high air content in the non-air-entrained concrete reflected the natural (entrapped) air voids, rather than the small bubbles from air-entrainment. Only four of the nine air-entrained mixes had spacing factors below the recommended 0.008 inch (0.20 mm). The non-air-entrained concrete

had spacing factors greater than 0.02 inch (0.51 mm) (0.022 to 0.041 inches (0.56 to 1.04 mm)), but exhibited excellent frost resistance. The authors attributed the good performance to greatly reduced freezable water content and increased tensile strength of the high-strength concrete.

Cohen, et al. [27] tested four mixes (two air-entrained and two non-air-entrained) for freeze-thaw resistance by ASTM C666 Procedure A. ASTM Type I portland cement and silica fume at 0 and 9 percent replacement by weight of cement were used. The total cementitious material content was approximately 660 lb/yd^3 (392 kg/m^3) with a water-to-cementitious material ratio of 0.35. High-range water-reducers were used in all mixes to obtain 6.5- to 8-in (165- to 203-mm) slumps. The coarse aggregate, a 0.5-in (13-mm) nominal maximum size crushed limestone, had proven frost resistance. Specimens were cured for 7, 14, 21 and 56 days in saturated lime-water at 73 °F (23 °C). Concrete strengths ranged from 9,570 to 11,240 psi (66 to 78 MPa). All air-entrained concrete specimens performed very well with relative dynamic moduli above 90 percent at 300 cycles. All non-air-entrained concrete with 9 percent silica fume performed poorly, dropping below 60 percent relative dynamic modulus well before reaching 300 cycles (between 150 and 225 cycles). The only non-air-entrained portland cement concrete mixes that passed the ASTM test (approximately 65 percent at 300 cycles) were cured for 21 and 56 days. Increasing the curing for non-air-entrained portland cement concrete improved the frost resistance, especially the increase from 7 to 21 days of curing. The spacing factors were very low for all concretes. Air-entrained concrete mixes (with and without silica fume) had spacing factors of 0.005 in (0.13 mm). The non-air-entrained concrete had spacing factors of 0.009 and

0.014 in (0.23 and 0.36 mm) for the silica fume and the portland cement concretes, respectively. The authors concluded that silica fume neither improved nor hindered the frost resistance of the concrete when it was properly air-entrained. For the non-air-entrained concrete, silica fume did not improve the inherent frost resistance of the concrete.

Burg and Ost [28] of the Portland Cement Association studied the freeze-thaw durability of non-air-entrained high-strength concrete by testing (ASTM C666 Procedure A) five concrete mixes with 28-day compressive strengths ranging from 11,400 to 17,250 psi (79 to 119 MPa). The concrete included a high cement content mix with no supplementary cementitious materials, concrete with silica fume added as a partial replacement of cement, and concrete incorporating both silica fume and fly ash. The total cementitious material contents were 900 to 1100 lb/yd^3 (534 to 653 kg/m^3), and ASTM Type I cement was used in all mixes. The water-to-cementitious material ratio ranged from 0.22 to 0.29. No intentional air-entrainment was used; air contents were all below 2 percent. The concrete was delivered by a ready-mix concrete supplier to the laboratory and, upon arrival, adjustments in high-range water-reducer content were made to attain 8- to 10-inch (203- to 254-mm) slumps. A 0.5-in (13-mm) nominal maximum size crushed dolomite aggregate was used. The concrete specimens were moist-cured (73 °F (23 °C) and 100 percent RH) for 28 days and then frozen until 102 days before testing.

The concrete mix containing 1100 lb/yd^3 (653 kg/m^3) total cementitious material, with 13.6 percent silica fume replacement of cement and a water-to-cementitious material ratio of 0.22, attained a 28-day compressive strength of 17,250 psi (119 MPa) and showed no

deterioration through 1800 cycles of freezing and thawing [28].

The concrete mix with 940 lb/yd^3 (558 MPa), 4.25 percent silica fume and 10.6 percent fly ash, with a water-to-cementitious material ratio of 0.29 and compressive strength of 12,840 psi (89 MPa), performed well, lasting over 300 cycles without failing [28].

The remaining three concrete mixes, although attaining high compressive strengths (11,400 to 15,500 psi (79 to 107 MPa)), showed significant deterioration between 75 and 300 cycles. The mix with 950 lb/yd^3 (564 kg/m^3) cement, having a water-to-cement ratio of 0.28 and attaining a 28-day strength of 11,400 psi (79 MPa), failed in less than 200 cycles. The concrete with 900 lb/yd^3 (534 kg/m^3) total cementitious material including 8.9 percent silica fume replacement of cement, having a water-to-cementitious material ratio of 0.29 and 28-day strength of 13,330 psi (92 MPa), failed at 75 cycles. Specimens from the concrete mix with 1100 lb/yd^3 (653 MPa) total cementitious material including 11.4 percent silica fume and 15.9 percent fly ash (replacement of cement), having a water-to-cementitious material ratio of 0.23 and 28-day strength of 15,520 psi (107 MPa), each failed suddenly between 229 and 361 cycles [28].

In addition to the five concrete mixes with 0.5-in (13-mm) nominal maximum size aggregates, a sixth concrete mix with 1-in (25-mm) nominal maximum size dolomite coarse aggregate was tested for freeze-thaw resistance. This concrete mix, with 743 lb/yd^3 (441 kg/m^3) total cementitious material content, 6 percent silica fume, 19.8 percent fly ash and 0.32 water-to-

cementitious material ratio, attained a 28-day compressive strength of 10,600 psi (73 MPa), but failed at 229 cycles of freezing and thawing [28].

Length change was measured in addition to the relative dynamic modulus. The three mixes that failed in less than 300 cycles showed large dilations (from 0.1 to 1.1 percent), while the two mixes that performed well showed small dilations. The relative dynamic modulus and length dilation failures appeared to correlate fairly well [28].

Water absorption characteristics of the concrete mixes were determined by placing 4x8-in (100x200-mm) cylinders in water and measuring weight gain over time. The weight gain measurements paralleled the rapid chloride permeability test results, and can be used as an indicator of concrete permeability. The concrete mix that withstood over 1800 cycles of freezing and thawing (i.e. the mix containing 1100 lb/yd^3 (653 kg/m^3) cementitious material with 13.6 percent silica fume) absorbed the least amount of water. The freeze-thaw performance of the other concrete, with the exception of the concrete specimens which failed suddenly during testing, correlated with absorption [28].

Tachibana, et al. [30] tested three non-air-entrained silica fume concrete mixes for freeze-thaw durability. ASTM Type I portland cement and silica fume (as a 10 percent replacement of cement) were used. High-range water-reducers were used to achieve water-to-cementitious material ratios of 0.22, 0.25, and 0.28 for the three concrete mixes. A crushed sandstone coarse aggregate (0.75-in (19-mm) nominal maximum size, 2.67 SSD-specific gravity)

was used. The specimens, with entrapped air contents of approximately 2 percent, were cured in water to 14 days. Compressive strengths greater than 14,500 psi (100 MPa) were achieved at 28 days. Freeze-thaw tests by ASTM Procedure A resulted in durability factors of 97 to 99 for the specimens, with little observed scaling of the concrete. The authors concluded that high-strength concrete without entrained air is highly durable to freeze-thaw exposure.

Pigeon, et al. [26] performed freeze-thaw tests according to ASTM C666 Procedure A on seventeen high-strength concrete mixes with and without air-entraining. Variables studied were cement type, aggregate type and length of curing. ASTM Type I and III cements were used, and silica fume was incorporated in some mixes as a 6 percent replacement of cement. High-range water-reducers were used to achieve water-to-cementitious material ratios of 0.30 and 0.26. The two aggregates used in the study, dolomitic limestone (0.70 percent absorption, 2.77 specific gravity) and granite (1.00 percent, 2.69), were dry at the time of mix. The concrete specimens were covered with plastic and air-cured, similar to field-curing, for 1, 3, 7 and 28 days. The reported 28-day moist-cured compressive strength was 10,800 to 12,900 psi (74 to 89 MPa) for the non-air-entrained and 8,700 to 10,000 psi (60 to 69 MPa) for the air-entrained concrete. All of the air-entrained and non-air-entrained concrete mixes with Type III cement (i.e. LS, LS w/SF, and GR w/SF) performed very well, with pulse velocities after testing (after 400 to 724 cycles) greater than before testing. The two non-air-entrained limestone concrete mixes with Type I cement and 6 percent silica fume were slightly damaged from freeze-thaw cycles (with all durability factors still greater than 87 after 300 cycles), indicating that cement type has an influence on the frost resistance of high-strength concrete.

Three conclusions were made by the authors. First, for Type III cement (with or without silica fume), air-entraining is not required for good frost resistance at a water-to-cementitious material ratio of 0.30, even after only one day of air curing. Second, at a water-to-cementitious material ratio of 0.30, silica fume does not significantly increase the frost resistance of concrete made with Type III cement (all performed well). Finally, the use of granite (instead of limestone) had no significant influence on freeze-thaw resistance, confirming that for Type III cement and 6 percent silica fume, air-entrainment is not required at a water-to-cementitious material content of 0.30 [26].

Hammer and Sellevold [31] investigated the freeze-thaw durability of four high-strength concrete mixes without air-entraining. A high-strength cement was used, and silica fume was used as 0, 5 and 10 percent replacement of cement to attain water-to-cementitious material ratios of 0.46, 0.37 and 0.28, respectively. High-range water-reducers were used in all concrete mixes. A 0.75-in (19-mm) nominal maximum size crushed gravel coarse aggregate was used in these three concrete mixes. Cube compressive strengths after 28 days in water were 11,140, 13,150 and 16,730 psi (77, 91 and 115 MPa), increasing with decreasing water-to-cementitious material ratio. The fourth concrete mix contained a light-weight aggregate, had a water-to-cementitious material ratio of 0.47 and attained a compressive strength of 12,200 psi (84 MPa). All specimens were air-cured for one month and then placed in seawater for one month prior to freeze-thaw testing similar to ASTM Procedure A.

Four specimens were tested from each mix, and the performance of each varied

considerably. One or more specimens from all concrete mixes suffered relatively severe damage. The authors believed the drying/resaturation treatment before freezing increased the amount of freezable water in the concrete [31].

The four specimens cast from the concrete without silica fume attained durability factors from 0 (severe damage of two specimens) to 100. Both concrete mixes with silica fume had durability factors between 60 and 100, indicating satisfactory performance. The light-weight aggregate concrete was severely damaged by 213 cycles. The authors pointed out the possibility that the light-weight aggregate concrete was less resistant to internal cracking because of the internal water reservoir in light-weight aggregate caused by water absorption in the fresh concrete. Almost no scaling was observed in any of the concrete specimens, even at relatively high levels of internal cracking. Air void analysis was performed in which hardened air contents were found to range from 1.0 to 6.3 in the non-air-entrained concrete, presumably due to the irregularity of natural air voids. Spacing factors ranged from 0.013 to 0.041 inch (0.34 to 1.03 mm) [31].

The authors suggested that the damage in the rapid freeze-thaw test may be due to the large difference between the thermal expansion coefficients of the aggregate and the paste, resulting in thermal fatigue during the numerous cycles. However, this explanation was not valid, according to Pigeon, et al. [26] who asserted that a critical air void spacing factor exists, and the concrete damage seen in Hammer and Sellevold's study was caused by freezing effects. Furthermore, with the thermal fatigue hypothesis one would expect that all of the specimens cast

from the same concrete batch would exhibit the same performance and there would not be the wide variation in performance that was seen in the results of this study [31].

Hooton [29] performed freeze-thaw tests on four non-air-entrained high-strength concrete mixes with 28-day compressive strengths in the range of 8,060 to 10,900 psi (56 to 75 MPa). ASTM Type V sulfate-resisting portland cement was used and silica fume was incorporated at 0, 10, 15 and 20 percent replacement of cement. The total cementitious material content was 676 lb/yd^3 (401 kg/m^3) with water-to-cementitious material ratios of 0.36 to 0.37. High-range water-reducers were used to achieve slumps of 1.5 to 3.5 in (38 to 89 mm). A 0.80-in (20-mm) nominal maximum size crushed limestone coarse aggregate (1.0 percent absorption) was used, and both coarse and fine aggregate were presoaked in water 24 hours prior to mixing. Six freeze-thaw specimens were cast from each mix and were cured for 14 days in lime-water before testing according to Procedure A of ASTM C666.

The control mix (with portland cement only) failed at 58 cycles, but the relative dynamic modulus of all silica fume mixes was greater than 90 percent after 300 cycles of freezing and thawing. The tests were extended to 600 cycles and then, because the durability factors all remained above 90 percent, half of the specimens continued testing while the other half of the concrete specimens were vacuum-saturated and immersed in water for 40 days before exposure to 300 more freeze-thaw cycles. The vacuum saturation had little adverse effect on the performance, since all durability factors remained above 90 percent for the silica fume concrete after 900 cycles of freezing and thawing [29].

The author attributed the excellent performance to self-desiccation obtained from a refined pore structure, combined with low permeability and an abundance of unreacted cementitious material, resulting in less-than-critical saturation levels. The silica fume concrete could become internally self-desiccated due to the combination of very low permeabilities and an abundance of very reactive but, as yet, unreacted material. Any penetrating water would be consumed immediately in hydration and make the concrete less permeable. The evidence supporting this theory included the finer pore size and the very low permeability of the silica fume mixes compared to the control mix [29].

Air void parameters determined by ASTM C457 have shown hardened air contents of 0.8 to 1.4 percent. Spacing factors were 0.027, 0.038, 0.020 and 0.028 in (0.69, 0.96, 0.50 and 0.70 mm) for the 0, 10, 15 and 20 percent silica fume concrete specimens, respectively. With the exception of the 10 percent silica fume mix, the observed internal microcracking increased with increased silica fume content. For this reason, 10 percent by mass replacement of portland cement by silica fume was deemed adequate with respect to resistance to freeze-thaw [29].

Whiting [37] looked at the durability of non-air-entrained and air-entrained high-strength concrete with nominal 28-day compressive strengths of 6,000, 8,000 and 10,000 psi (41, 55 and 69 MPa) and water-to-cementitious material ratios of approximately 0.47, 0.32 and 0.27, respectively. ASTM Type I portland cement was used in varying quantities from 588 to 1158 lb/yd^3 (349 to 687 kg/m^3), and a Class C fly ash was incorporated as a 10-18 percent replacement of cement. High-range water-reducers were used to obtain slumps of 2 to 3.5 in

(50 to 90 mm). Two separate gradations of a crushed, subangular dolomitic limestone coarse aggregate (1.6 percent absorption and 2.74 and 2.69 SSD specific gravity) were used in the concrete mixes and were soaked in water for 18 to 24 hours prior to mixing. Two curing methods were investigated: a 28-day moist-cure and a 7-day moist-cure followed by 21 days of air-drying and 3 days in lime-water prior to testing. Two freeze-thaw cycles (-10 °F to 55 °F (-23 °C to 13 °C)) were completed per day.

All air-entrained concrete specimens had relative dynamic moduli of 99 percent or greater after 300 cycles of freezing and thawing. The non-air-entrained concrete performed poorly with the exception of one mix. As the strength of the concrete increased, the number of cycles required to produce failure increased. The highest strength (10,000 psi (69 MPa)) non-air-entrained concrete with 15 percent fly ash, given a period of air-drying before testing, achieved a durability factor of 70 percent, showing satisfactory frost resistance. The authors suggest that the good performance of this concrete was a result of the increased concrete strength and the period of air-drying before testing. Air-drying would result in a reduction in the degree of saturation of the concrete prior to testing. During this period continued hydration would lead to a decrease in permeability of the concrete, making it more difficult for water to re-enter the pore system of these concrete specimens during the thawing phase of subsequent freeze-thaw cycles [37].

The results of these studies of the freeze-thaw durability of high-strength concrete provide the basis for explaining the findings of the current investigation in Chapter 4.

CHAPTER 3

DESCRIPTION OF TEST PROGRAM

INTRODUCTION

The freeze-thaw durability study was completed in two phases. Phase I included seventeen high-strength concrete mixes batched in the laboratory and concrete specimens taken from each of the two project girder mixes and a typical girder mix cast at a local precasting plant. Phase II involved preparing and testing replicates of ten of the Phase I mixes in the laboratory.

Variables studied included aggregate type, pozzolan type and content, and curing condition. In the laboratory mixes, five types of local aggregate were used. Fly ash and silica fume were incorporated individually and in combination. Combinations of these variables describe the 17 concrete mixes investigated. For example, using round gravel aggregate, a reference mix, a 20 percent fly ash mix, a 7.5 percent silica fume mix, and a 20 percent fly ash with 7.5 percent silica fume mix were produced. In terms of cementitious material composition, reference mixes, for example, were made using round gravel, partially-crushed gravel, granite, high-absorption limestone, and low-absorption limestone aggregate. The complete list of the 17 mix designs for the Phase I laboratory mixes is given in the next section. Heat-cured and 7-day moist-cured specimens were investigated in Phase I. In addition to these curing conditions, the

ASTM C666 method of curing (14-day moist-cure) was investigated in Phase II.

This chapter provides a description of the test program for the laboratory concrete mixes. The description of the test procedures and results for the girder concrete specimens are provided in Appendix E.

PREPARATION OF TEST SPECIMENS

Mix Composition

The concrete mix variables included the type of aggregate and the cementitious material composition. The five types of aggregate included round gravel (RG), partially-crushed gravel (PCG), granite (GR), high-absorption limestone (LS-H) and low-absorption limestone (LS-L). During the investigation it was determined that the aggregate referred to as "limestone" may, more accurately, be classified as dolomite. In this report, however, the aggregate is referred to as "limestone." The cementitious material comprised portland cement and two pozzolans, fly ash (FA) and silica fume (SF), added to the mixes individually and in combination. Fly ash and silica fume were added as 20 percent and 7.5 percent replacements, respectively, of the portland cement on an equal weight basis. The combinations given in Table 3.1 were selected to explore the effects of aggregate type, cementitious material composition and curing condition on the freeze-thaw durability of high-strength concrete.

Table 3.1 Mix Composition

Cementitious Material Composition	Aggregate				
	RG	PCG	GR	LS-H	LS-L
Ref	X	X	X	X	X
20% FA	X	X	X		
7.5% SF	X	X	X		X
20% FA & 7.5% SF	X	X	X	X	X

Several parameters in the concrete mix designs were held constant. The water-to-cementitious material ratio was 0.30. A total cementitious material content of 750 lb/yd^3 (445 kg/m^3) was used. The coarse-to-fine aggregate ratio was 1.5 for all of the concrete mixes.

The mix proportions, as batched, and the date of batching are given in Table A.1 of Appendix A for each of the concrete mixes. Table A.2 in Appendix A provides the mix proportions per unit volume of concrete.

Materials

The cementitious material comprised low-alkali ASTM C150 Type III portland cement, ASTM C618 Class C fly ash and slurried silica fume.

All aggregates used in the high-strength concrete mixes were obtained from local sources. The nominal maximum particle size was 0.5 in (13 mm). The gradation of the aggregates used

was "as received" from the sources.

The coarse aggregate properties for each of the mixes is given in Table 3.2. The table contains the saturated, surface-dry specific gravities and the absorption capacities of the coarse aggregates. Different absorption capacities are listed for the high-absorption limestone aggregate in Phase I because the aggregate was obtained from the same source at different times. Care was taken to insure that the aggregate came from the same ledge in the quarry. There are also different absorption capacities listed for the Phase II aggregates (repeat mixes) in comparison to the aggregates used in the corresponding Phase I mixes. Additional aggregate was required to batch these mixes. The aggregate for each of the Phase II mixes came from the same source as in Phase I.

The moisture contents of the fine and the coarse aggregate at the time of mixing in the laboratory are also given in Table 3.2. The coarse aggregate for the laboratory mixes was washed in the laboratory prior to measuring the aggregate properties. Using the measurements of the coarse aggregate moisture content and the absorption capacities of the coarse aggregates, the percent saturation was calculated and is also given in

Table 3.2. The level of saturation of the coarse aggregate was calculated as:

$$\text{Saturation (\%)} = (\text{moisture content})/(\text{absorption}) * 100 \qquad \text{(Eq. 3-1)}$$

Table 3.2: Aggregate Properties

Mix	SSD Coarse Aggregate Specific Gravity	Coarse Aggregate Absorption (%)	Coarse Aggregate Moisture Content (%)	Saturation of Coarse Aggregate (%)	Fine Aggregate Moisture Content (%)
PHASE I MIXES					
RG Ref	2.65	1.11	1.47	132	2.77
RG w/FA	2.65	1.11	1.50	135	1.78
RG w/SF	2.65	1.11	1.54	139	1.38
RG w/FA&SF	2.65	1.11	1.45	131	1.45
PCG Ref	2.74	1.39	2.57	185	2.76
PCG w/FA	2.74	1.39	2.67	192	2.25
PCG w/SF	2.74	1.39	2.11	152	3.11
PCG w/FA&SF	2.74	1.39	2.22	160	2.65
GR Ref	2.68	1.00	1.00	100	3.77
GR w/FA	2.68	1.00	1.00	100	3.42
GR w/SF	2.68	1.00	0.70	70	2.99
GR w/FA&SF	2.68	1.00	0.98	98	3.40
LS-H Ref	2.77	2.05	2.48	121	3.83
LS-H w/FA&SF	2.74	2.97	1.85	62	2.13
LS-L Ref	2.75	1.50	2.70	180	4.10
LS-L w/SF	2.75	1.50	3.24	216	2.37
LS-L w/FA&SF	2.75	1.50	2.54	169	2.17
PHASE II MIXES					
(RG Ref)R	2.66	1.44	1.22	85	7.18
(RG w/SF)R	2.66	1.44	1.18	82	2.36
(RG w/SF)AE	2.66	1.44	0.74	51	1.62
(LS-H Ref)R	2.71	2.08	1.98	95	2.12
(LS-H w/SF)R	2.71	2.08	1.53	74	2.21
(LS-H w/FA&SF)R	2.71	2.08	1.48	71	10.83
(LS-L Ref)R	2.69	1.67	1.88	113	1.25

The absorption capacity of the coarse aggregate was based on only the aggregate particles retained on the no. 4 sieve in accordance with ASTM procedures. These particles (retained on the no. 4 sieve) have a lower surface area per unit volume than the smaller particles (those passing through the no. 4 sieve and not used in the measurement). The moisture content was measured from the washed aggregate "as received" from the sources (i.e. fine particles and particles retained on the no. 4 sieve). The moisture content was measured this way because the aggregate was washed and then used in the concrete mix "as received" from the sources. The moisture content of the aggregate before mixing was needed in order to proportion the mix water so that a 0.30 water-to-cementitious material ratio was attained for each concrete mix. Inclusion of the fine particles in the moisture content measurement provided more surface area per unit volume, and more water could be adsorbed onto the surface of these particles. Therefore, calculating the percent saturation by comparing the actual moisture content to the absorption capacity results in a somewhat higher number than the actual saturation. This explains some of the seemingly high coarse aggregate saturations reported in Table 3.2.

The natural coarse sand used in all mixes had a fineness modulus of 2.80. The absorption capacity of the fine aggregate measured 0.50 percent, and the saturated, surface-dry specific gravity was 2.63.

Two admixtures were used in the high-strength concrete mixes. A modified naphthalene sulfonate high-range water-reducer was used in varying quantities (8.5 to 15 oz/cwt (13 to 23 ml/kg) of cement) to attain a target slump of 4 to 6 in (100 to 150 mm).

No air-entraining agents were used in any of the Phase I mixes, in conformance with typical precast girder production. Two Phase I mixes that exhibited poor freeze-thaw durability were remixed in Phase II with the addition of an air-entraining agent composed of an aqueous solution of completely neutralized vinsol resin to assess its affect on improving the concrete freeze-thaw durability.

Mix Procedure

As previously noted, the coarse aggregate was washed and the fine and coarse aggregate moisture contents were measured prior to mixing. The moisture content minus the absorption capacity of the aggregate is the amount of free water present in the aggregate. The free water in the aggregates and the water content of the silica fume slurry and high-range water-reducer were considered in proportioning the mix water so that a water-to-cementitious material ratio of 0.30 was attained for each concrete mix. The moisture contents of the aggregates are given in Table 3.2, and the mix proportions, as batched, are given in Table A.1 of Appendix A.

The mixing and curing was conducted in the Structural Laboratory of the University of Minnesota. A 10 ft^3 (0.3 m^3) fixed-drum mixer powered by an electric motor was used to mix all of the laboratory concrete batches. For each mix investigated, all specimens were cast from a single batch. The freeze-thaw beams were cast in heavy-gauge reusable steel molds and the cylindrical specimens (for compression strength tests) were cast in plastic molds. One day prior to mixing, the insides of all molds were lightly coated with a non-oil-based form release agent.

Following evaluation of a few trial batches, the standard laboratory mixing and batching procedures recommended by ASTM C192 were modified slightly to facilitate an easy and uniform production technique. The mixing procedure followed these steps:

1. Spray interior of mixer with water. Empty the mixer and drain it.
2. Load the mixer with all coarse aggregate and half of the mixing water. Mix for 30 seconds.
3. Stop the mixer and allow the coarse aggregate to soak in the water for 10 minutes.
4. Turn on the mixer and add sand, cementitious material, remaining water and high-range water-reducer. Mix for 5 minutes.
5. Stop the mixer for 1 minute. Evaluate the workability. Add additional high-range water-reducer (up to a total of 15 oz/cwt (23 ml/kg) of cement) if needed.
6. Turn on the mixer for 3 more minutes.
7. Do a final slump test and discharge the concrete into a clean, moist, metal bin.
8. Fill molds and manually rod in accordance with the provisions of ASTM C192.

For each of the mixes, measurements of the slump were taken according to ASTM C143, and the air content was measured according to the volumetric method of ASTM C173. The results of these measurements are given in Table 3.3.

Table 3.3: Slumps and Air Contents

Mix	Slump in (mm)	Air Content %
PHASE I MIXES		
RG Ref	5.0 (127)	2.0
RG w/FA	5.5 (140)	2.5
RG w/SF	2.75 (70)**	1.5
RG w/FA&SF	5.5 (140)	1.5
PCG Ref	0.5 (13)*	1.5
PCG w/FA	3.5 (89)**	2.0
PCG w/SF	3.5 (89)**	1.5
PCG w/FA&SF	3.0 (76)**	2.0
GR Ref	1.75 (44)*	1.5
GR w/FA	4.0 (102)	1.5
GR w/SF	NR	1.5
GR w/FA&SF	4.0 (102)	1.0
LS-H Ref	6.0 (152)	1.5
LS-H w/FA&SF	6.0 (152)	1.5
LS-L Ref	1.5 (38)*	1.5
LS-L w/SF	4.5 (114)	2.0
LS-L w/FA&SF	NR	1.0
PHASE II MIXES		
(RG Ref)R	1.0 (25)	2.0
(RG w/SF)R	1.0 (25)	3.5
(RG w/SF)AE	5.5 (140)	5.0
(LS-H Ref)R	4.0 (102)	2.0
(LS-H w/SF)R	2.25 (57)	2.0
(LS-H w/FA&SF)R	4.0 (102)	1.5
(LS-L Ref)R	3.75 (95)	2.0

NR Indicates measurement not recorded.

* It was not possible to achieve the desired slump range of 4-6 in (100-150 mm) without exceeding the maximum high-range water-reducer dosage of 15 oz/cwt (23 ml/kg) of cement.

** For these mixes, adequate workability was achieved without meeting target slump range of 4-6 in (100-150 mm).

Description of Test Specimens

The test specimens for the freeze-thaw durability study were 3 x 4 x 16 in (76 x 102 x 406 mm) concrete beams. Quarter-inch (6-mm) diameter and approximately 0.816-in (21-mm) long gage studs were embedded in the center of each end of each concrete beam. Figure 3.1 shows the placement of the gage studs in the steel molds prior to casting a concrete beam for freeze-thaw testing, and a single gage stud is shown in Figure 3.2. These gage studs allowed for the accurate measurement of the length change of the specimens during the period of aging and during freeze-thaw testing.

HANDLING OF THE TEST SPECIMENS

Curing

An exception to the ASTM C666 standard test procedure was made in order to investigate the effect of curing on the freeze-thaw durability. The standard procedure requires freeze-thaw concrete specimens to be cast and continuously moist-cured for a period of 14 days prior to placement in the freeze-thaw testing machine. To investigate curing effects, all Phase I concrete beam specimens were either moist-cured for 7 days or heat-cured to simulate the precasting process. After the prescribed curing, the specimens were stored in a relatively constant temperature and humidity environment for a period of time. This procedure was intended to

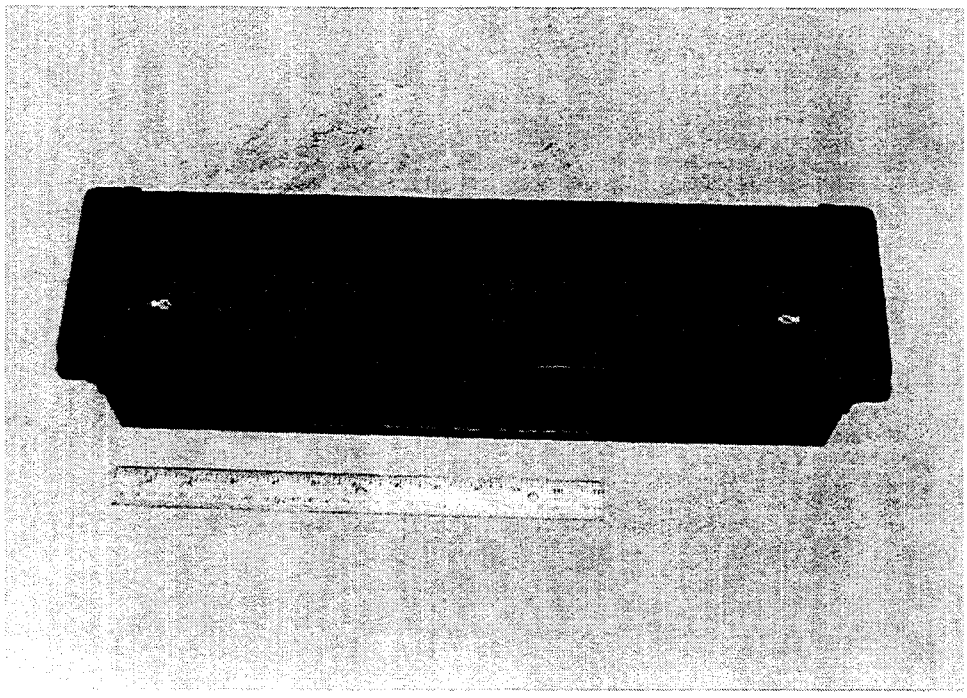

Figure 3.1 Steel mold for casting freeze-thaw beam

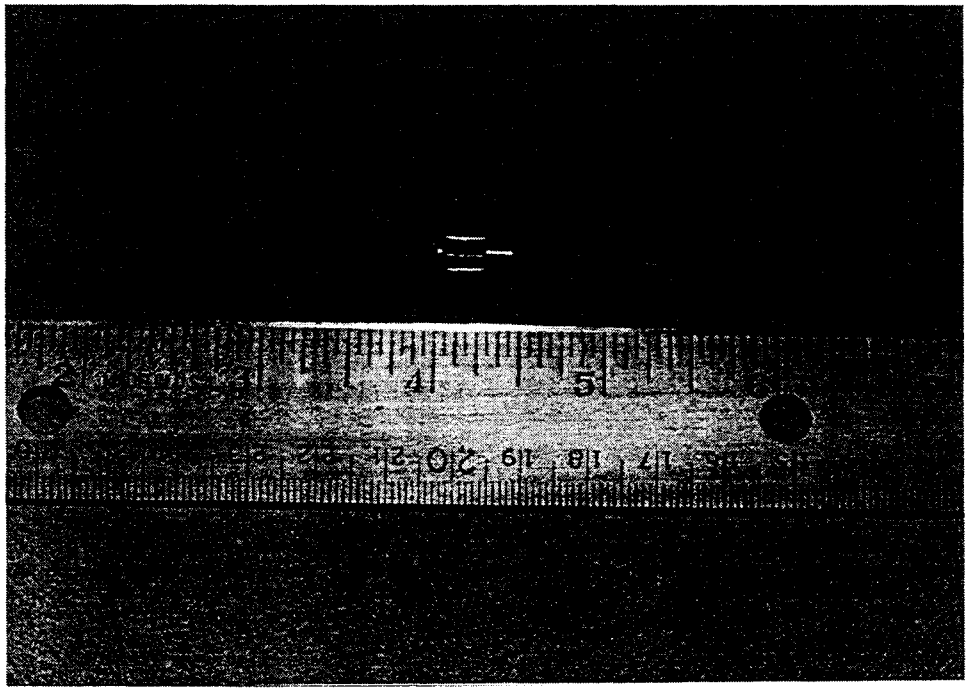

Figure 3.2 Gage stud

simulate casting and aging of cast-in-place and precast/prestressed members prior to exposure to freeze-thaw conditions. This procedural modification for testing the durability of high-strength concrete is supported by many experts. For example, Philleo recommended altering the age-at-test and specimen conditioning to test the frost resistance of specimens to more typical exposures. Stating that the ASTM C666 freeze-thaw test is an extremely severe test because of the young age of the concrete, the lack of drying period, and the rapid cooling cycle, Philleo argued that high-strength concrete without air entrainment that may ultimately become durable cannot be expected to do well in the test [11].

Four concrete beams were cast from each Phase I mix to investigate the effects of moist- versus heat-cured concrete performance. In all cases two concrete specimens were treated identically to provide a direct comparison in the results. Thus, from the four beams cast from each mix, two of the specimens were moist-cured in saturated lime-water for 7 days and two were heat-cured. Following the freeze-thaw tests, slices were obtained from the selected concrete specimens to investigate the air void system and to observe the failure mechanisms in each of the tested beams.

Three concrete beams were cast for each curing condition from each Phase II mix. The three specimens were treated identically (in curing and aging condition) up until the time the specimens were placed in the freeze-thaw testing machine. After removal from the constant temperature water bath, two of the specimens were placed in the freeze-thaw machine and tested. The third specimen was sliced and a linear traverse study was conducted to provide information

on the air void characteristics of the concrete prior to freeze-thaw exposure. The curing conditions studied in Phase II included a 7-day and a 14-day moist-cure in saturated lime-water and a heat-cure. The 14-day moist-cured specimens were cast to compare the ASTM C666 prescribed method of cure to the curing conditions used in this study.

A 386-gallon (1460-liter) curing tank equipped with a thermostatically controlled electric heater was used for moist-curing the concrete specimens. The specimens to be moist-cured were placed into the 73 °F (23 °C) saturated lime-water bath immediately after casting. To avoid damage to the young specimens, molds were stripped after 48 hours (instead of 24+/- 8 hours, as specified by ASTM C192). The specimens were immediately returned to the saturated lime-water bath where they remained for a total of seven days for the "moist-cured" specimens and 14 days for the "ASTM-cured" specimens.

To simulate the accelerated heat-curing process typical of precast/prestressed concrete manufacturers, an electronically-controlled environmental chamber was used. The temperature in the chamber was varied according to the following procedure: 3 hours at room temperature (preset period after casting), temperature increased to 150 °F (65 °C) over the next 2.5 hours, temperature held constant for 12 hours, and specimens returned to room temperature over 2 hours. To prevent loss of moisture from the fresh concrete, the surface of each heat-cured specimen was covered immediately after casting with a piece of plastic wrap held in place by a rubber band. The heat-cured specimen molds were stripped after 24 hours.

Period of Aging

Following the specified curing period, the length and weight of each specimen was measured. The specimen was then placed in an environment of relatively constant temperature and humidity (73 °F (23 °C) and 50 percent relative humidity).

Phase I mixes were aged 189 days (approximately six months) to simulate the aging of precast/prestressed members prior to exposure to freeze-thaw conditions. To accelerate the repeated tests, Phase II concrete specimens were aged only 28 days.

Immersion in Constant Temperature Water Bath

Following the period of aging, the concrete beam specimens were taken from the environment of relatively constant temperature and humidity and placed in a constant temperature water bath at 40 °F (4.5 °C) for 21 days prior to placement in the freeze-thaw testing machine. The three-week period of immersion was intended to enable at least partial saturation of the concrete beam specimens prior to freezing and thawing. This was considered to be a severe condition because bridge girders are not typically maintained in a saturated moisture condition.

Period of Constant Freeze

Following the 21-day immersion in the constant temperature water bath, the first set of Phase I concrete beam specimens (and some beams from subsequent Phase I mixes) were placed in a chest freezer and kept at an approximately constant temperature (0 °F (-18 °C)) until calibration of the new freeze-thaw testing machine was completed. This was done in accordance with ASTM C666, which specifies storage of the concrete specimens in a frozen condition if the sequence of freezing and thawing is interrupted. The length of time the specimens were kept frozen varied from 0 to 41 days and is given in Table 4.7 along with the freeze-thaw test results. Three Phase II concrete mixes were used to investigate the validity of this procedure by comparing the freeze-thaw test results of specimens placed directly in the freeze-thaw testing machine versus specimens that repeated the time frozen prior to placement in the freeze-thaw testing machine.

ASTM Curing Procedure

The handling procedure described above was used to investigate the effect of curing on the freeze-thaw durability of high-strength concrete. As mentioned above, the ASTM C666 standard test procedure requires freeze-thaw specimens to be cast and continuously moist-cured for a period of 14 days prior to placement in the freeze-thaw testing machine. Two of the beam specimens from each of the Phase II concrete mixes were cast and cured according to the standard ASTM procedure. These "ASTM-cured" beam specimens were cast, moist-cured for

14-days in the 73 °F (23 °C) lime-water tank, and then placed in the constant temperature water bath at 40 °F (4.5 °C) for approximately 2 hours before placement in the freeze-thaw testing machine. The constant temperature water bath lowered the temperature of the concrete beam specimens to the temperature at which freeze-thaw test measurements were taken. Thus, the initial length measurement was taken when the concrete beam specimens were at a temperature of approximately 40 °F (4.5 °C).

FREEZE-THAW TESTING MACHINE

A freeze-thaw testing machine was obtained from Scientemp Company of Adrian, Michigan and installed in the Structures Laboratory of the University of Minnesota in December of 1993. Figures 3.3 (a) and (b) show the freeze-thaw testing machine as well as the constant temperature water bath and the chest freezer in the Structures Laboratory.

The freeze-thaw testing machine was set up to operate ASTM C666 Procedure B (Rapid Freezing in Air and Thawing in Water). The machine was programmed to complete eight freeze-thaw cycles per day. One freeze-thaw cycle consisted of lowering the temperature of the specimens from 40 °F to 0 °F (4.4 °C to -17.8 °C) in 111 minutes and raising it from 0 °F to 40 °F (-17.8 °C to 4.4 °C) in 66 minutes. Thus, one freeze-thaw cycle took 177 minutes, approximately 3 hours. Figure 3.4 shows the freeze-thaw test profile followed in this freeze-thaw study (obtained from the Michigan Department of Transportation (DOT)). As the profile shows, the chamber is empty (no water) during the freeze mode (freezing in air) and full of

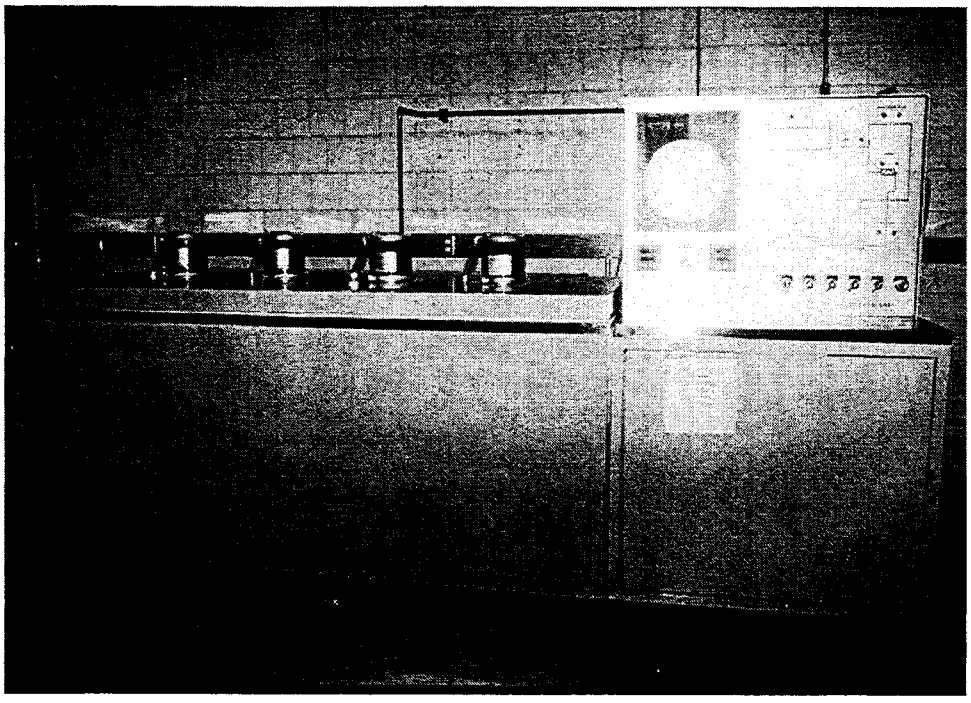

(a) Freeze-thaw testing machine

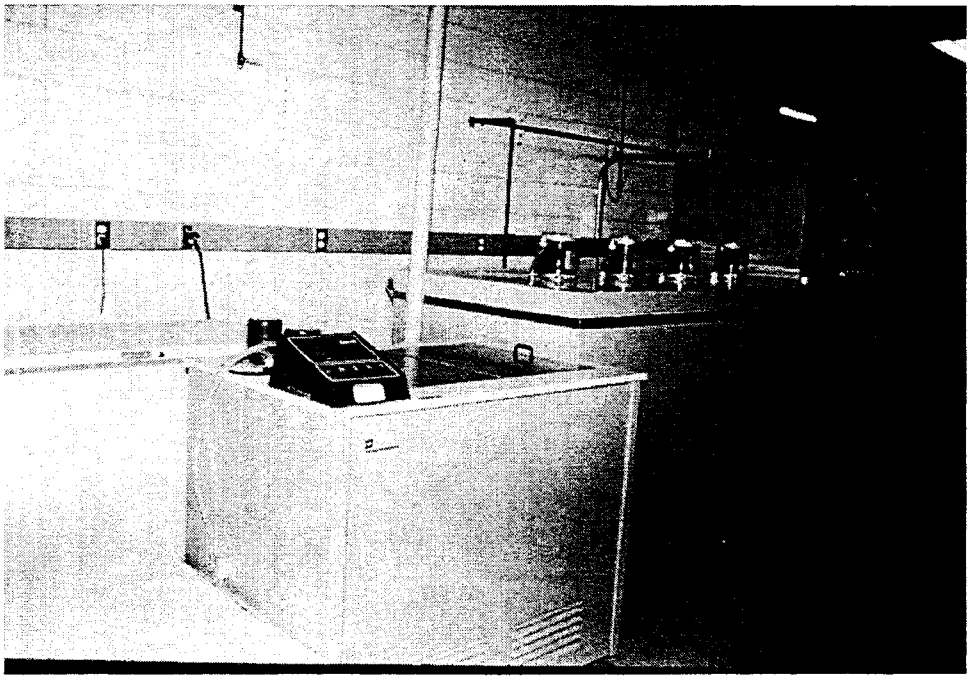

(b) Chest freezer (left), constant temperature water bath (middle), and freeze-thaw testing machine (right)

Figure 3.3 Freeze-thaw testing machine

water during the thaw mode. During the last nine minutes of the thaw mode the drain valve on the freeze-thaw chamber was open to allow the water to drain out prior to freezing again; it takes approximately five minutes for all of the water to drain out of the chamber. The difference between the University of Minnesota test profile and the Scientemp test profile (used by the Minnesota DOT (shown in Figure 3.5)) is the length of time in which the beam specimens are immersed in water in the thaw mode of the cycle. The University of Minnesota test profile allows the beam specimens to be immersed in water for as long as possible during the thaw cycle, while the Scientemp test profile calls for the draining of the water from the freeze-thaw testing machine earlier and results in more time for the beam specimens to dry prior to freezing again.

The freeze-thaw testing machine chamber during a freeze-thaw cycle is shown in Figure 3.6. During the freeze mode (Figure 3.6 (a)) the chamber is empty (freezing in air), and during the thaw mode (Figure 3.6 (b)) the chamber is full (thaw in water). The approximately 3.5 ft x 7.5 ft (1 m x 2.3 m) chamber of the freeze-thaw testing machine contained four steel racks that supported the concrete test beams in a vertical position, as can be seen in Figures 3.6 (a) and (b). Each steel rack, equally spaced, held 20 concrete beam specimens, so the freeze-thaw testing machine held 80 concrete beams for simultaneous testing. Three of the concrete beams had embedded thermocouples to measure the temperature of the center of the concrete specimens during each cycle. One of these three concrete beams served as the control beam; its measured temperature was used by the cycle controller to maintain the temperature of the center of the specimen within the programmed temperature profile. The control beam remained in the same

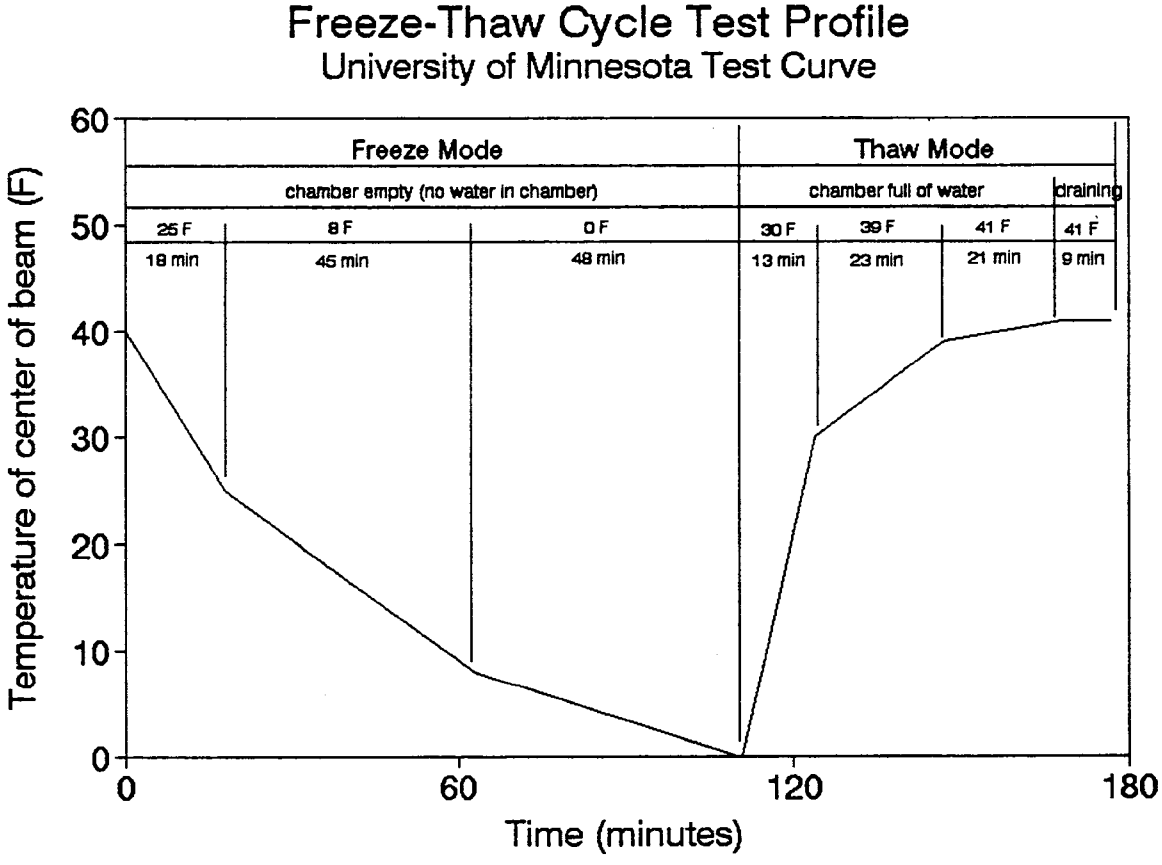

Figure 3.4 University of Minnesota freeze-thaw test profile

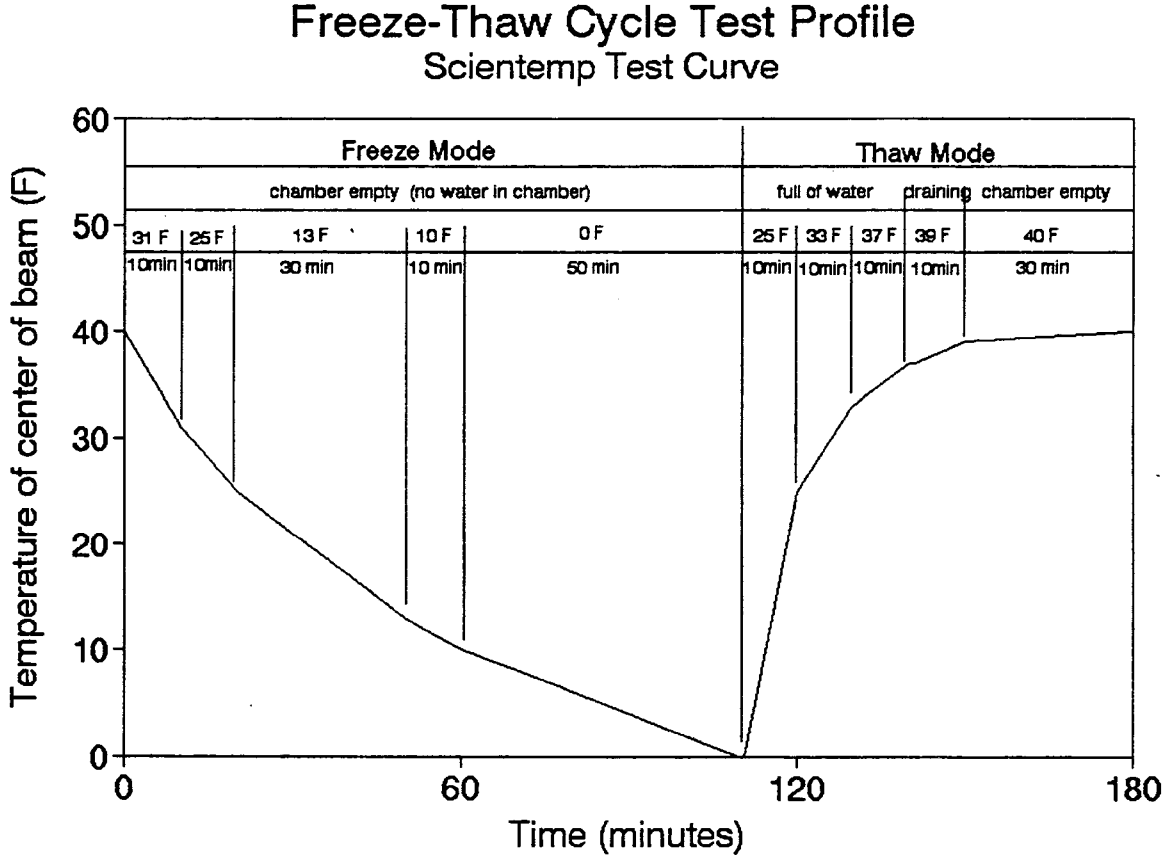

Figure 3.5 Scientemp freeze-thaw test profile

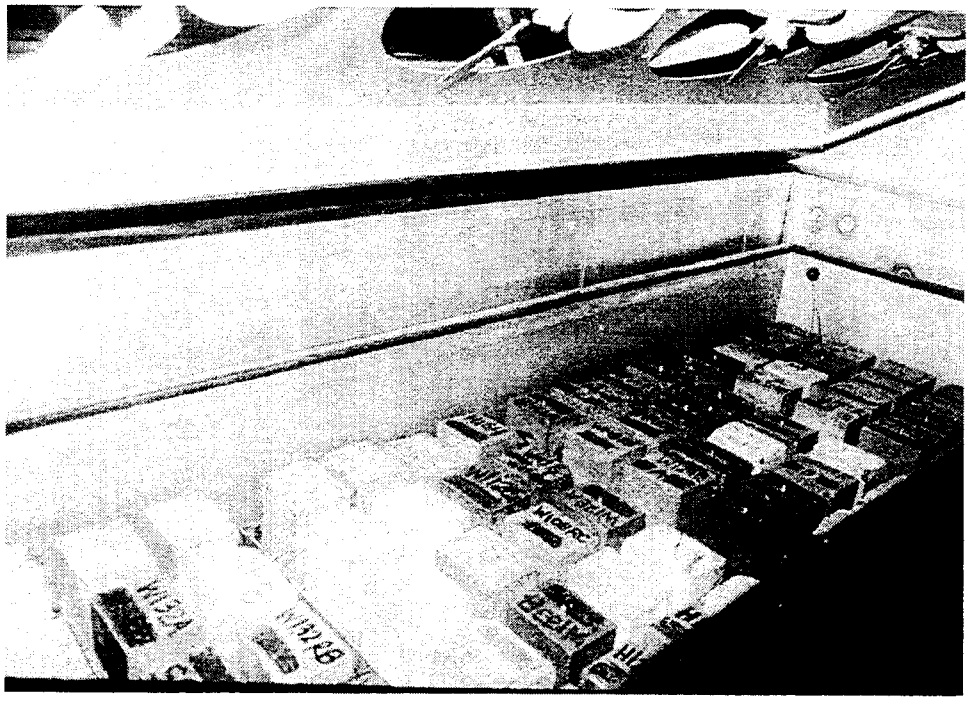

(a) Freezing in air

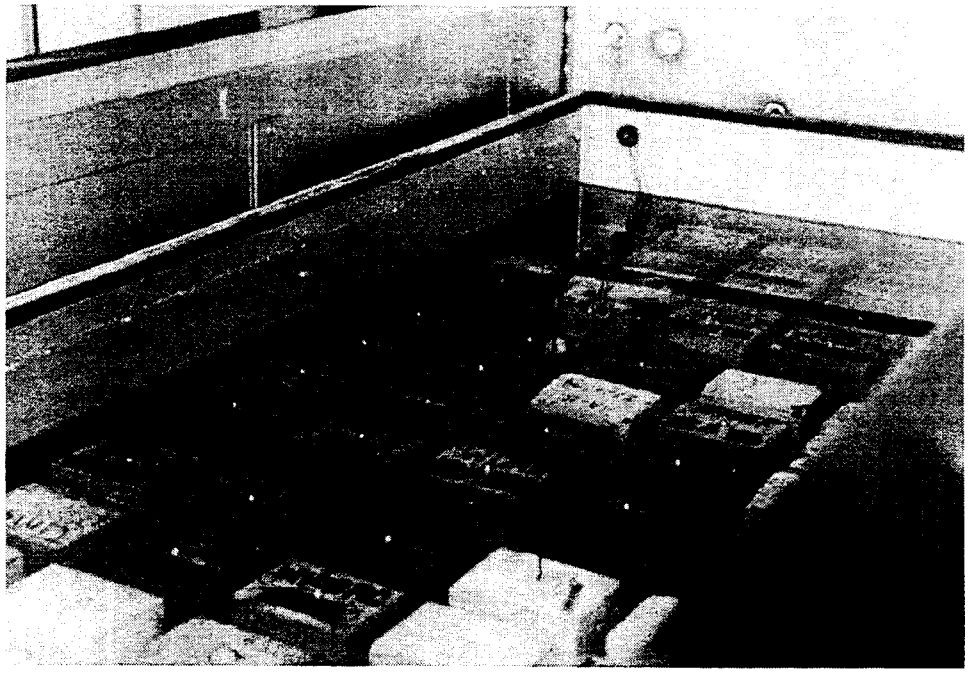

(b) Thawing in water

Figure 3.6 Freeze-thaw testing machine chamber

location in the freeze-thaw testing machine for the entire duration of testing. The fundamental transverse frequency of this control beam was tested periodically, and no deterioration was measured or observed during the entire duration of testing. The remaining two thermocouple-embedded concrete beams were rotated to different locations of the freeze-thaw testing machine during testing to monitor the temperature variation within the freeze-thaw testing machine. All locations within the freeze-thaw test machine were maintained within +/- 3 °F (+/- 1.7 °C) of the programmed temperature profile.

The freeze-thaw testing machine operated automatically by way of a Watlow Series 942 controller (which controlled the timing functions), and an Allen Bradley SLC 500 programmable controller (which provided the input/output for the equipment starting and status indication). The thermocouple cast in the center of the control beam served as the temperature control signal. The thermocouple was attached to the input of the Watlow Series 942 temperature controller. The controller sent an output to the temperature chart to record the control specimen temperature and to the refrigeration system to keep the center of the control specimen following the rate of change of cooling as input in the time-based test profile (Figure 3.4), as described above. The temperature of the concrete specimens in the thaw cycle was controlled by two parameters: time and the thaw water temperature. The thaw time followed the time-based test profile, as entered in the Watlow Series 942 cycle controller. The temperature of the thaw water was critical in maintaining the specimens within the prescribed time-temperature profile. Before freeze-thaw testing was begun, the temperature of the thaw water was optimized to achieve the desired results. The thaw water circulated in the chamber, as called for by the controller, to follow the

thaw rate programmed into the Watlow Series 942 cycle controller.

The concrete test beam specimens were placed randomly in the steel rack spaces and were rotated following removal and deterioration measurements. This procedure allowed each beam specimen to be subjected to the random temperature variations (+/-3 °F (1.7 °C)) throughout the freeze-thaw testing machine. In addition, the beams were turned end-for-end upon returning to the freeze-thaw testing machine for uniform deterioration of the beam (the beam bottoms tend to remain moist longer than the beam tops as water drains from the chamber at the conclusion of the thaw mode of the freeze-thaw cycle). Because the freeze-thaw testing machine must operate at full capacity for uniformity of freezing and thawing conditions, failed test beam specimens were replaced with "dummy" concrete beams (i.e. concrete beams cast for the purpose of filling the empty spaces in the chamber, not to be tested for freeze-thaw durability).

DESCRIPTION OF EXPERIMENTAL MEASUREMENTS

Measurements were taken at intervals conforming to the requirements of ASTM C666 to monitor specimen deterioration caused by the freeze-thaw cycles. Measurements included weight, length and fundamental transverse frequency. The concrete beam specimens were removed from the freeze-thaw testing machine when they were in the thawed condition and at a temperature of approximately 38 °F (3.3 °C). The beams were then patted dry with a cotton towel to remove surface moisture, and the measurements were taken.

FREEZE-THAW TESTS

Length

Length measurements were taken according to ASTM C490. The length comparator used in the study, shown in Figure 3.7, was designed and built by the Minnesota Department of Transportation. The length comparator for determining length changes had a dial micrometer, shown in Figure 3.8, graduated to read 0.0001-in (0.0025-mm) units, with a 0.5-in (13-mm) range to allow for small variations in the actual length of the various beam specimens. The length comparator provided a means for checking the concrete beam specimen length relative to the length of a reference bar (Figure 3.7). The reference bar had an overall length of 16.0000 in (406.4000 mm). A positioning mark on the invar reference bar ensured that the reference bar was positioned the same for each reading. Each concrete beam specimen was also marked (with an arrow) and placed in the same position each time a length comparator reading was taken (Figure 3.9).

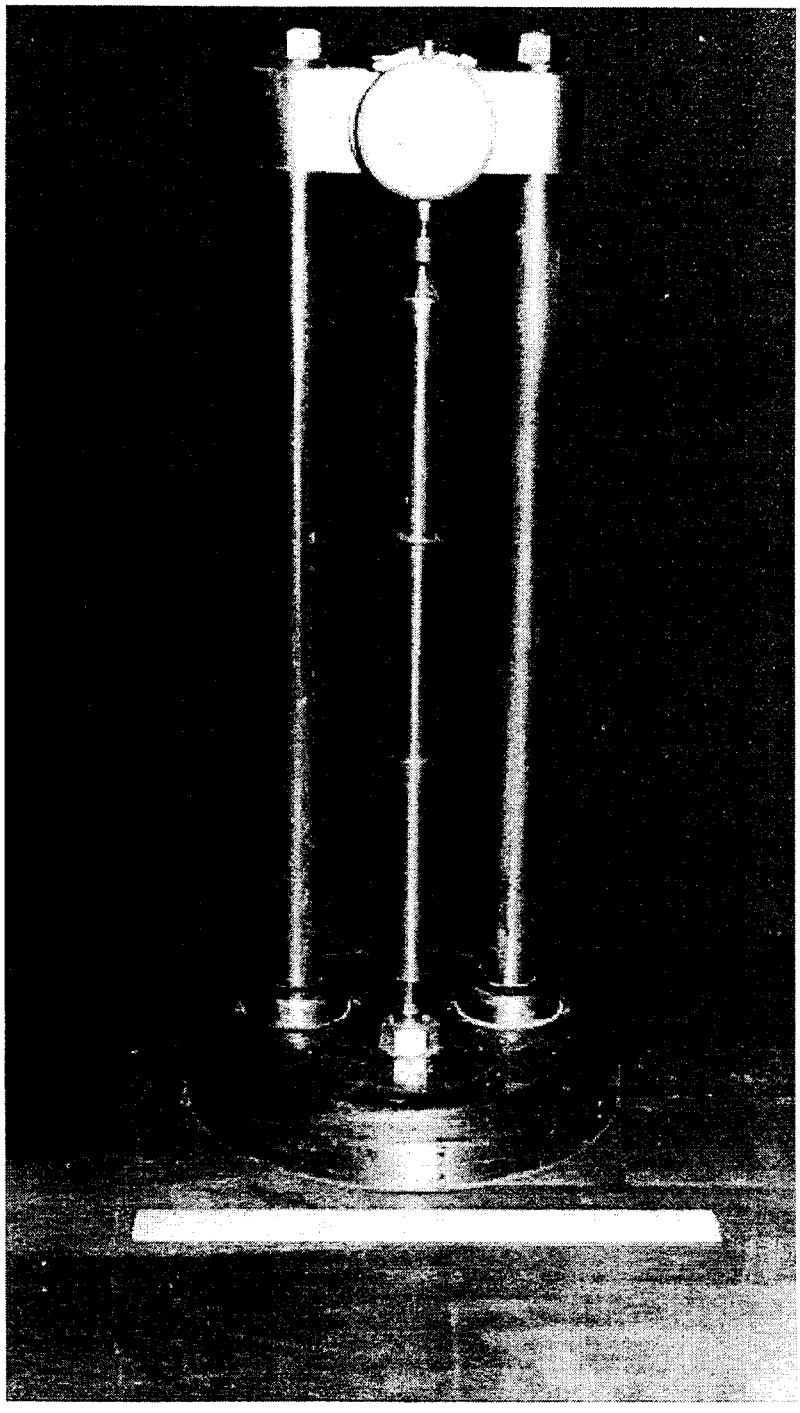

Figure 3.7 Length comparator: reference bar measurement

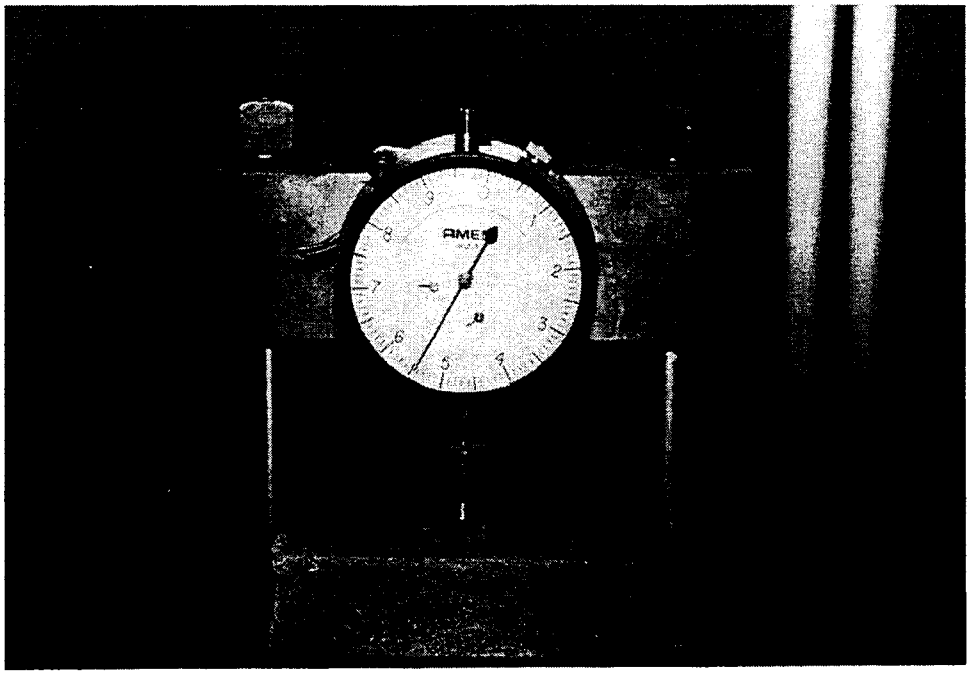

Figure 3.8 Dial micrometer on length comparator

Figure 3.9 Length comparator: freeze-thaw test beam measurement

The length change was calculated as follows:

$$\text{Length Change (\%)} = [(l_c - l_o) / L_g] \times 100 \qquad \text{(Eq. 3-2)}$$

l_o = initial length (0 cycles)
l_c = length at time of test (c cycles)
L_g = initial gage length of beam
= initial beam length minus twice the length of a gage stud

Length change is considered by many to be a highly reliable indicator of internal cracking. Although dilation is possible without microcracking, microcracking generally accompanies dilation.

Weight

An Ohaus Model IP12KS top loading balance with a capacity of 12,000 grams (26.5 lb), readable to the nearest 0.1 gram (2.2×10^{-4} lb), was used to measure the specimen weight, as shown in Figure 3.10.

Concrete beam specimen weight was measured to the nearest 0.1 gram (2.2×10^{-4}), and weight change was calculated as follows:

$$\text{Weight Change (\%)} = [(W_c - W_o) / W_o] \times 100 \qquad \text{(Eq. 3-3)}$$

W_o = initial weight (0 cycles)
W_c = weight at time of test (c cycles)

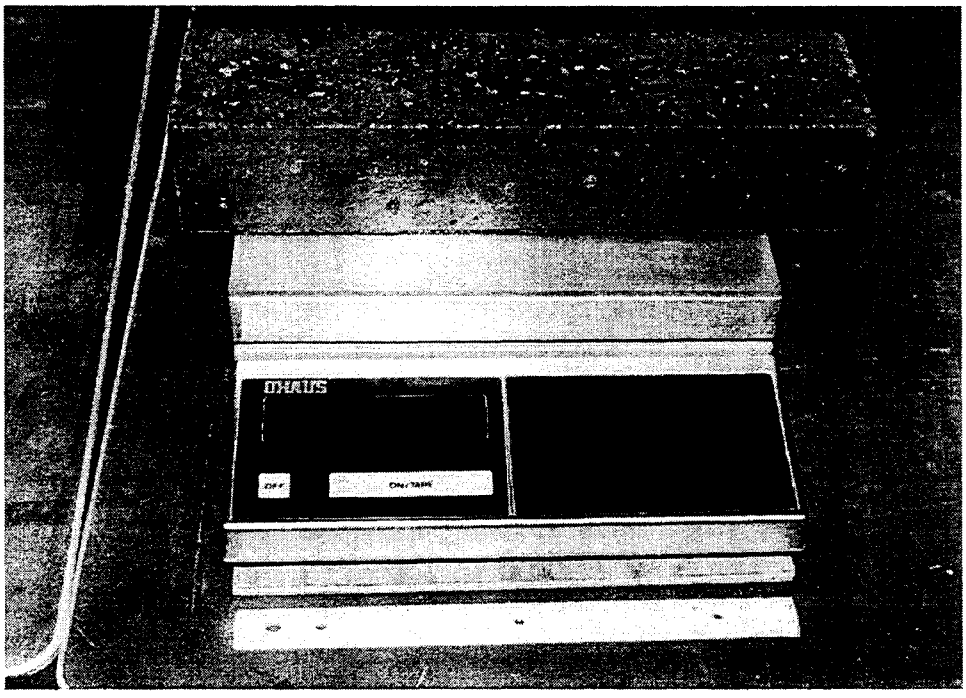

Figure 3.10 Weight measurement

Weight gain is an indicator of concrete microcracking since water is drawn into the microcracks by capillarity during the thaw phase of the freeze-thaw cycle [14]. ASTM C666 does not use weight change as a failure criterion, but observation of weight change was beneficial during freeze-thaw testing. Weight loss was an indication of spalling of concrete off the beam specimen. Weight gain, on the other hand, resulted from the ingress of water in the concrete beam specimen, and served as an indicator of impending failure of the concrete beam specimen.

Dynamic Modulus of Elasticity

The fundamental transverse frequency of the concrete beam was measured in accordance with ASTM C215 using the Impact Resonance Method. Figure 3.11 shows the test setup for the fundamental transverse frequency measurement. The procedure to measure the fundamental transverse frequency involved the following, as depicted in Figure 3.12: the specimen was supported on piano wires to allow free vibration of the concrete beam in the transverse direction, the specimen was struck with a small instrumented impactor and the specimen response was measured using a lightweight piezoelectric accelerometer that was held in place by a small rubber band. A frequency analyzer (shown in Figure 3.11) received the output from both the impactor and the accelerometer. The resonant frequency of the specimen was determined by analyzing the ratio of the impact and accelerometer signals over the response frequency spectrum to determine the peak ratio, which occurs at the resonant frequency.

The fundamental transverse frequency can be used to calculate the Dynamic Modulus of Elasticity.

$$\text{Dynamic } E = C * p * n^2 \qquad \text{(Eq. 3-4)}$$

where p = mass of specimen
n = fundamental transverse frequency of beam
$C = 0.9464\ (L^3 * T)/(b*t^3)$
L = length of specimen
t,b = dimensions of cross section of prism, t in direction of vibration
T = correction factor which depends on the ratio of the radius of gyration, K, to the length of the specimen, L, and on Poisson's ratio, (values of T are tabulated in ASTM C215)

Relative Dynamic Modulus

Calculation of the Relative Dynamic Modulus of Elasticity of each specimen may then be made using the fundamental transverse frequency measurement.

The Relative Dynamic Modulus of Elasticity may be calculated as:

$$RDM\ (\%) = (E_c / E_o) * 100 \qquad \text{(Eq. 3-5)}$$

E_c = Dynamic Modulus of Elasticity at cycle c
E_o = Initial Dynamic Modulus of Elasticity (0 cycles)

According to ASTM C666, when the test is to be used to make comparisons between the Relative Dynamic Moduli of different concrete specimens, it is adequate to assume that the weight and the dimensions of the specimens remain constant throughout the test. Therefore, the

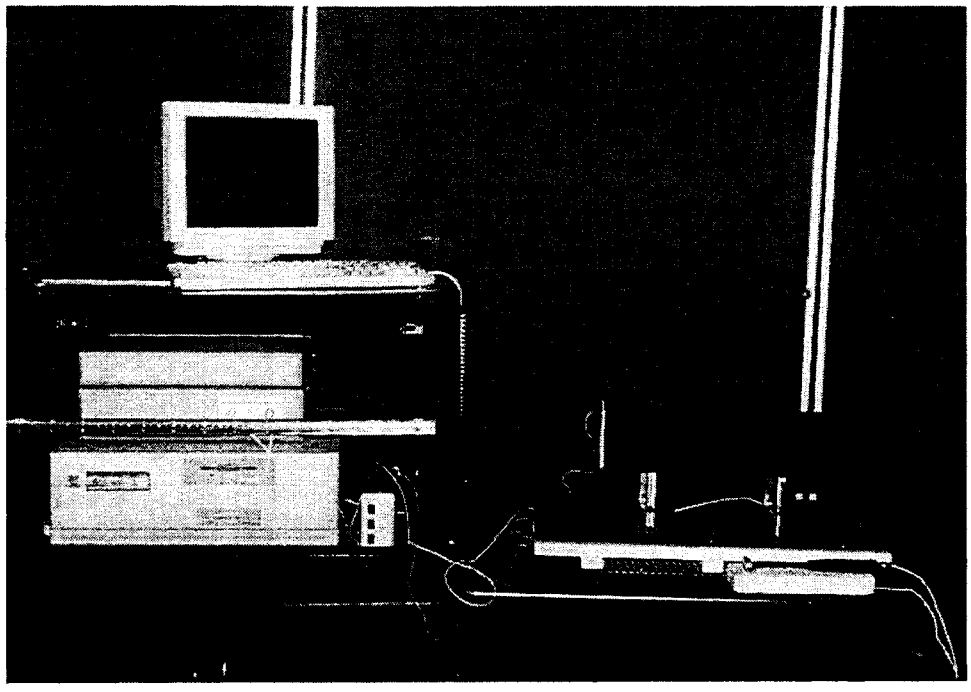

Figure 3.11 Fundamental transverse frequency test setup

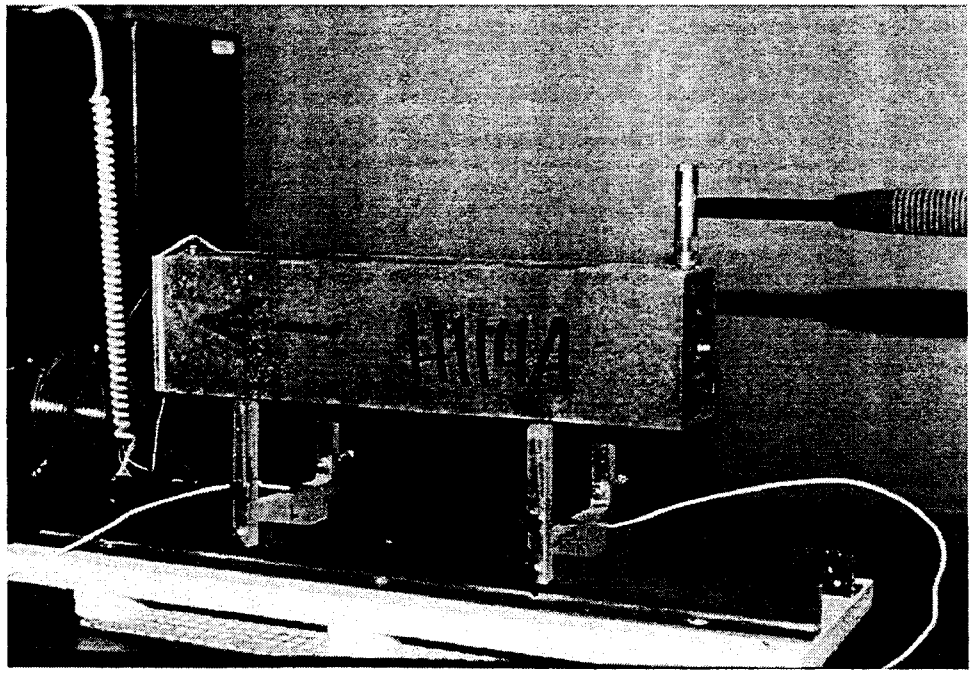

Figure 3.12 Fundamental transverse frequency measurement

Relative Dynamic Modulus was calculated in this study (as given in ASTM C666) as:

$$RDM\ (\%) = (n_c^2 / n_o^2) * 100 \qquad \text{(Eq. 3-6)}$$

n_c = fundamental transverse frequency at c cycles
n_o = initial fundamental transverse frequency (0 cycles)

Durability Factor

The freeze-thaw durability of different concrete mixes may be compared by way of the Durability Factor, which was calculated in this study (as given in ASTM C666) as:

$$DF = [(RDM)_n * n] / M \qquad \text{(Eq. 3-7)}$$

$(RDM)_n$ = Relative Dynamic Modulus of Elasticity at n cycles
n = number of cycles when RDM > 60% or M, whichever is less
M = specified number of cycles at which testing is to end, typically 300.

FAILURE

ASTM C666 Failure Criteria

ASTM C666 requires that the testing of each specimen continue until it has been subjected to 300 freeze-thaw cycles or until it has reached the failure criterion, whichever occurs first. ASTM defines the failure criteria as the Relative Dynamic Modulus of Elasticity reaching

60 percent of the initial modulus or, optionally, a 0.10 percent length expansion. In this study, both failure criteria were considered and the specimens were removed from the freeze-thaw testing machine when the Relative Dynamic Modulus of Elasticity generally reached 50 percent of the initial modulus. During early tests, some specimens were monitored to well below 50 percent Relative Dynamic Modulus before removal from the freeze-thaw testing machine. Even at very low RDM values, most specimens remained intact (i.e. little to no concrete spalled off beam) with a small amount of cracking (in most cases) the only visible sign of deterioration (see Figures 3.13 and 3.14).

Except for ranking in relative order of frost resistance, there are no established criteria for acceptance or rejection of concrete aggregate based on ASTM C666. Neville proposed the following durability factor scale to evaluate freeze-thaw performance in ASTM C666: concrete with DF greater than 60 is probably satisfactory for frost resistance; concrete with DF between 40 and 60 is of doubtful performance; and concrete with DF less than 40 is probably unsatisfactory for frost resistance [49]. This scale was used in the evaluation of the freeze-thaw durability of concrete.

The ASTM C666 test procedure has shown some variability in the results. However, the variability is much less for very good and very poor concrete than for those of intermediate durability [41].

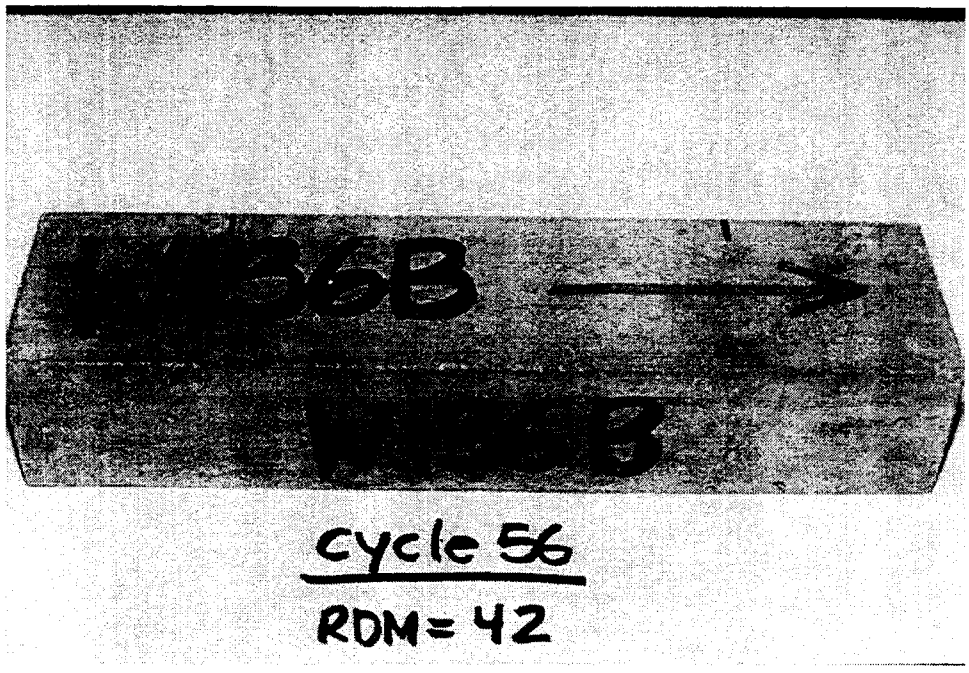

Figure 3.13 Freeze-thaw tested concrete beam: moist-cured granite reference mix

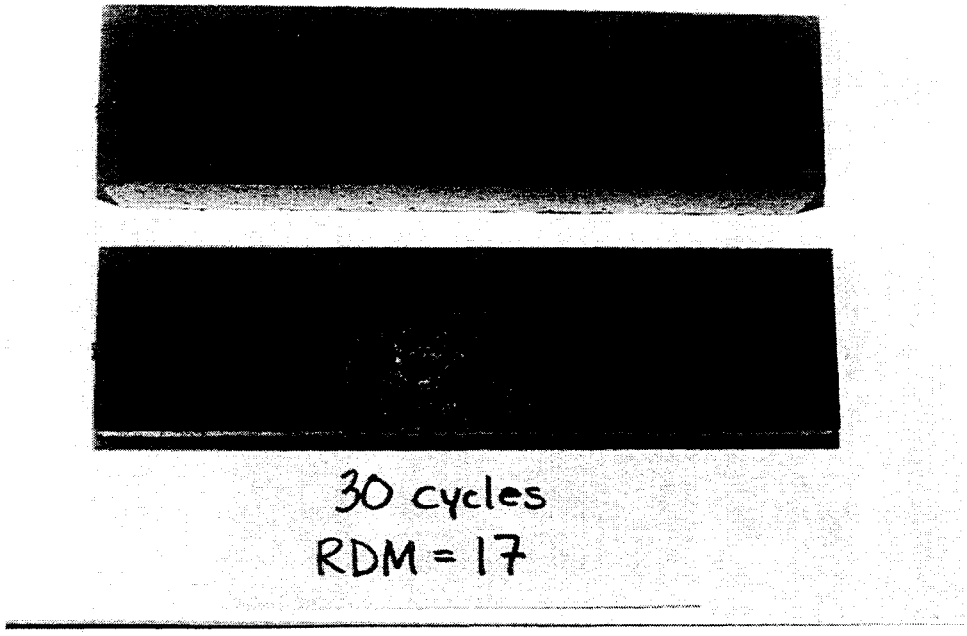

Figure 3.14 Freeze-thaw tested beams: moist-cured granite with silica fume mix

Observed Failure Mechanisms

After failing both the Relative Dynamic Modulus and the dilation criteria or completing over 1500 or 500 cycles (for Phase I and Phase II mixes, respectively), the beam specimens were removed from the freeze-thaw testing machine. Slices were prepared from selected specimens for visual microscopic investigation (same samples used for the linear traverse study, described below) to determine the failure mechanism in each case.

AIR VOID SYSTEM

The air void system of the hardened concrete was investigated in accordance with ASTM C457 Procedure A (linear traverse method). The linear traverse procedure estimates the volumetric composition of the concrete by measuring the size of air voids and amount of paste traversed along a series of regularly spaced lines in one plane intersecting the sample. Each air void encountered by the intersection of the cross hairs was both measured and recorded on a counter to determine the total number of air voids in the cross section. The data gathered were the total length traversed (T_t), the length traversed through air voids (T_a), the length traversed through paste (T_p), and the total number of air voids (N). These data were used to calculate the hardened air content and various other measures of the air void system.

ASTM C457 provides the following definitions and equations for the calculation of the linear-traverse parameters:

air void: a space enclosed by the cement paste and that was filled with air or other gas prior to the setting of the paste.

air content (A): the proportion of the total volume of the concrete that is air voids, expressed as percentage by volume.

$$A = (T_a/T_t)x100 \qquad \text{(Eq. 3-8)}$$

specific surface (S): the total surface area of the air voids divided by the volume of air in the concrete, expressed in compatible units so that the unit of specific surface is a reciprocal length.

$$S = (4xN)/T_a \qquad \text{(Eq. 3-9)}$$

paste-to-air ratio (p/a): the ratio of the volume of hardened cement paste to the volume of the air voids in the concrete.

$$p/a = T_p/T_a \qquad \text{(Eq. 3-10)}$$

spacing factor (L): the average maximum distance of any point in the cement paste from the periphery of an air void, the unit is a length.

$$L = 3[1.4(1+(p/a))^{1/3}-1]/S \qquad \text{(Eq. 3-11)}$$

Air Content

Air content of the hardened concrete is an important indicator of frost-resistant concrete. Air contents between 3 and 6 percent of the volume of concrete are typically believed to be satisfactory for producing frost-resistant concrete. According to the ACI 201.2 Guide for

Durable Concrete, an air content of 5.5 percent is needed to ensure durable concrete in moderate exposure, the level of exposure of bridge girders in freezing environments. However, a high air content can be detrimental to concrete strength. Therefore, it is desirable to keep the air content as low as possible, yet still provide durability. **Also, in terms of providing frost-resistant concrete, it is not the total volume of air that is important, but the size and distribution of the air voids and the distance between them.**

A short discussion of the parameters that are determined from the linear traverse method is presented below. These parameters provide an indication of the air void sizes and distribution in the hardened concrete.

Spacing Factor

Of the parameters determined by linear traverse, the spacing factor is generally regarded as the most significant indicator of the durability of the cement paste to freezing and thawing exposure of the concrete. Closely-spaced air voids minimize the hydraulic pressure buildup during freezing. The maximum value of the spacing factor for concrete in moderate exposure is usually accepted as 0.008 in (0.20 mm). Larger values may be adequate for mild exposure or for high-strength concrete, as discussed in Chapter 2.

Specific Surface

With low air content, a concrete with larger surface area of air voids is more likely to withstand rapid freezing. The specific surface of air voids in concrete containing entrained air is higher than in concrete without air entrainment. When air entrainment is used, producing many small air voids in the concrete, the total surface area of the air voids increases more rapidly than the total volume of the air voids.

ASTM C457 reports that, for air-entrained concrete designed in accordance with ACI 201.2R and ACI 211.1, the paste-air ratio is usually in the range of 4 to 10, the specific surface is usually in the range of 600 to 1100 in^{-1} (23.6 to 43.3 mm^{-1}), and the spacing factor is usually in the range 0.004 to 0.008 in (0.10 to 0.20 mm).

Procedure

For each beam investigated, a slice approximately 1 inch (25 mm) thick was sawed from the center of the concrete beam. The surface was prepared by lapping with successively finer abrasive until a suitable surface for microscopic observation was achieved. Figures 3.15 and 3.16 show examples of slices taken from tested freeze-thaw beams and prepared for microscopic investigation. A magnification of approximately 40X was used in the linear traverse study. This magnification was deemed appropriate because all of the air voids in the concrete for this linear traverse study were entrapped air voids (complete air void analysis was not performed on the

air-entrained concrete specimens). Entrapped air voids are typically 0.04 in (1 mm) or more in diameter and irregular in shape because the voids tend to follow the contours of the surrounding aggregate particles. Entrained air voids are usually much smaller in size than the entrapped air voids, with diameters ranging from 0.0004 to 0.004 inches (10 to 100 microns). Entrained air voids are also mostly spherical in shape.

The total area traversed in each 3 x 4-in (76 x 102-mm) slice was 6.6 in^2 (4260 mm^2) and the total length traveled was 55.0 in (1400 mm). The paste content (i.e. the proportion of the total volume of the concrete that is hardened cement paste) was calculated from the batched mix proportions and ranged from 29 to 30 percent of the total concrete volume.

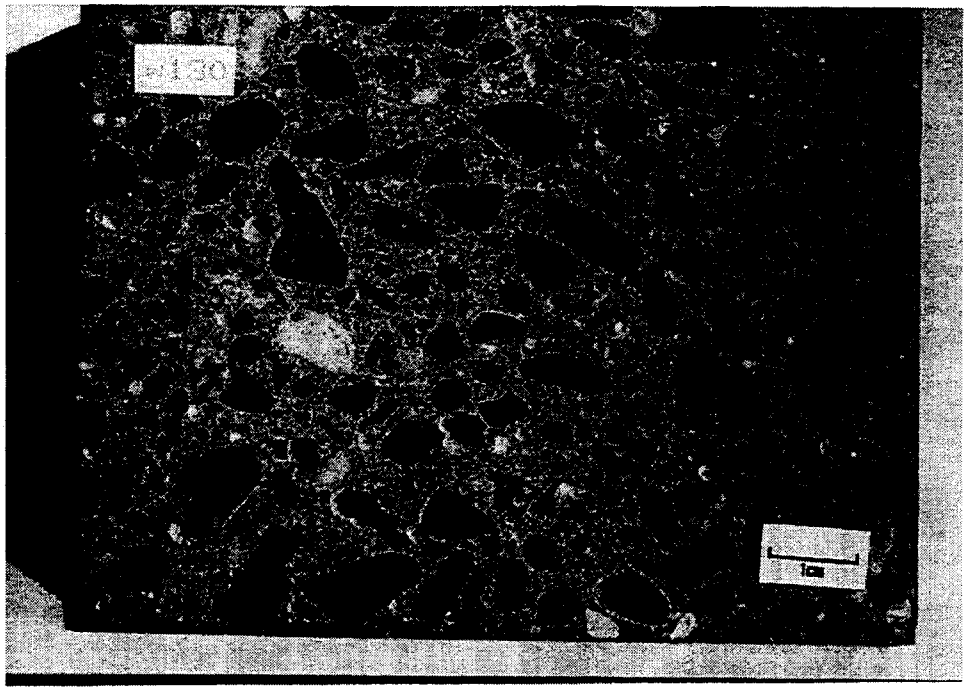

Figure 3.15 Prepared cross section: moist-cured PCG w/FA mix

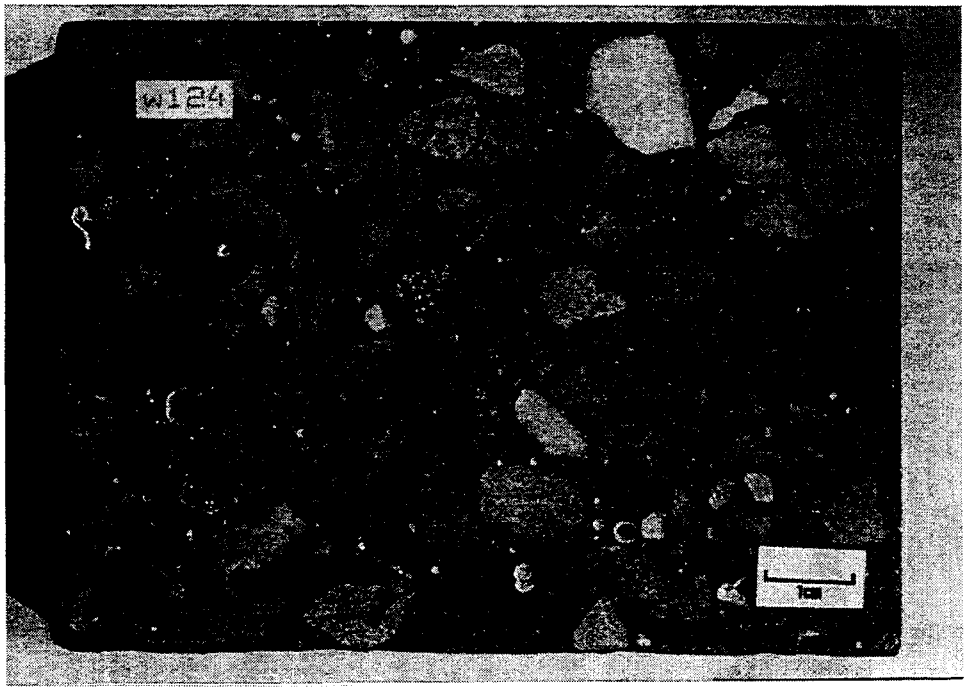

Figure 3.16 Prepared cross section: moist-cured LS-H ref.mix

CHAPTER 4

EXPERIMENTAL RESULTS AND DISCUSSION

DATA TAKEN WHILE AGING SPECIMENS

Length and weight measurements were taken on all beam specimens at the time they were placed in the storage room (i.e. at age of 1 day for the heat-cured specimens and at an age of 7 days for the moist-cured specimens). Measurements were also taken upon removal of the specimens from this environment. These measurements permit the calculation of weight and length change while aging. Length and weight change from the time the specimens were placed in storage to the time the specimens were removed from storage were calculated as:

$$\text{Change } (\%) = [(m_f - m_i) / (m_i)] \times 100 \qquad \text{(Eq. 4-1)}$$

m_i = initial measurement when placed in storage room (after initial curing)
i = day placed in storage room
= 1 for heat-cured specimens
= 7 for moist-cured specimens

m_f = measurement when taken from storage room
f = day removed from storage room
= 189 for Phase I mix specimens
= 28 for Phase II mix specimens

The length and weight changes of the heat- and moist-cured specimens after aging are given in Table 4.1. Each number represents the average of the two specimens tested for each mix curing condition.

Table 4.1: Specimen Length and Weight Change After Aging

Mix	Average Length Change (%)		Average Weight Change (%)	
	heat-cured	moist-cured	heat-cured	moist-cured
PHASE I MIXES (Aged 189 days)				
RG Ref	-0.053	-0.056	-0.983	-1.113
RG w/FA	-0.036 *(6)*	-0.052	-0.960	-1.126
RG w/SF	-0.031	-0.044	-0.696	-0.866
RG w/FA&SF	-0.035	-0.054	-0.812	-1.269
PCG Ref	-0.057	-0.051	-0.808	-0.917
PCG w/FA	-0.062	-0.055	-0.973	-1.189
PCG w/SF	-0.038	-0.057	-0.894	-1.272
PCG w/FA&SF	-0.034	-0.060	-0.749	-1.249
GR Ref	-0.053	-0.029 *(17)*	-0.929	-1.065
GR w/FA	-0.040	-0.023 *(15)*	-0.832	-1.138
GR w/SF	-0.027	-0.018 *(17)*	-0.582	-0.919
GR w/FA&SF	-0.038	-0.019 *(15)*	-0.923	-1.128
LS-H Ref	-0.056	-0.052	-1.162	-1.098
LS-H w/FA&SF	-0.039	-0.052	-1.004	-1.670
LS-L Ref	-0.069	-0.038 *(20)*	-1.089	-1.105
LS-L w/SF	-0.044	-0.049	-0.850	-1.148
LS-L w/FA&SF	-0.054	-0.019 *(20)*	-0.971	-1.321
PHASE II MIXES (Aged 28 days)				
(RG Ref)R	-0.011	-0.035	-0.280	-0.400
(RG w/SF)R	-0.013	-0.029	-0.227	-0.424
(RG w/SF)AE	-0.021	-0.039	-0.246	-0.627
(LS-H Ref)R	-0.037	-0.038	-0.557	-0.739
(LS-H w/SF)R	-0.017	-0.060	-0.305	-0.527
(LS-H w/FA&SF)R	-0.006	-0.037	-0.220	-0.974
(LS-L Ref)R	-0.032	-0.037	-0.530	-0.591

( ) Indicates day initial measurement was taken following placement in the storage room.
\+ Indicates increased weight or length
\- Indicates decreased weight or length

For the Phase I concrete mixes, the difference between each weight change measurement compared with the average value of the two test beam specimens was less than 10 percent for all but one set of beam specimens. In fact, 30 of the 37 beam specimen pairs (81 percent) had a difference of less than 5 percent from the calculated average. In terms of length change, in which length is measured to the nearest 0.0001 in (0.0025 mm), 34 of the 37 beam specimen pairs (92 percent) had less than 0.0005 in (0.0130 mm) difference between the measurements of the two test beam specimens. In addition, 25 of the 37 concrete mixes (68 percent) had less than 0.0002 in (0.0050 mm) difference.

The Phase II concrete mixes exhibited a greater variation between the measurements of the two test beam specimens than the Phase I concrete mixes. The difference between each weight change measurement and the calculated average of the two test beam specimens was less than 10 percent for 10 of the 17 (59 percent) concrete mixes. Fourteen of the 17 concrete mixes (82 percent) had less than 0.0003 in (0.0080 mm) difference between the lengths of the two test beam specimens. All the data taken while the concrete beam specimens were aged can be found in Appendix F.

Several sets of specimens were not measured for length at the time they were placed in the storage room because of failure of the dial indicator on the length comparator. Upon replacement of the dial indicator, these beam specimens were measured and this measurement was used as the initial reading to monitor length change. Table 4.1 indicates the specimens affected and the day the "initial" length measurement was taken. In the table, a negative value

indicates a decrease in the length or weight of the specimen.

In addition to initial and final measurements, weekly measurements were taken on all four concrete beam specimens of selected Phase I mixes to monitor changes in weight and length while aging. All four of the concrete mixes containing round gravel (i.e., RG Ref, RG w/FA, RG w/SF and RG w/FA&SF) and the additional four reference mixes (i.e., PCG Ref, GR Ref, LS-H Ref and LS-L Ref) were arbitrarily chosen for this purpose (giving a total of 8 mixes x 4 beams/mix = 32 beams).

To compare the effect of cementitious material content and curing condition, Figures 4.1 (a) and (b) show the weight changes of the heat- and moist-cured round gravel concrete mixes, and Figures 4.2 (a) and (b) provide the length changes of the heat- and moist-cured round gravel concrete mixes. In all four round gravel concrete mixes, the moist-cured specimens lost more weight and experienced greater length change while aging than the heat-cured specimens. This expected result was due to the moist-cured specimens' wet condition at the time of the initial measurement (having just been removed from the curing (water) tank) whereas the heat-cured concrete specimens had no exposure to water and were dry when placed in storage.

Based on cementitious material content, the order of decreasing measurement for both the weight and length changes of the heat-cured specimens was the same. The reference mix experienced the greatest weight loss and length change, followed by the fly ash mix, the combination fly ash with silica fume mix and the mix containing only silica fume. For the

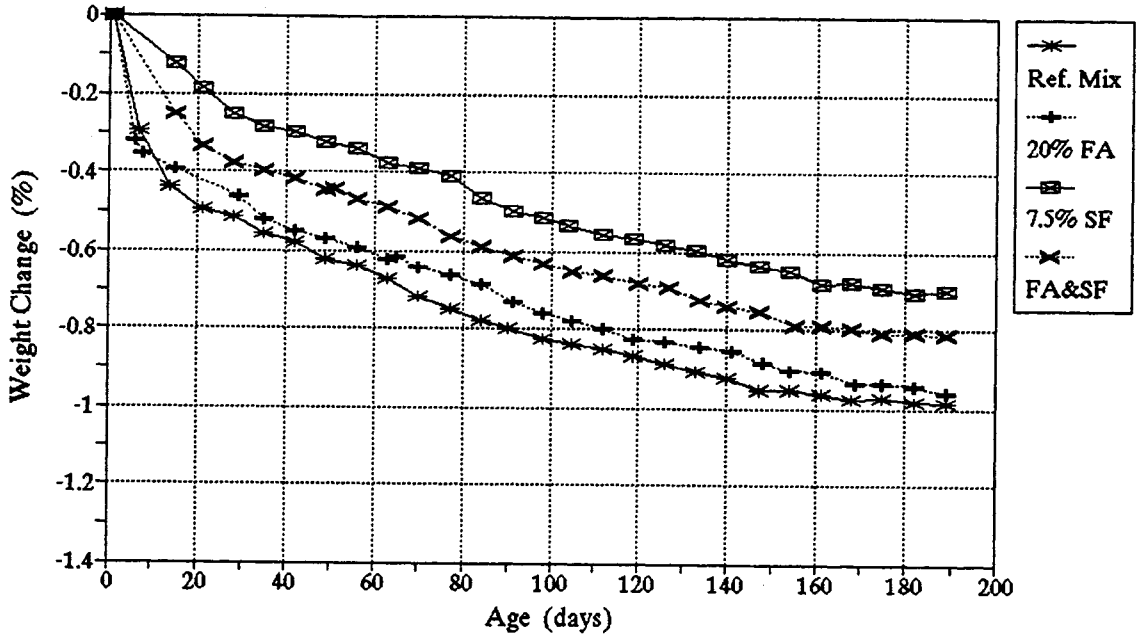

(a) heat-cured concrete specimens

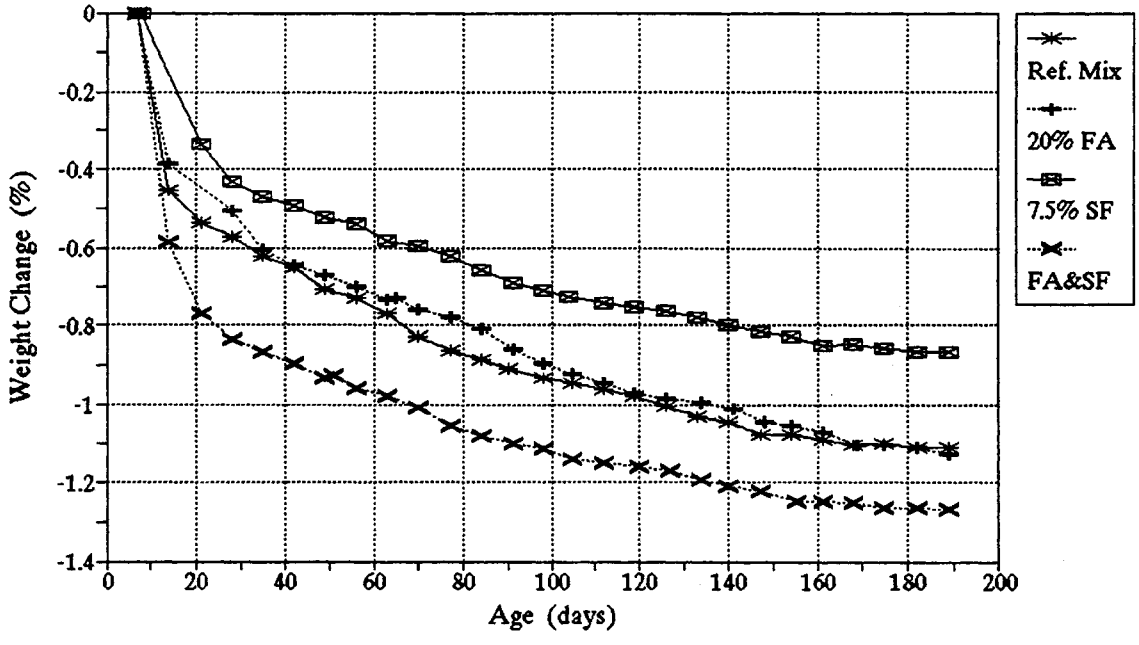

(b) moist-cured concrete specimens

Figure 4.1 Weight change while aging: round gravel concrete mixes

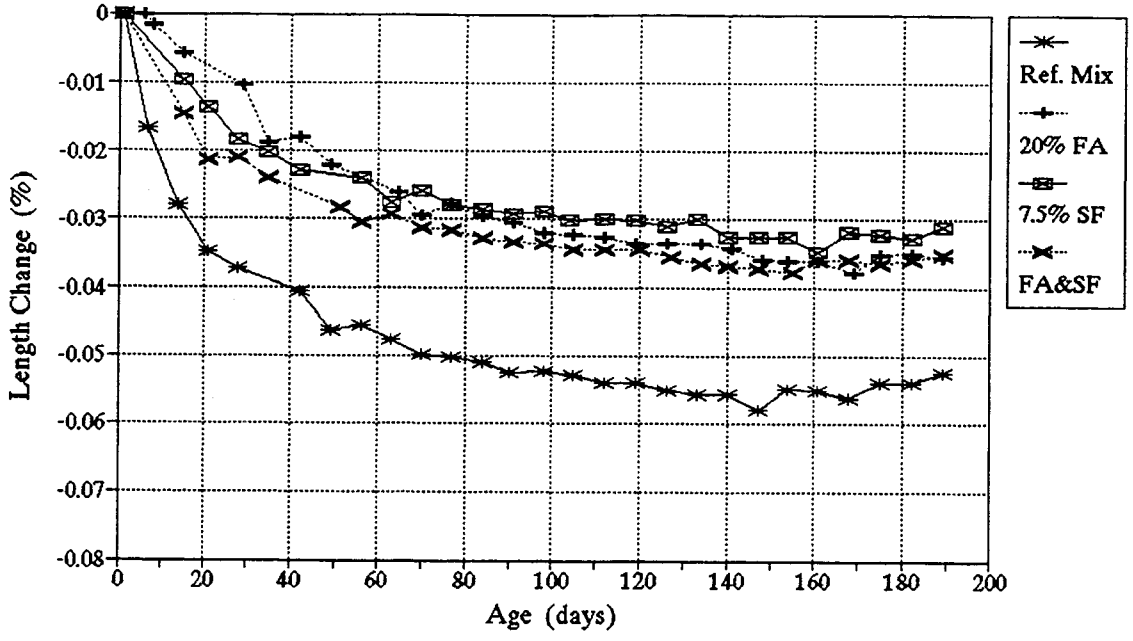

(a) heat-cured concrete specimens

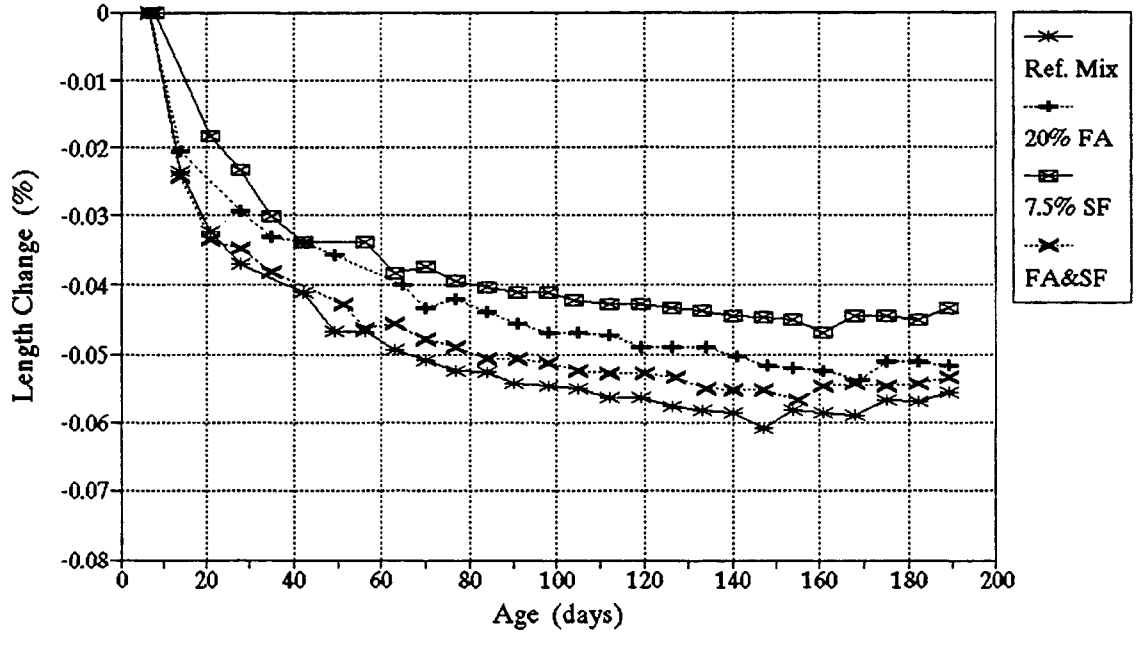

(b) moist-cured concrete specimens

Figure 4.2 Length change while aging: round gravel concrete mixes

moist-cured specimens, the silica fume mix again experienced the least amount of weight or length change, followed by the fly ash mix. The moist-cured reference mix experienced a slightly greater length change than the fly ash with silica fume mix, even though it did not lose as much weight as the fly ash with silica fume mix.

These measurements are consistent with current knowledge of the effects of pozzolans in concrete. As discussed in Chapter 2, the use of a pozzolan reduces the permeability of concrete. With a lower permeability, the rate that water will be lost from the concrete on drying is slower than for a concrete without a pozzolan. In addition, Bayasi [38] has shown that the inclusion of fly ash in silica fume concrete increases the permeability of the concrete. Therefore, in this investigation, one would expect the reference mix (without pozzolan) to experience the greatest weight loss followed by the fly ash concrete mix and the fly ash with silica fume concrete mix. The silica fume concrete mix, presumably with the lowest permeability, would be expected to experience the least amount of weight loss. These behaviors were, in fact, seen in the results of the weight change while aging (with the exception of the moist-cured fly ash with silica fume concrete mix).

The effect of curing condition may also be discussed by looking at the difference between the heat- and moist-cured measurements for weight change in each round gravel concrete mix. For example, in the round gravel reference mix, the difference between the measurements of the heat- and moist-cured specimen pairs for weight change was small. In the concrete mix with 20 percent fly ash and in the concrete mix with 7.5 percent silica fume, the gap widens between

the measurements of the moist- and heat-cured specimens. The difference in the measurements for weight change of the heat- and moist-cured specimens was greatest for the 20 percent fly ash with 7.5 percent silica fume mix. In this case, the difference between the heat- and moist-cured measurements was over four times the difference between the measurements of the reference mix. From these observations, one could conclude that the curing condition had a much greater effect on the concrete mixes containing fly ash and silica fume (especially in the mix containing a combination of fly ash and silica fume) than it did on the reference mix. Similar observations may be found when looking at the difference between the heat- and moist-cured length change measurements of the round gravel mixes. Again, these results are consistent with the understanding that use of a pozzolan in concrete may require a longer period of curing. The benefits of moist-curing the concrete (in comparison to heat-curing) were more evident in the concrete mixes containing a pozzolan than in the reference concrete mixes (in which both the heat- and moist-cured concrete specimens behaved similarly).

To compare the effect of aggregate type and curing condition, Figures 4.3 (a) and (b) show the weight changes of the heat- and moist-cured reference mixes, and Figures 4.4 (a) and (b) show the length changes of the heat- and moist-cured reference mixes.

In Figure 4.4 (b), note that the initial length change of the concrete mixes containing granite and low-absorption limestone was taken at a later time. Thus, the curves for these two concrete mixes shows the percent length change from this later "initial" length measurement, and cannot be compared directly with the curves of the other three concrete mixes (containing round

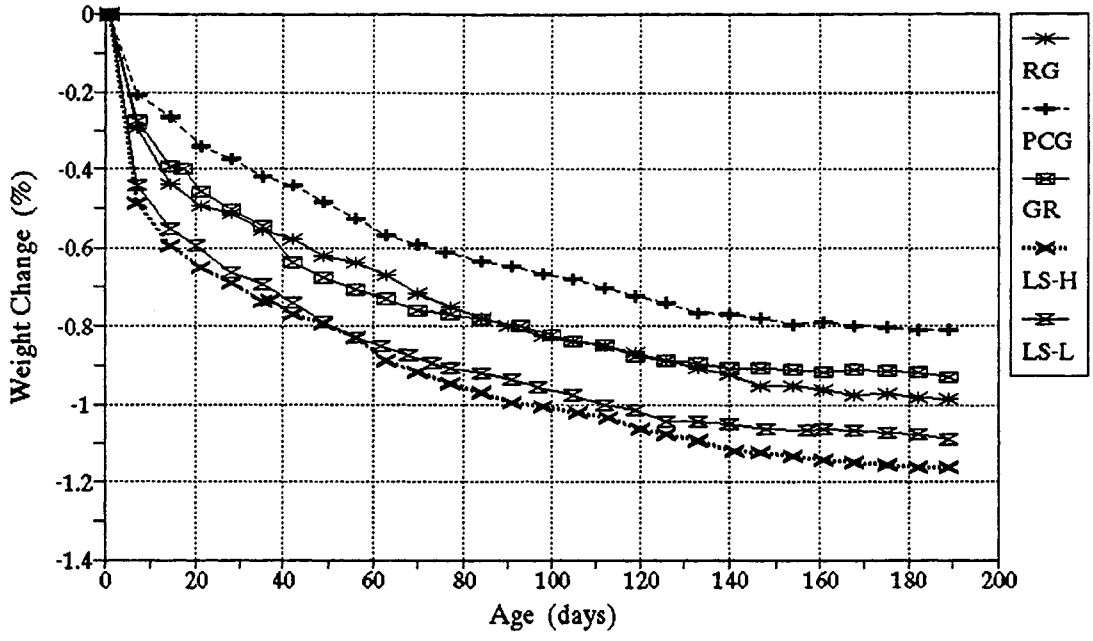

(a) heat-cured concrete specimens

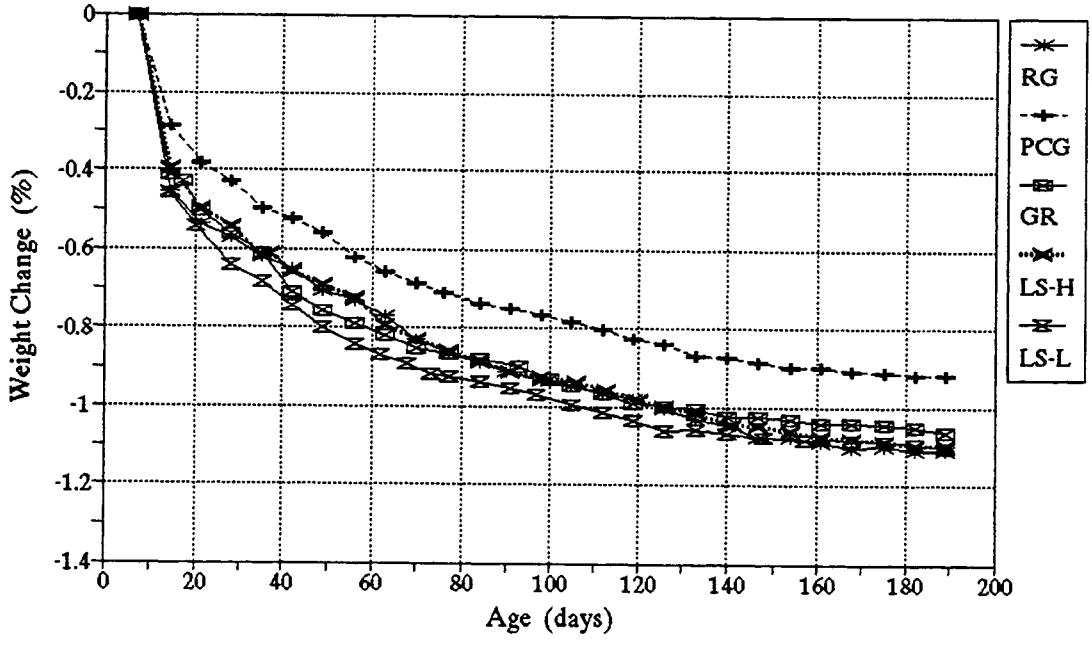

(b) moist-cured concrete specimens

Figure 4.3 Weight change while aging: reference concrete mixes

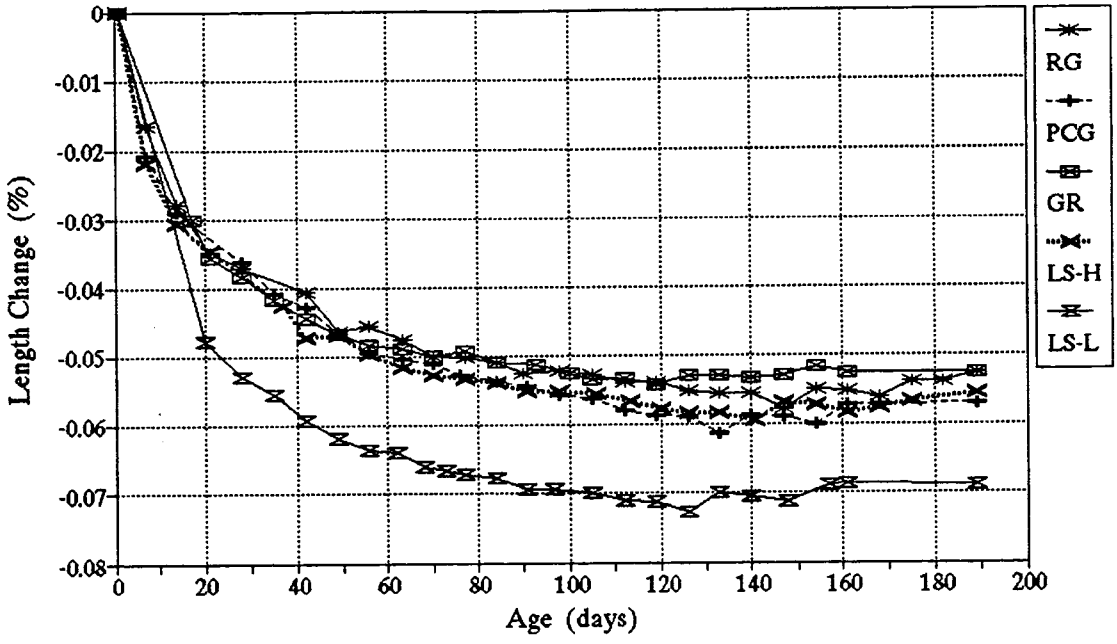

(a) heat-cured concrete specimens

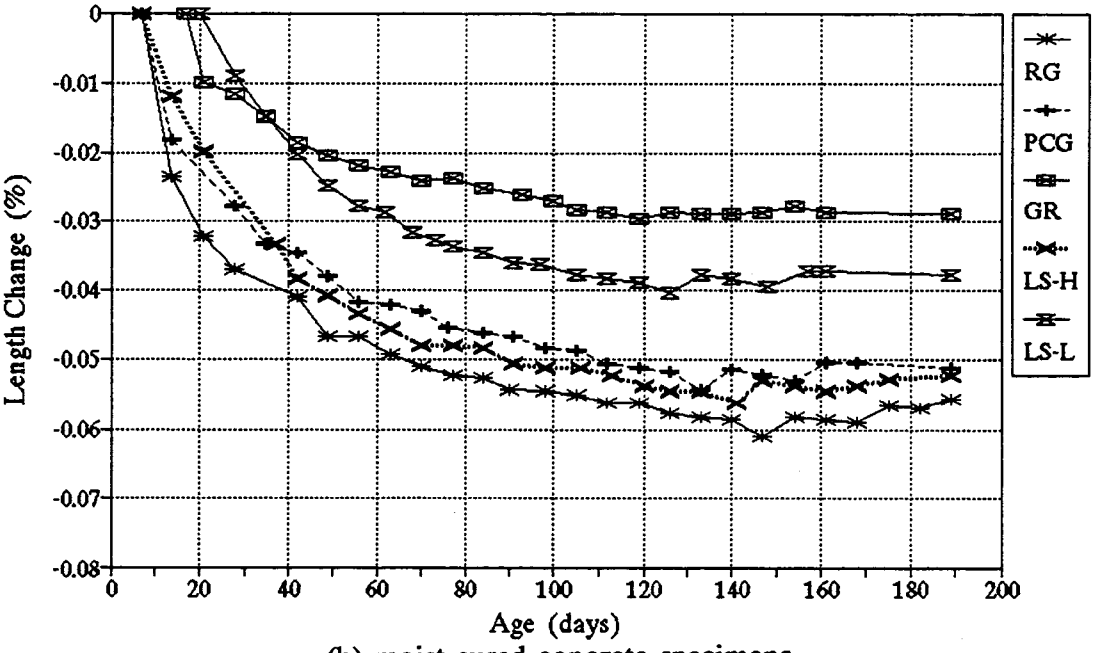

(b) moist-cured concrete specimens

Figure 4.4 Length change while aging: reference concrete mixes

gravel, partially-crushed gravel and high-absorption limestone).

Comparing the five reference mixes for effect of curing condition, the moist-cured specimens generally lost more weight and experienced greater length change than the heat-cured specimens, as expected.

Based on aggregate type, the concrete specimens with limestone generally experienced the greatest weight loss and length change. The partially-crushed gravel concrete specimens consistently lost the least amount of weight while aging, although the length changes of these specimens were close to those of the limestone concrete specimens.

As discussed in Chapter 2, whether or not water will be drawn from an aggregate particle depends upon the relative size of the pores in the aggregate particle and in the cement paste. During a period of drying, water will be drawn by capillarity from the aggregate particles containing only voids which are larger than those in the paste. Aggregate particles containing small, interconnected voids are capable of retaining a high degree of saturation in concrete. In this study, the limestone aggregate had the highest absorption capacity; the limestone concrete also experienced the greatest weight loss upon drying. A possible explanation is that the pore sizes of the limestone were of a size that permitted easy absorption and easy drainage of water.

The effect of curing condition on each aggregate type, in terms of the difference between the heat- and moist-cured measurements in each of the reference concrete mixes, may also be

explored. In the limestone concrete specimens the difference between the heat- and moist-cured measurements for weight change was very small (especially for the low-absorption limestone concrete specimens). Following the limestone concrete in the order of increasing effect of curing condition was the concrete containing partially-crushed gravel. The concrete mixtures containing granite and round gravel appeared to be most affected by the curing condition.

Some of the observations of the selected Phase I concrete specimens that were monitored weekly during aging can be extended to all of the concrete specimens. Looking at Table 4.1, all of the moist-cured concrete specimens consistently lost more weight while aging than the heat-cured specimens. The moist-cured concrete specimens generally experienced greater length change than the heat-cured. In most of the cases in which the heat-cured specimens showed a greater tabulated length change, the initial measurement of the moist-cured specimen was delayed due to an inoperable length comparator (e.g. Fig. 4.4), giving a shorter period of time for which the measurement was compared. Since the moist-cured specimen length change in the first 20 days was observed to be greater than the heat-cured specimen length change for the other specimens, the total length change would be expected to be greater for the moist-cured specimens had the length been measured when the concrete specimens were placed in storage.

In comparison of the cementitious material content, the reference mixes generally experienced the greatest weight and length change and the 7.5 percent silica fume mixes generally experienced the least. Curing condition had the smallest effect on the reference mixes and the greatest effect on the concrete containing the combination of fly ash with silica fume.

In comparison of the aggregate type, the limestone concrete mixes experienced the greatest weight and length changes while the partially-crushed gravel and granite concrete mixes experienced the least. Curing condition had the least effect on the limestone reference concrete. However, in the limestone concrete containing silica fume and fly ash with silica fume, large differences between the measurements of the heat- and moist-cured specimens were seen. Generally, the effect of curing condition seems to depend more on cementitious composition than on aggregate type.

As previously mentioned, the Phase II concrete mixes were only aged 28 days before beginning the freeze-thaw testing procedure. To aid in the comparison of the Phase II concrete mixes with the Phase I concrete mixes, the 28-day weight and length changes of the Phase I mixes that were measured weekly are given in Table 4.2.

The Phase I mixes generally experienced greater weight loss and length change at 28 days than the Phase II mixes (see Table 4.1). Because the Phase II mixes were intended to be exact replicates of the Phase I mixes, one of the few variables was the moisture content of the aggregate at the time of mixing. The final water-to-cementitious material ratio in all mixes, however, was 0.30 since batch water was adjusted for the free water in the aggregate at the time of mixing. Although most of the length change measurements do not appear to be influenced by the aggregate moisture content, there does seem to be a correlation between the coarse aggregate moisture content and the measured weight change. For example, the Phase I round gravel reference mix experienced much greater weight loss by the age of 28 days than the Phase

Table 4.2: Specimen Aging Data (end of curing to 28 days)

Mix	Length Change (%)		Weight Change (%)	
	heat-cured	moist-cured	heat-cured	moist-cured
PHASE I MIXES				
RG Ref*	-0.037	-0.037	-0.515	-0.572
RG w/FA	-0.011	-0.030	-0.460	-0.508
RG w/SF*	-0.019	-0.024	-0.250	-0.431
RG w/FA&SF	-0.021	-0.035	-0.376	-0.835
PCG Ref	-0.036	-0.028	-0.372	-0.426
GR Ref	-0.038	-0.012	-0.505	-0.534
LS-H Ref*	NR	NR	-0.688	-0.545
LS-L Ref*	-0.053	-0.009	-0.665	-0.643

NR Indicates measurement not reported due to failure of dial indicator.
* Indicates Phase I mix repeated in Phase II.

II round gravel reference mix, especially for the heat-cured specimens. The coarse aggregate saturation of the Phase I concrete mix (that experienced the greater weight loss) was 132 percent (see Eq. 3-1) whereas the saturation of the coarse aggregate in the Phase II concrete mix was only 85 percent. However, in the Phase I and Phase II round gravel with silica fume concrete mixes, which had coarse aggregate saturations of 139 percent and 82 percent, respectively, there is relatively little difference between the weight and length changes. This could result from the presence of unreacted silica fume at the transition zone that would use any expelled water from the aggregate for hydration or prevent water from escaping. In the cases of the limestone reference concrete mixes, both the Phase I and Phase II concrete mixes contained coarse aggregate that was (or was close to) saturated at the time of mixing. For the heat-cured

limestone mixes, a larger weight loss is seen in the Phase I reference concrete mix containing more saturated coarse aggregate (than the Phase II reference concrete mix). These observations are less evident for the moist-cured limestone reference mixes.

SPECIMEN DATA AFTER IMMERSION IN CONSTANT TEMPERATURE BATH

Length and weight measurements were taken on all beam specimens immediately upon removal from the constant temperature water bath. These measurements permit the calculation of length and weight change of the concrete beam specimens while immersed in the 40 °F (4.5 °C) water bath. Length and weight change were calculated as follows:

$$\text{Change } (\%) = [(m_c - m_f) / (m_f)] \times 100 \qquad \text{(Eq. 4-2)}$$

m_f = measurement when taken from storage room
f = day removed from storage room
= 189 for Phase I mix specimens
= 28 for Phase II mix specimens
m_c = measurement when removed from constant temperature bath (after 21 days in 40 °F (4.5 °C) water)

The length and weight changes of the heat- and moist-cured specimens after immersion in the constant temperature water bath are given in Table 4.3. Again, each number represents the average of the two specimens tested for each mix curing condition. In the table, a positive value indicates an increase from the initial measurement, while a negative value indicates a decrease in the measurement.

For the Phase I concrete mixes, the difference between each weight change measurement

Table 4.3: Specimen Length and Weight Change After Immersion in Constant Temperature Bath

Mix	Length Change (%)		Weight Change (%)	
	heat-cured	moist-cured	heat-cured	moist-cured
PHASE I MIXES				
RG Ref	0.022	0.021	1.421	1.159
RG w/FA	0.025	0.019	1.579	1.178
RG w/SF	0.012	0.009	1.055	0.960
RG w/FA&SF	0.012	0.010	1.064	1.206
PCG Ref	0.021	0.014	1.082	0.848
PCG w/FA	0.025	0.018	1.555	1.196
PCG w/SF	0.011	0.010	1.139	1.354
PCG w/FA&SF	0.009	0.011	0.855	1.201
GR Ref	0.022	0.015	1.627	1.075
GR w/FA	0.014	0.012	1.383	1.137
GR w/SF	0.009	0.006	0.890	0.963
GR w/FA&SF	0.006	0.005	1.379	1.164
LS-H Ref	0.023	0.023	1.396	1.142
LS-H w/FA&SF	0.012	0.008	1.439	1.710
LS-L Ref	0.023	0.021	1.121	1.022
LS-L w/SF	0.008	0.006	0.931	1.148
LS-L w/FA&SF	0.008	0.007	0.954	1.187
PHASE II MIXES				
(RG Ref)R	0.010	0.006	0.890	0.415
(RG w/SF)R	-0.002	-0.003	0.383	0.468
(RG w/SF)AE	0.004	0.004	0.517	0.619
(LS-H Ref)R	0.015	0.012	0.951	0.668
(LS-H w/SF)R	-0.001	0.031	0.477	0.512
(LS-H w/FA&SF)R	0.005	0.001	0.797	0.850
(LS-L Ref)R	0.009	0.009	1.058	0.634

\+ Indicates increased length or weight.
\- Indicates decreased length or weight.

and the average value of the two test beam specimens was less than 10 percent for all but one set of beam specimens. In fact, 31 of the 37 beam specimen pairs (84 percent) had a difference of less than 5 percent from the calculated average. In terms of length change, in which length is measured to the nearest 0.0001 in (0.0025 mm), 36 of the 37 concrete mixes (97 percent) had less than 0.0002 in (0.0050 mm) difference between the measurements of the two test beam specimens.

The Phase II concrete mixes exhibited a greater variation between the measurements of the two test beam specimens than the Phase I concrete mixes. The difference between each weight change measurement and the calculated average of the two test beam specimens was less than 10 percent for 12 of the 17 (71 percent) concrete mixes. For the length change, 15 of the 17 concrete mixes (88 percent) had less than 0.0002 in (0.0050 mm) difference between the measurements of the two test specimens. The data used for these calculations can be found in Appendices F, G and H.

These length and weight change measurements may be used to compare the concrete mixes. All of the heat-cured concrete specimens experienced greater dilation while in the constant temperature water bath than the moist-cured specimens. In addition, the heat-cured specimens from the reference and 20 percent fly ash concrete mixes gained more weight than the moist-cured concrete specimens from these mixes, while the opposite was generally true for the concrete specimens containing silica fume. Incorporated in a concrete mix, silica fume can have merely a filler effect (i.e. filling in voids due to its fineness) and, in the presence of water,

silica fume can produce additional hydration products that also fill in voids in the cement paste. In the moist-cured concrete specimens, in the presence of water, the silica fume would have the opportunity for both effects. However, in the heat-cured concrete specimens, with the amount of water limited to the mix water, the benefits of silica fume would be realized mainly through its filler effect. In the concrete mixes containing silica fume, the filler effect of the silica fume (in the heat-cured specimens) appeared to produce a less permeable structure than the structure created by the additional products of the silica fume reaction (moist-cured).

There was no apparent correlation with weight (or length) change (while immersed in the constant temperature water bath) and cementitious material composition or aggregate type.

Figures 4.5 (a) through 4.6 (b) compare the specimen weight loss while aging with the specimen weight gain after immersion in the constant temperature water bath for the heat- and moist-cured Phase I and Phase II concrete specimens. These Figures show that each heat-cured specimen generally gained back much more water weight than it had lost during the period of drying. The moist-cured specimens, on the other hand, generally gained back the same approximate weight they had lost while drying. These observations are expected. The heat-cured specimens, placed into storage dry, would lose a relatively small amount of water compared to the water gain they would experience upon placement in a water bath. The moist-cured specimens, placed into storage wet, would have lost water-weight through evaporation upon drying and then gain it back when placed in the water bath. The dilation while immersed in the water bath, however, was not nearly the length change (shrinkage) that the concrete beam

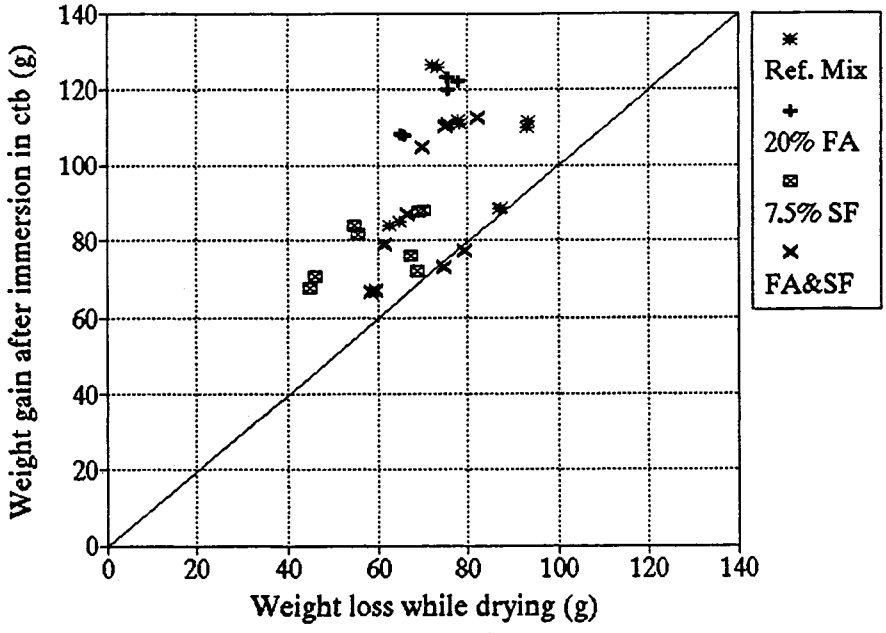

(a) heat-cured concrete specimens

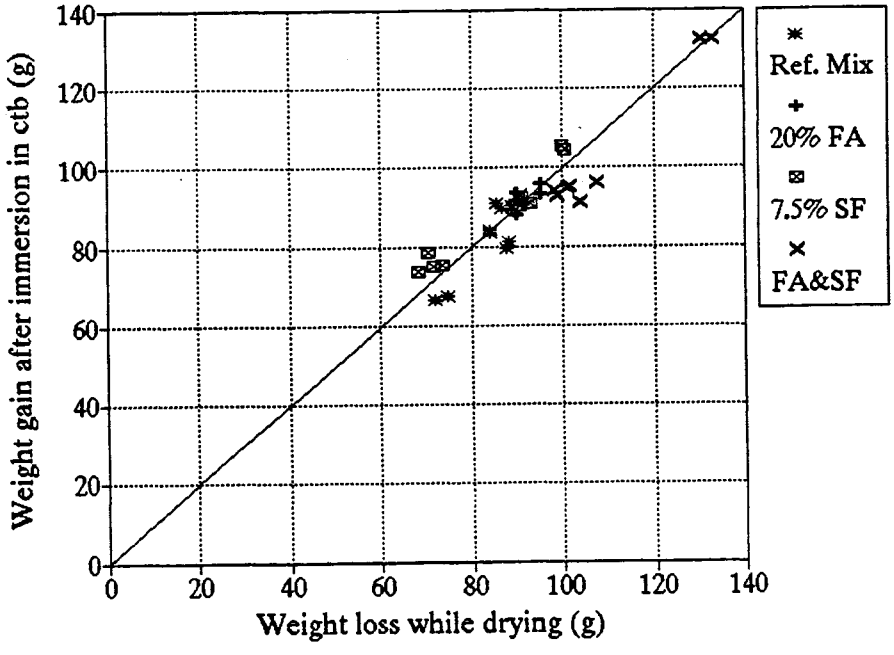

(b) moist-cured concrete specimens

Figure 4.5 Specimen weight gain vs. weight loss: Phase I mixes

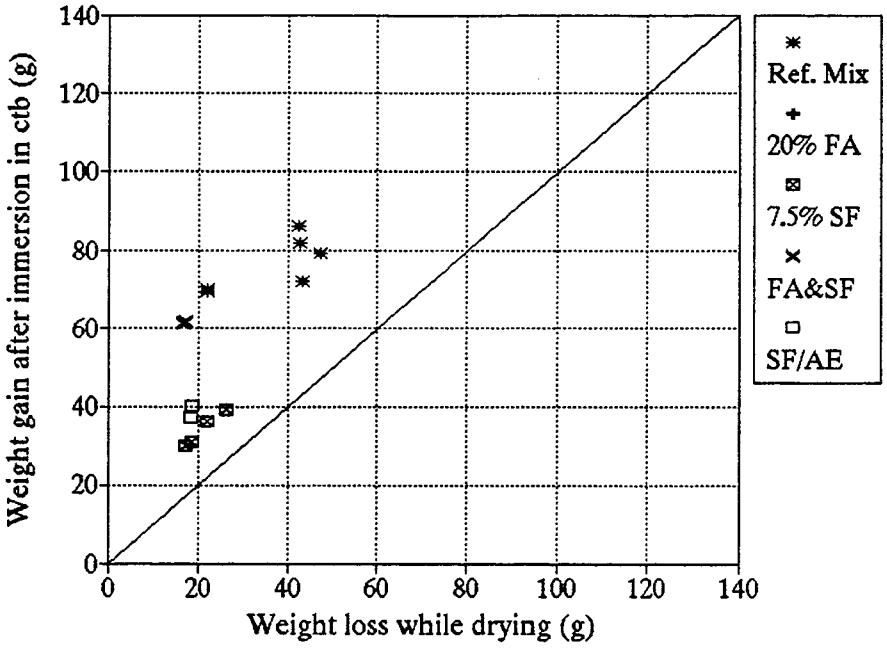

(a) heat-cured concrete specimens

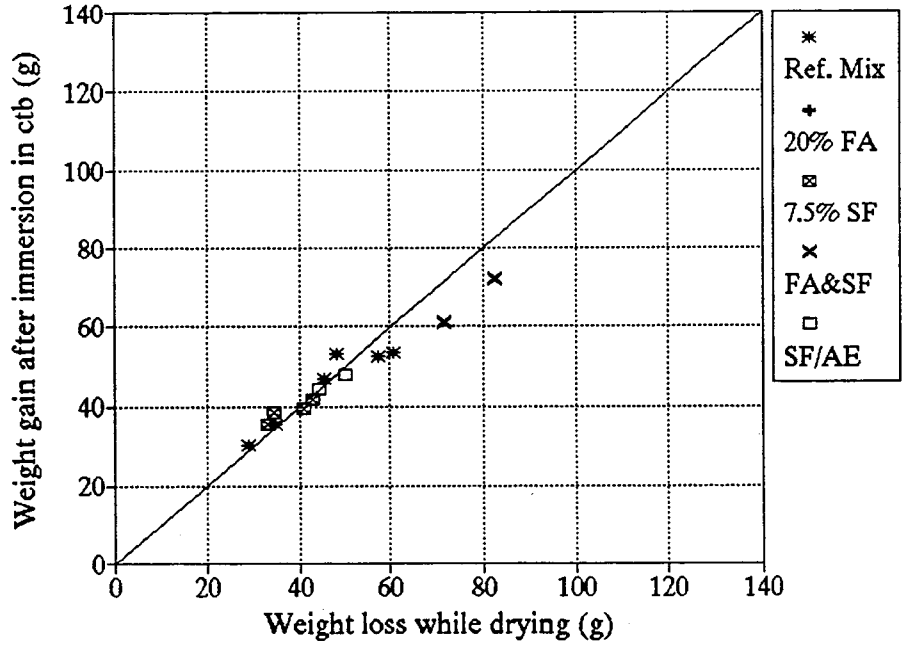

(b) moist-cured concrete specimens

Figure 4.6 Specimen weight gain vs. weight loss: Phase II mixes

specimens had experienced upon drying while aging. Comparing the two figures (4.5 and 4.6), the Phase II concrete specimens, aged for a shorter period of time, did not lose (during aging) or gain (while immersed in the constant temperature water bath) as much water weight as the Phase I specimens.

CONCRETE ABSORPTION POTENTIAL

Concrete absorption potential tests were conducted as a portion of the study dealing with the mechanical properties of high-strength concrete [3]. As discussed in Chapter 2, the PCA research program had shown that absorption potential serves as an indirect indicator of concrete permeability [28].

Measurements were taken on all Phase I concrete mix specimens; absorption potential tests were not performed on Phase II concrete specimens. In each Phase I concrete batch, companion 4 x 8-inch (100 x 200-mm) cylindrical specimens were cast and tested to determine absorption potential. The concrete specimens for these measurements were heat-cured at 150 °F (65 °C) or moist-cured for 28 days (in lime water). The moist-cured freeze-thaw beam specimens were moist-cured for seven days. However, data for the 28-day moist-cured specimens are presented to provide a comparison of moist- versus heat-curing. After the specified curing period, the absorption potential specimens were stored in an environment of 73 °F (23 °C) and 50 percent relative humidity until 56 days old. At the age of 56 days, each specimen was weighed (initial measurement) and then submerged in water and the weight gain

was measured and analyzed with respect to time. Results of the concrete absorption potential are given in Table 4.4 for the heat-cured and 28-day moist-cured specimens at 196 days of age. The concrete absorption is given as a percentage of the weight of the concrete specimen. The concrete absorption results are presented for the age of 196 days because the age correlated the closest to that of the Phase I concrete beam specimens at the time of immersion in the constant temperature water bath (age of 189 days).

For the effect of curing condition, the results indicate that the heat-cured specimens consistently absorbed much more water than the moist-cured specimens. As explained previously, the heat-cured concrete specimens were expected to absorb more water than the moist-cured concrete specimens, due to more microcracking in the dry, heat-cured concrete compared to the "dried-out" moist-cured concrete.

In terms of effect of aggregate type, the limestone concrete specimens typically exhibited the highest absorption. The partially-crushed gravel and the round gravel concrete specimens typically absorbed the least amount of water. This ranking did not completely agree with the order of the aggregates according to absorption capacities. The limestone aggregate had the highest absorption capacity, and the concrete made with limestone experienced the highest absorption. However, the granite aggregate had the lowest absorption capacity, but the granite concrete did not absorb the least amount of water.

Table 4.4: Concrete Absorption Potential Test Results: Phase I Mixes [3]

Mix	Concrete Absorption @ 196 days (% of weight)	
	heat-cured	moist-cured for 28 days
RG Ref	1.35	0.70
RG w/FA	1.72	0.79
RG w/SF	0.84	0.54
RG w/FA&SF	1.14	0.73
PCG Ref	1.28	0.65
PCG w/FA	1.65	0.80
PCG w/SF	1.03	0.72
PCG w/FA&SF	0.96	0.74
GR Ref	1.66	0.81
GR w/FA	1.50	0.87
GR w/SF	0.99	0.61
GR w/FA&SF	1.18	0.74
LS-H Ref	1.69	0.85
LS-H w/FA&SF	1.31	1.03
LS-L Ref	1.46	0.88
LS-L w/SF	0.98	0.73
LS-L w/FA&SF	0.99	0.82

With regard to cementitious material composition, the absorption tests have shown that the fly ash concrete specimens typically absorbed the most water, followed by the reference mix concrete specimens. The silica fume concrete specimens absorbed the least water, with the silica fume and fly ash with silica fume concrete specimens exhibiting similar performance (with a slightly higher absorption observed for the specimens containing the combination of fly ash with silica fume).

The absorption potential of all the heat-cured concrete specimens correlated exactly with the measurement of weight change while the freeze-thaw concrete specimens were immersed in the constant temperature water bath. A clear correlation was not seen in the moist-cured concrete specimens. However, since the absorption potential concrete specimens were moist-cured for 28 days and the freeze-thaw concrete specimens were moist-cured for seven days, the differences seen may be due to the differing length of moist-curing. Additional moist-curing will allow continued hydration and theoretically, result in less permeable concrete. Thus, as observed, the 28-day moist-cured concrete specimens would be less permeable and absorb less water than the seven-day moist-cured concrete specimens.

LINEAR TRAVERSE DATA

Table 4.5 provides the air void system parameters obtained from the linear traverse study of the hardened concrete of selected Phase I and Phase II concrete specimens. The Phase I mix specimens were tested for freeze-thaw durability prior to obtaining the samples for the linear traverse study. However, the Phase II concrete samples were obtained from concrete beams cast specifically for the purpose of conducting the linear traverse study; they were not tested for freeze-thaw durability prior to measuring the air-void system. Measurements for these Phase II specimens were obtained from samples cut from concrete beam specimens after their removal from the constant temperature water bath.

As expected with non-air-entrained concrete, all spacing factors of the Phase I and the non-air-entrained Phase II concrete mixes were much greater than the 0.008 in (0.20

Table 4.5: Specimen Air-void Parameters

Mix	Total # air voids*		Spacing Factor inch (mm)		Specific Surface inch^{-1} (mm^{-1})		Paste to Air Ratio	
	heat-cured	moist-cured	heat-cured	moist-cured	heat-cured	moist-cured	heat-cured	moist-cured
PHASE I MIXES								
RG Ref	62	44	0.039 (0.99)	0.050 (1.27)	168.9 (6.65)	143.5 (5.65)	10.90	13.05
RG w/FA	44	50	0.046 (1.17)	0.043 (1.09)	168.2 (6.62)	174.3 (6.86)	16.03	14.62
RG w/SF	53	NT	0.039 (0.99)	NT	191.3 (7.53)	NT	14.74	NT
RG w/FA&SF	40	NT	0.056 (1.42)	NT	127.1 (5.00)	NT	13.16	NT
PCG Ref	88	61	0.033 (0.84)	0.045 (1.14)	170.2 (6.70)	134.4 (5.29)	7.74	8.82
PCG w/FA	73	66	0.043 (1.09)	0.046 (1.17)	125.6 (4.94)	122.8 (4.83)	7.10	7.67
PCG w/SF	27	NT	0.074 (1.88)	NT	106.2 (4.18)	NT	16.06	NT
PCG w/FA&SF	66	NT	0.043 (1.09)	NT	140.2 (5.52)	NT	8.94	NT
GR Ref	52	57	0.039 (0.99)	0.038 (0.97)	192.0 (7.56)	187.0 (7.36)	14.78	13.13
GR w/FA	40	NT	0.047 (1.19)	NT	170.1 (6.70)	NT	17.25	NT
GR w/SF	40	NT	0.046 (1.17)	NT	181.7 (7.15)	NT	18.56	NT
GR w/FA&SF	21	31	0.062 (1.57)	0.054 (1.37)	171.7 (6.76)	166.3 (6.55)	33.27	21.83
LS-H Ref	32	41	0.048 (1.22)	0.052 (1.32)	193.8 (7.63)	139.6 (5.50)	24.23	13.62
LS-H w/FA&SF	56	41	0.042 (1.07)	0.049 (1.24)	165.4 (6.51)	160.1 (6.30)	12.23	16.16
LS-L Ref	28	63	0.052 (1.32)	0.040 (1.02)	186.5 (7.34)	156.4 (6.16)	26.66	9.93
LS-L w/SF	43	40	0.052 (1.32)	0.054 (1.37)	140.0 (5.51)	137.1 (5.40)	13.52	14.24
LS-L w/FA&SF	51	39	0.041 (1.04)	0.047 (1.19)	185.7 (7.31)	173.8 (6.84)	14.82	18.14

NT Indicates measurement not tested.

* Total length traversed = 55 in (1400 mm).

Table 4.5: Specimen Air-void Parameters, continued

Mix	Total # air voids*		Spacing Factor inch (mm)		Specific Surface inch^{-1} (mm^{-1})		Paste to Air Ratio	
	heat-cured	moist-cured	heat-cured	moist-cured	heat-cured	moist-cured	heat-cured	moist-cured
PHASE II MIXES (specimens not tested for freeze-thaw durability)								
(RG Ref)R	69	74	0.034 (0.86)	0.031 (0.79)	205.1 (8.07)	223.0 (8.78)	12.2	12.4
(RG w/SF)R	74	50	0.039 (0.99)	0.038 (0.97)	159.9 (6.30)	224.5 (8.84)	9.5	19.6
(RG w/SF)AE	349	193	0.012 (0.30)	0.019 (0.48)	405.6 (15.97)	264.8 (10.43)	5.3	6.0
(LS-H Ref)R	47	35	0.054 (1.37)	0.058 (1.47)	119.2 (4.69)	133.1 (5.24)	10.5	15.7
(LS-H w/SF)	69	44	0.043 (1.09)	0.053 (1.35)	134.7 (5.30)	134.9 (5.31)	8.2	12.9
(LS-H w/FASF)R	43	40	0.055 (1.40)	0.056 (1.42)	125.5 (4.94)	130.4 (5.13)	12.2	13.6
(LS-L Ref)R	53	53	0.037 (0.94)	0.045 (1.14)	217.2 (8.55)	149.9 (5.90)	17.0	11.7

NT Indicates measurement not tested.
* Total length traversed = 55 in (1400 mm).

mm) recommended for durable concrete. The Phase II concrete mix that was air-entrained also produced spacing factors greater than 0.008 in (0.20 mm). Table 4.5 shows that the Phase II air void system parameters were generally similar to the Phase I air void system parameters, allowing for the variability of entrapped air voids. With intentional air-entraining, the air voids are usually well-distributed through the concrete; entrapped air voids (in non-air-entrained concrete) are generally much larger in size and randomly distributed through the specimen.

The air void parameters of the round gravel concrete specimens of Phase II were slightly different from the Phase I concrete specimens. The specific surface measurements of the round

gravel reference mix were much larger in the Phase II concrete specimens than in the Phase I concrete specimens, indicating the presence of more small entrapped air voids. Generally, the spacing factors of the moist-cured concrete specimens were greater than the spacing factors of the heat-cured specimens. Generally, the reference concrete mixes had smaller spacing factors and more total air-voids than the companion mixes containing fly ash and/or silica fume (except for the limestone concrete mixes). The smaller spacing factor may be due to the ability of the fly ash and silica fume to fill the voids in the concrete with additional hydration products as well as unreacted material. For the limestone aggregate concrete, the spacing factors of the limestone reference mixes were greater than the spacing factors of the reference mixes of the gravel and granite aggregate. However, the spacing factors of the limestone concrete mixes containing silica fume were less than the spacing factors of the gravel and the granite silica fume and fly ash with silica fume concrete mixes.

Table 4.6 provides the air content measured in the fresh concrete and the air content in the hardened concrete determined from linear traverse. Figure 4.7 is a plot of the air content measured in the hardened concrete versus the air measured in the fresh concrete. There was generally a good correlation between these two measurements. In the cases where there was a large difference in the measurements, such as the Phase I low-absorption limestone reference mix, which measured 2.93 percent for the moist-cured and 1.09 percent for the heat-cured hardened concrete while the fresh concrete had 1.5 percent air content (see Table 4.6), more large air-voids were present in the particular cross section taken from the moist-cured beam specimen. In this study, the air content is a measure of the entrapped air in the concrete (since

Table 4.6: Air Content in Fresh and Hardened Concrete

Mix	Air in Fresh Concrete (%)	Air in Hardened Concrete, (%)	
		heat-cured	moist-cured
PHASE I MIXES			
RG Ref	2.0	2.67	2.23
RG w/FA	2.5	1.90	2.09
RG w/SF	1.5	2.02	NT
RG w/FA&SF	1.5	2.29	NT
PCG Ref	1.5	3.76	3.30
PCG w/FA	2.0	4.23	3.91
PCG w/SF	1.5	1.85	NT
PCG w/FA&SF	2.0	3.42	NT
GR Ref	1.5	1.97	2.22
GR w/FA	1.5	1.71	NT
GR w/SF	1.5	1.60	NT
GR w/FA&SF	1.0	0.89	1.36
LS-H Ref	1.5	1.20	2.14
LS-H w/FA&SF	1.5	2.46	1.86
LS-L Ref	1.5	1.09	2.93
LS-L w/SF	2.0	2.23	2.12
LS-L w/FA&SF	1.0	2.00	1.63
PHASE II MIXES			
(RG Ref)R	2.0	2.45	2.41
(RG w/SF)R	3.5	3.37	1.62
(RG w/SF)AE	5.0	6.26	5.30
(LS-H Ref)R	2.0	2.87	1.91
(LS-H w/SF)	2.0	3.73	2.37
(LS-H w/FA&SF)R	1.5	2.49	2.23
(LS-L Ref)R	2.0	1.77	2.57

NT Indicates measurement not tested.

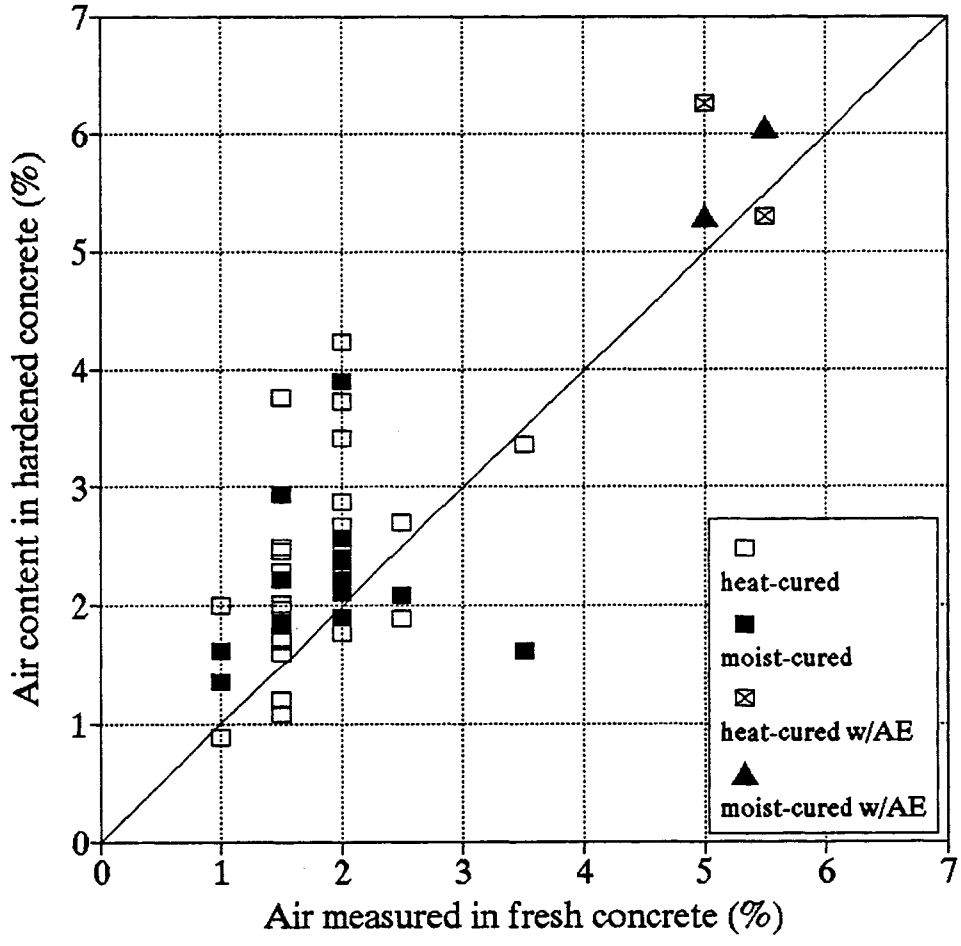

Figure 4.7 Air content in hardened concrete vs. measured air in fresh concrete: heat- and moist-cured Phase I and Phase II mixes

all but two mixes have no air-entrainment).

PHASE I FREEZE-THAW TEST RESULTS

The average number of cycles after which the failure criteria were met and the corresponding average durability factor for each pair of specimens are given in Table 4.7. Measurements for each specimen may be found in Appendix G. Generally, the specimen measurements were very close to one another (Figure 4.8). In the cases where the measurements differed considerably (Figure 4.9), both measurements are given. All of the plots of Relative Dynamic Modulus versus cycles of freezing and thawing are given for each specimen, similar to Figures 4.8 and 4.9, in Appendix C.

In Table 4.7, the number of "cycles to observed failure" are given for both the relative dynamic modulus and the dilation failure criteria. As can be seen in the table, there is generally a strong correlation between the two failure criteria. However, the dilation criterion in the limestone aggregate concrete mixes was generally reached much more quickly than the relative dynamic modulus criterion (e.g. the heat-cured LS-L w/SF mix failed dilation at 229 cycles and lasted 640 cycles before RDM failure). This may be due to the ability of the more porous limestone to expand with the expanding cement mortar (without failing the relative dynamic modulus criterion) when compared to concrete containing the harder gravel and granite aggregates. More importantly, it suggests that the limestone aggregates developed a stronger bond with the mortar, allowing dilation without cracking (failing) at the transition zone between

Table 4.7: Phase I Freeze-Thaw Test Results

Mix	Age placed in freeze-thaw testing machine* (days)	Cycles to Observed RDM Failure *Length Change Failure*		Durability Factor	
		heat-cured	moist-cured	heat-cured	moist-cured
RG Ref	228	34 *34*	80 *80*	5	14
RG w/FA	251	26 *30*	85 *85*	5	15
RG w/SF	242	34 *34*	26 *30*	6	5
RG w/FA&SF	237	48 *41*	26 *26*	7	4
PCG Ref	214	71 *62*	1507+(346) *1507+(346)*	12	97
PCG w/FA	214	55 *48*	201 *180*	10	40
PCG w/SF	210	30 *26*	26 *26*	4	2
PCG w/FA&SF	210	68 *58*	35 *38*	12	6
GR Ref	210	46 *30*	52 *48*	9	9
GR w/FA	210	53 *53*	59 *62*	10	11
GR w/SF	210	30 *30*	20 *20*	3	2
GR w/FA&SF	210	53 *53*	19 *22*	10	4
LS-H Ref	223	469(149) *59*	1507+ *1507+(1132)*	66(30)	97
LS-H w/FA&SF	216	119 *62*	26 *26*	24	5
LS-L Ref	210	1520+ *1520+(1166)*	1520+ *1520+*	96	98
LS-L w/SF	210	640 *229*	1510+ *420(240)*	77	81
LS-L w/FA&SF	210	308 *161*	1366 *116*	61	71

* Age = (210 days) + (days frozen prior to testing).

\+ Indicates that the specimens had not yet failed the test criteria.

( ) Indicates value for companion specimen if different.

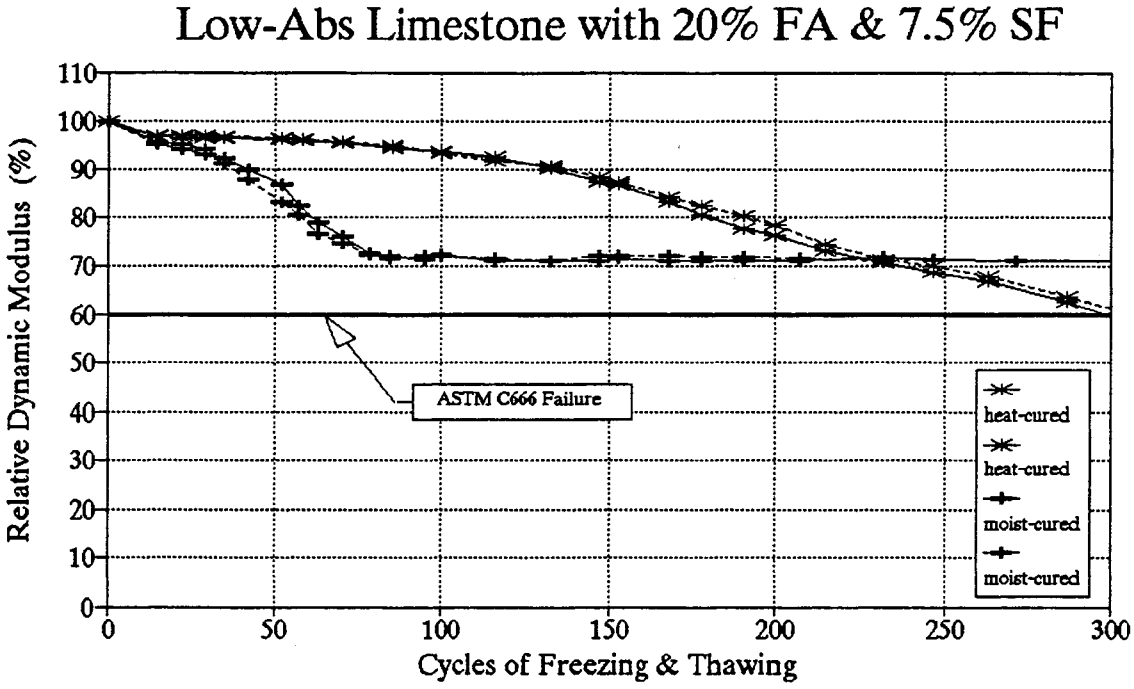

Figure 4.8 Relative Dynamic Modulus vs. cycles of freezing and thawing: Low-absorption limestone with 20% fly ash and 7.5% silica fume mix

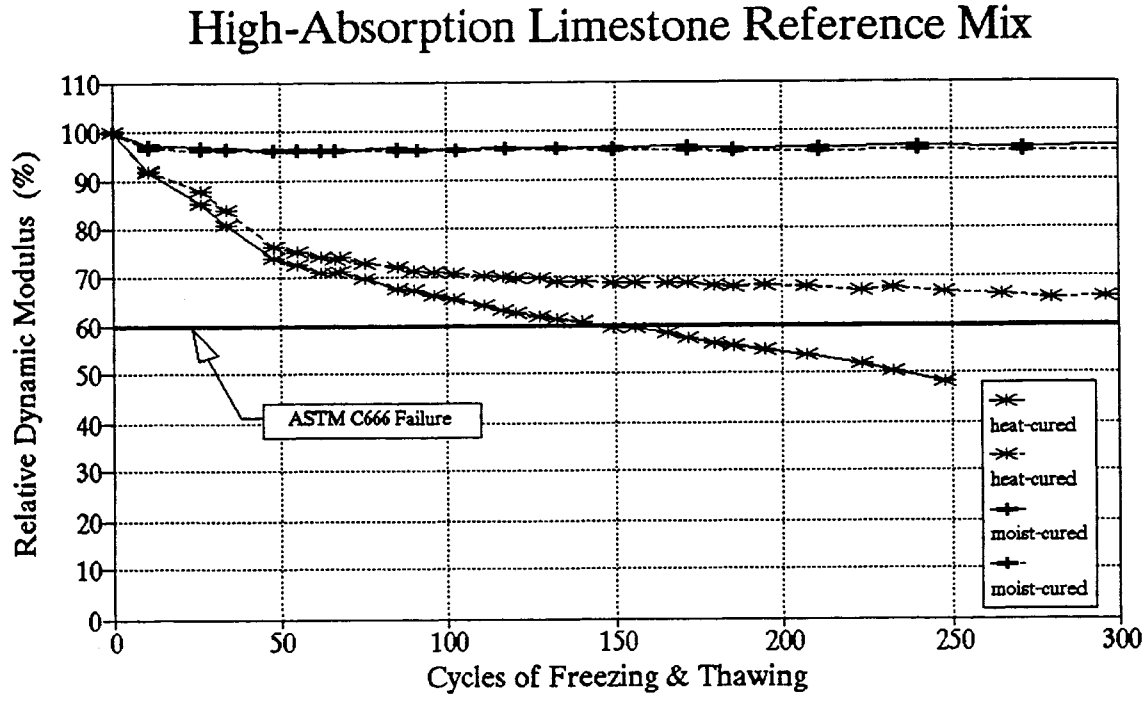

Figure 4.9 Relative Dynamic Modulus vs. cycles of freezing and thawing: High-absorption limestone reference mix

the aggregate and the cement paste. Furthermore, it demonstrates the strength of the aggregate itself and the strength of the surrounding cement paste, each able to withstand the possibly high tensile forces due to the expansion.

Table 4.8 gives the length change and the weight change of the concrete specimens at the cycle the RDM failure was observed. Representative plots of RDM versus percent length change are given in Figures 4.10 and 4.11 for the heat-cured round gravel and high-absorption limestone concrete specimens. Figure 4.10 shows that the round gravel concrete specimens failed both criteria at approximately the same time. Figure 4.11 shows that the limestone concrete specimens failed the dilation criterion much sooner than the relative dynamic modulus criterion. The complete set of plots of RDM versus Length Change and RDM versus Weight Change are given in Appendix C.

The durability factors for the heat- and moist-cured specimens from Table 4.7 are presented graphically in Figures 4.12 (a) and (b), respectively. Results shown in these figures are grouped according to aggregate type and cementitious material composition. Generally, the moist-cured concrete specimens exhibited better frost resistance than the heat-cured concrete specimens. In terms of aggregate type, the limestone concrete specimens showed the best performance. Regarding cementitious material composition, the reference mixes performed better than the mixes containing pozzolan. Detailed descriptions of these effects are presented in the following sections.

Table 4.8: Length and Weight Change at Cycle RDM Failure Observed

Mix	Length Change (%)		Weight Change (%)	
	heat-cured	moist-cured	heat-cured	moist-cured
PHASE I MIXES				
RG Ref	0.148*	0.120	0.334	0.251
RG w/FA	0.097	0.117	0.224	0.244
RG w/SF	0.100	0.093	0.426	0.273
RG w/FA&SF	0.174	0.172*	0.542	0.337
PCG Ref	0.200	0.008 *(101, 1507)** 0.125*	0.501	-0.196 *(101, 1507)** 0.117*
PCG w/FA	0.168	0.139	0.426	0.264
PCG w/SF	0.199	0.215*	0.642	0.344
PCG w/FA&SF	0.186	0.112	0.709	0.340
GR Ref	0.163	0.171*	0.287	0.312
GR w/FA	0.131	0.113	0.393	0.284
GR w/SF	0.182	0.148	0.535	0.309
GR w/FA&SF	0.121	0.383	0.368	0.227
LS-H Ref	0.211*	0.127 *(85, 1507)*	0.490	0.198 *(85, 1507)*
LS-H w/FA&SF	0.252*	0.114	0.524	0.216
LS-L Ref	0.042 *(101, 1520)** 0.135 *(87,1520)**	0.020 *(101, 1520)*	0.060 *(101, 1520)** 0.346 *(87, 1520)**	-0.109 *(101, 1520)*
LS-L w/SF	0.245	0.201 *(79, 1511)*	0.709	0.428 *(79, 1511)*
LS-L w/FA&SF	0.320*	0.379*	0.774	0.793

* Indicates measurement for one beam specimen (not an average of two measurements).

(a,b) Indicates measurement on beam specimen that did not fail RDM criterion. Measurement taken at RDM value = *a* and at cycle = *b*.

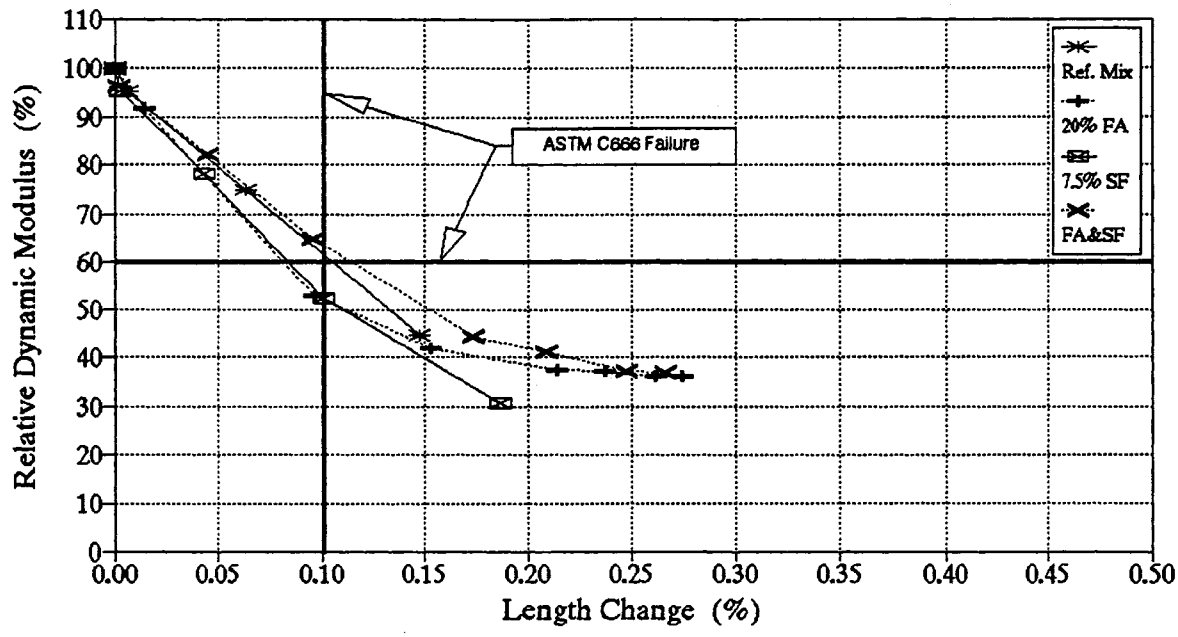

Figure 4.10 Relative Dynamic Modulus vs. Length Change: Heat-cured round gravel mixes

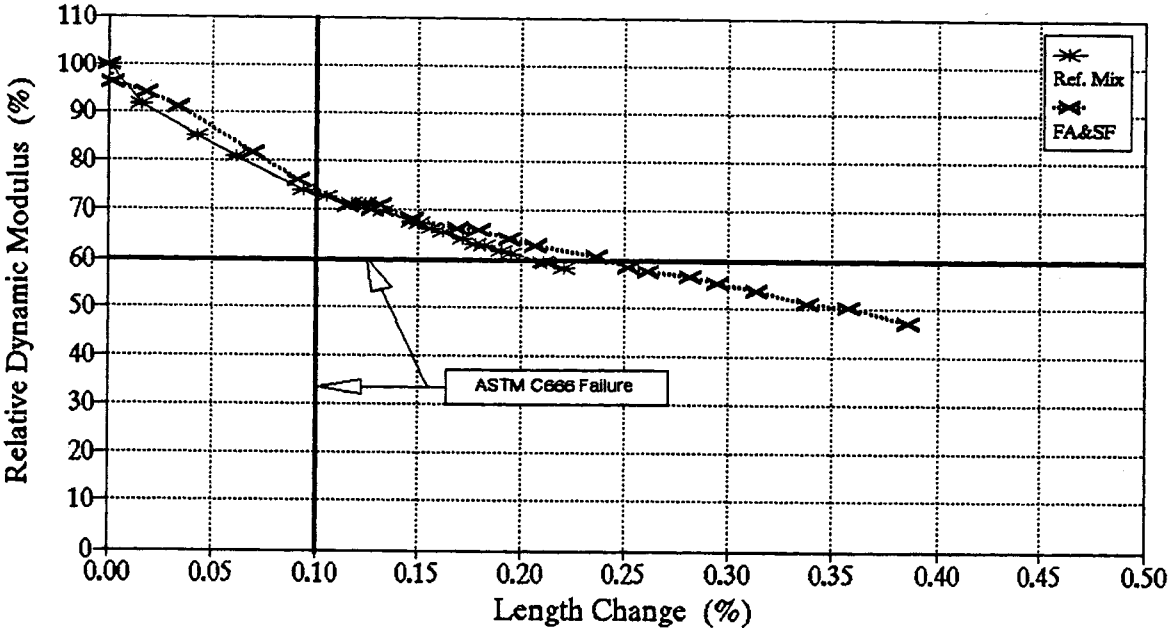

Figure 4.11 Relative Dynamic Modulus vs. Length Change: Heat-cured high-absorption limestone mixes

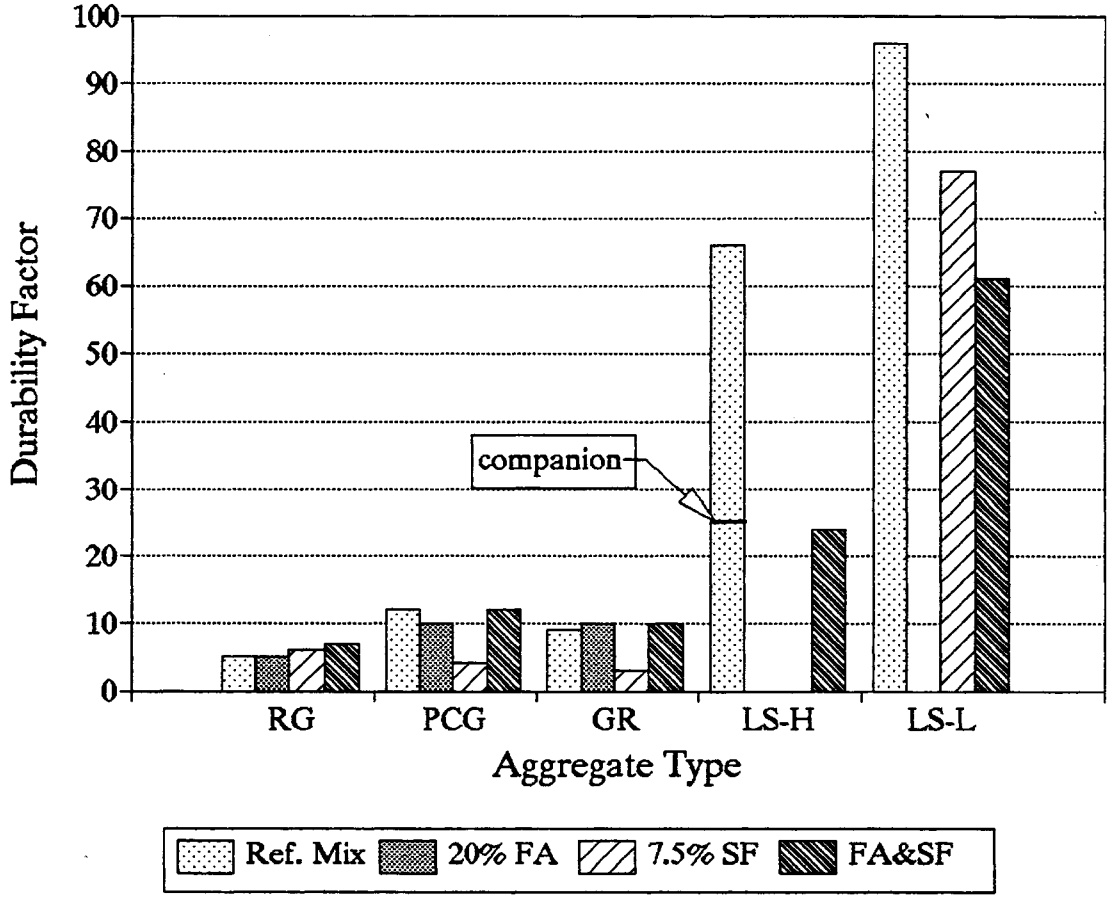

Figure 4.12 (a) Freeze-thaw durability: Phase I heat-cured specimens

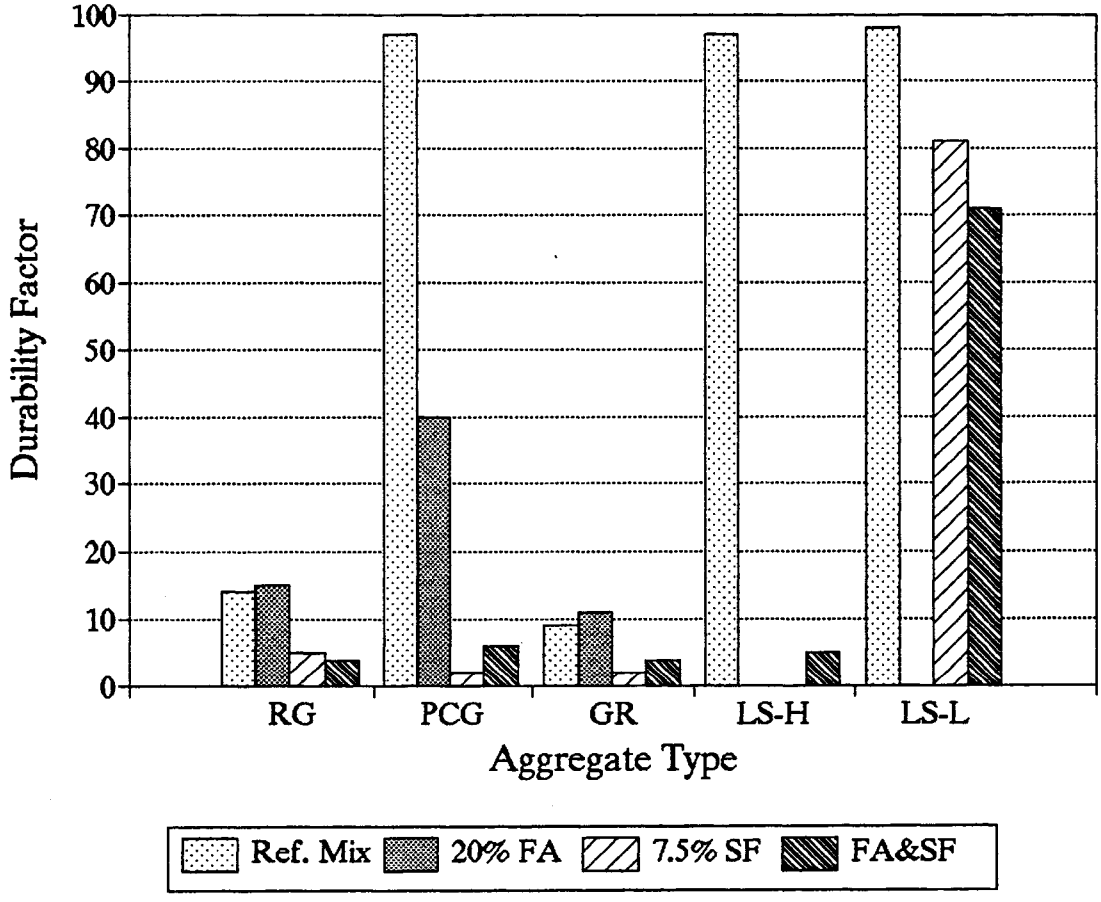

Figure 4.12 (b) Freeze-thaw durability: Phase I moist-cured specimens

Effect of Curing Condition

The water weight gain measurements after the concrete freeze-thaw specimens were immersed in the constant temperature water bath served as a good predictor of freeze-thaw test performance; the concrete specimens that had gained the most water performed worst. In the reference concrete mixes and the 20 percent fly ash concrete mixes, the moist-cured specimens absorbed less water than the heat-cured specimens (Table 4.3) and performed better in terms of durability. Whereas in the mixes containing silica fume (i.e. the 7.5 percent silica fume and the 20 percent fly ash with 7.5 percent silica fume), the heat-cured specimens absorbed less water (Table 4.3) and performed slightly better than the moist-cured specimens. Figures 4.13(a) and (b) are plots of the weight gain versus the cycles of freezing and thawing that show this behavior. The plot given is for the heat- and moist-cured partially-crushed gravel concrete mixes; the complete set of plots for all of the Phase I concrete mixes are given in Appendix C. Figure 4.13 (a) shows that all of the heat-cured concrete specimens gained water weight at approximately the same rate. However, Figure 4.13 (b) shows that the moist-cured reference and 20 percent fly ash concrete mixes did not gain water weight at the rate that the concrete mixes containing silica fume did and performed better in the test.

In the instances where the heat-cured specimens did perform better, the durability factors were less than 25 for both the heat- and moist-cured specimens (unsuitable for frost resistance). Both heat- and moist-cured specimens performed satisfactorily (DF > 60) for all low-absorption limestone concrete mixes, although moist-curing appeared to provide better durability.

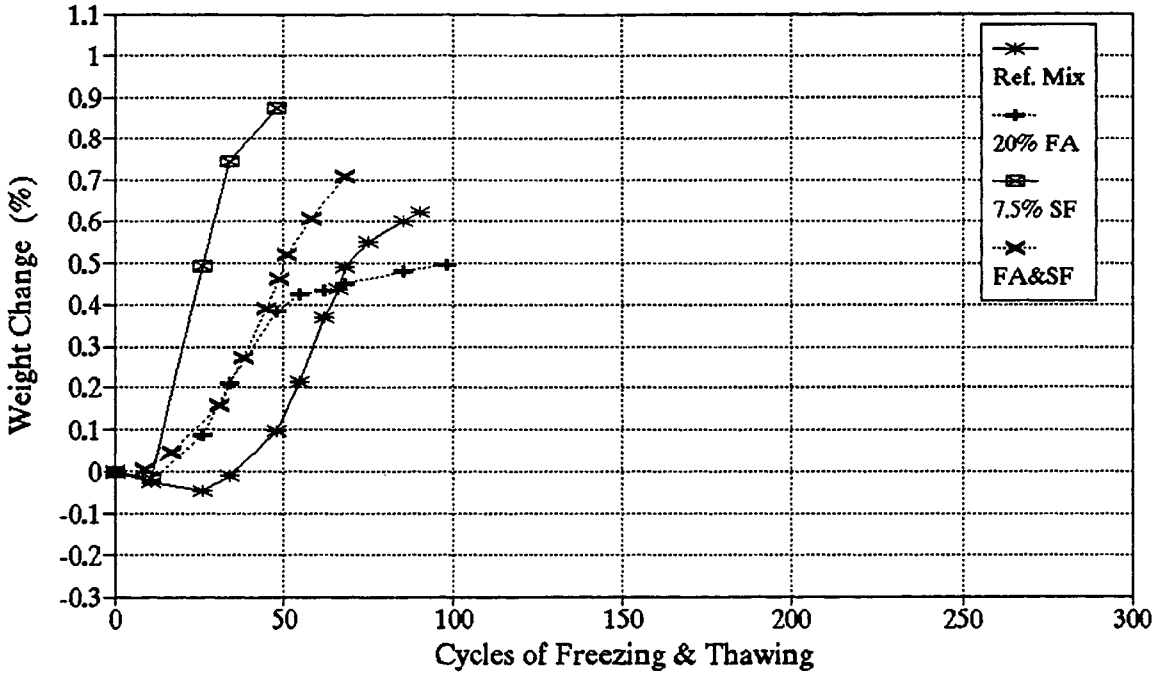

(a) Heat-cured partially-crushed gravel mixes

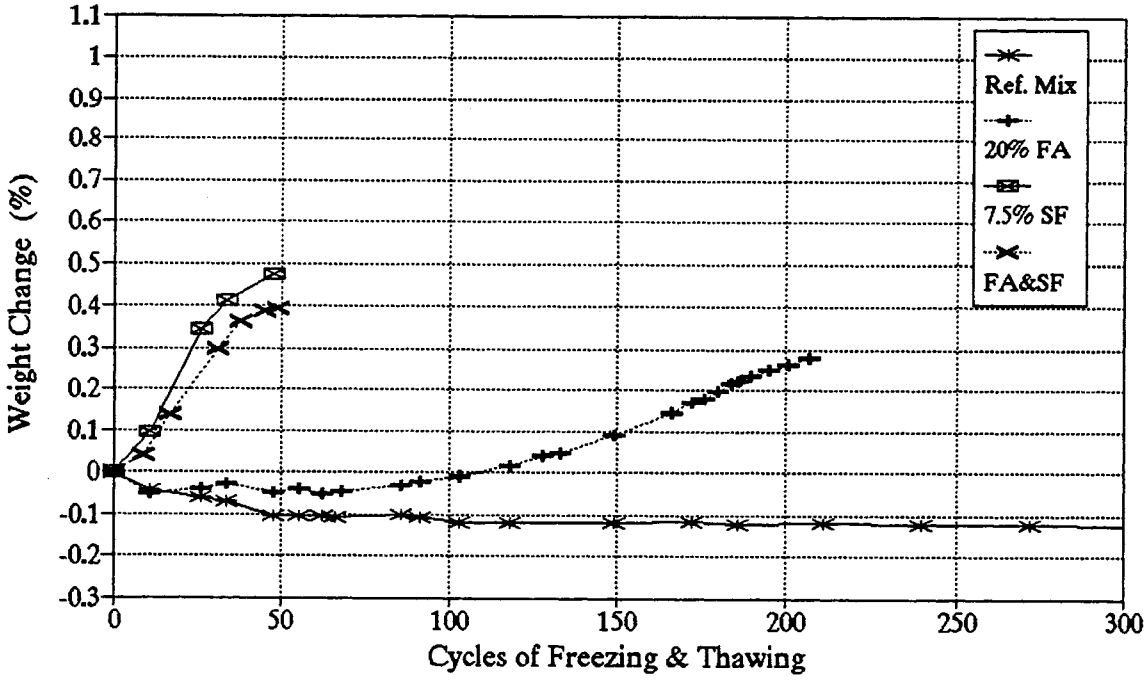

(b) Moist-cured partially-crushed gravel mixes

Figure 4.13 Weight change vs. cycles of freezing and thawing

These observations on the effect of curing condition correlated fairly well with the results of the concrete absorption potential tests in which all moist-cured concrete specimens absorbed less water than the heat-cured concrete specimens. It is expected that the moist-cured concrete specimens would be less permeable than the heat-cured concrete specimens. The moist curing allowed continuous hydration of the cementitious materials, and the concrete developed a less permeable pore structure. The hydration in heat-curing was limited by the amount of mix water. Microcracking could also develop upon drying, weakening the strength of the transition zone between the aggregate and the cement paste. These factors resulted in an increase in permeability. As Figures 4.13(a) and (b) show, moist-curing seems to have provided a less permeable pore structure for the reference and the 20 percent fly ash concrete mixes, but the permeability of the concrete mixes containing silica fume (7.5 percent silica fume and 20 percent fly ash with 7.5 percent silica fume) did not benefit as much from moist-curing.

Effect of Aggregate Type

The low-absorption limestone concrete specimens consistently performed the best of all the specimens (reference, 7.5 percent silica fume, and combination of 20 percent fly ash with 7.5 percent silica fume) for both types of curing, with durability factors ranging from 61 to 98 (Table 4.7). Several of the low-absorption limestone specimens endured more than 1500 freeze-thaw cycles without failing (RDM criterion) before they were removed from the freeze-thaw testing machine. The moist-cured high-absorption limestone and partially-crushed gravel reference concrete mixes also exhibited excellent performance. The round gravel and granite specimens performed the poorest (DF < 15).

The order of performance, with the exception of the limestone aggregate concrete specimens, was consistent with the results of the concrete absorption tests. In other words, the concrete specimens fabricated with limestone aggregate exhibited the highest absorptions, but showed the best performance. This provides evidence of the strong bond that must have developed between the limestone aggregate particles and the cement paste; the limestone concrete absorbed the most water but provided the best freeze-thaw durability. As discussed earlier in this chapter, perhaps the pore sizes of the limestone aggregate were of a size that permitted easy absorption and easy drainage of water. Improved performance of the other mixes correlated with reduced concrete absorption.

Although the limestone concrete specimens achieved high durability factors, they generally failed the dilation criterion quite early compared to the relative dynamic modulus criterion. Dilation of the limestone concrete mixes which failed the ASTM criteria ranged from 0.114 percent to 0.379 percent at RDM failure, where a 0.10 percent length expansion defines failure (see Table 4.8). As previously mentioned, the large dilations observed in the limestone concrete specimens (without failing the RDM criterion) may be attributed to the strength of the bond between the limestone aggregate and the cement paste. It may also, in part, be due to the ability of the more porous limestone to expand with the expanding cement mortar to accommodate the increased volume without failing. It demonstrates the low modulus of the limestone aggregate (enabling it to undergo large deformations) and/or the high strength of the aggregate and surrounding cement paste (enabling them to withstand the possibly high tensile forces created by the expansion). The low-absorption limestone reference mix, however, exhibited excellent freeze-thaw durability in terms of both RDM and dilation, withstanding over

1100 cycles without failing. In the reference concrete mix, the structure of the concrete (including the cement paste, the transition zone and the aggregate) may have consisted of pore sizes that permitted easy flow of water.

Figures showing the Relative Dynamic Modulus versus the number of cycles of freezing and thawing are provided to further aid in the evaluation of aggregate type used in the concrete. Figures 4.14 (a) through 4.17 (b) show results of all Phase I heat- and moist-cured mixes (reference, 20 percent fly ash, 7.5 percent silica fume and 20 percent fly ash with 7.5 percent silica fume, respectively). These figures show that the concrete specimens made with limestone aggregate performed well for both heat- and moist-curing. The performance of the round gravel concrete specimens improved slightly when moist-curing, and the partially-crushed gravel concrete specimens improved greatly when moist-curing for the reference and fly ash mixes and not for the silica fume and fly ash with silica fume mixes, leading to the conclusion that the aggregate was sound; the paste was the critical component in the frost resistance of the concrete. For the concrete specimens containing granite aggregate, no improvement was seen when moist-curing the specimens. The granite aggregate was suspect as the reason for the failure of these specimens and will be discussed in later sections of this chapter.

Effect of Cementitious Composition

Comparing the results in Figures 4.12(a) and (b), it can be seen that the reference mixes generally performed the best for any given aggregate type. For the moist-cured specimens, the reference mixes prepared using limestone and partially-crushed gravel achieved durability factors

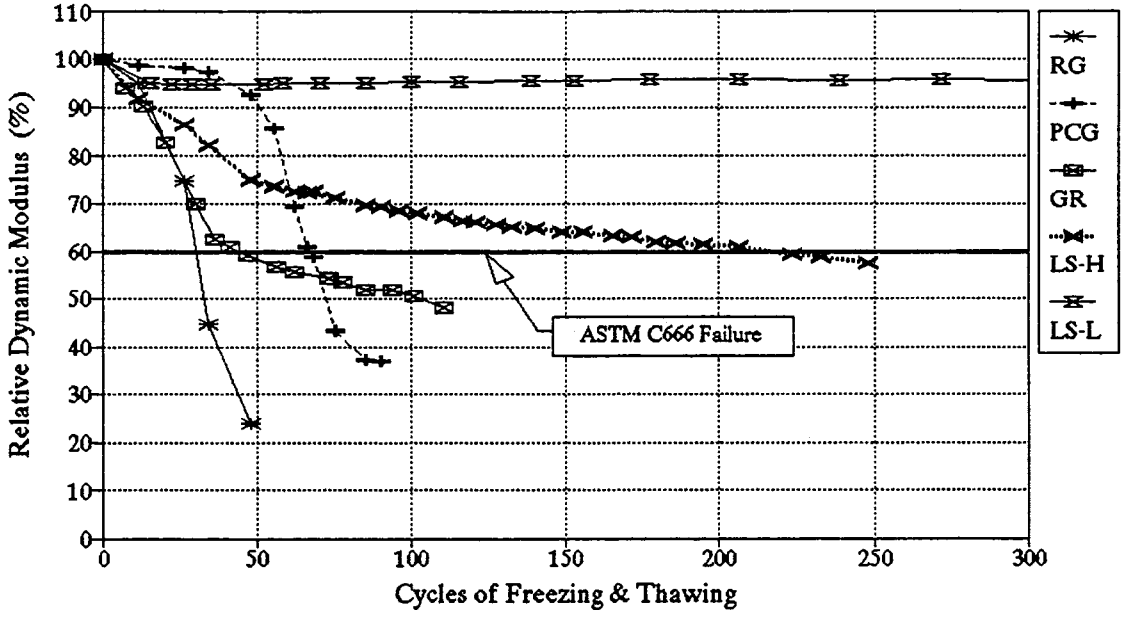

(a) heat-cured reference mixes

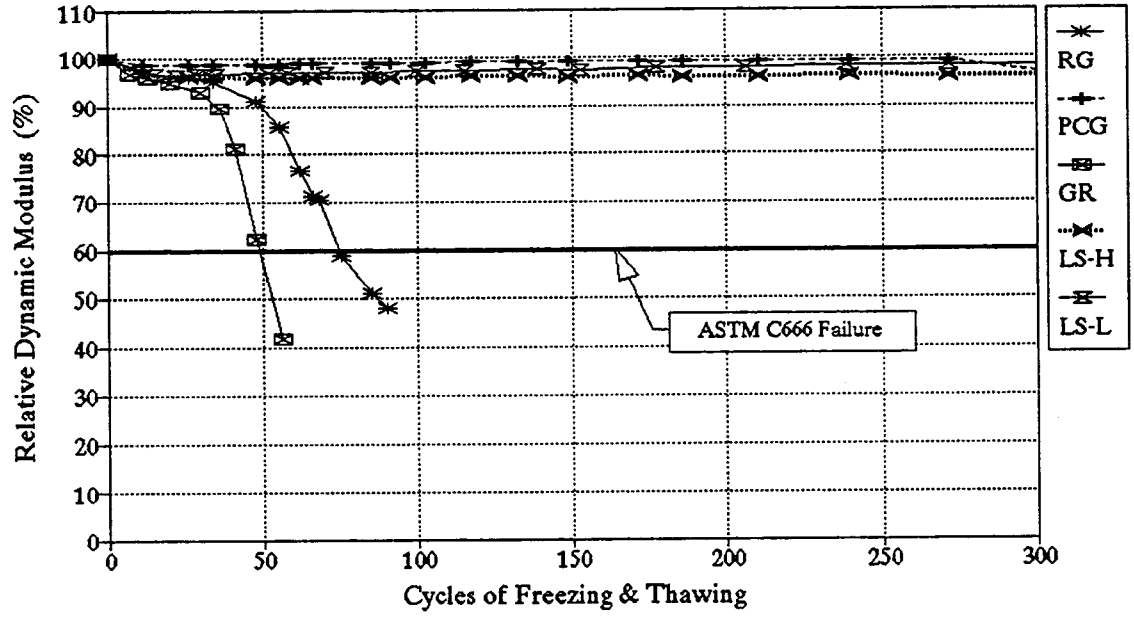

(b) moist-cured reference mixes

Figure 4.14 Relative Dynamic Modulus vs. cycles of freezing and thawing

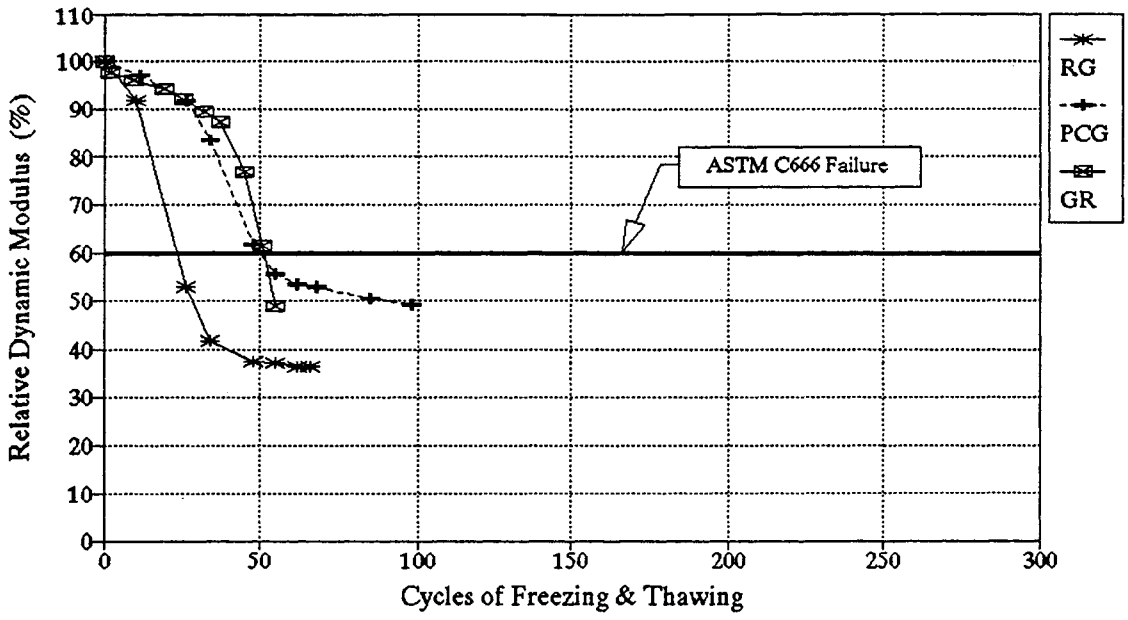

(a) heat-cured 20% fly ash mixes

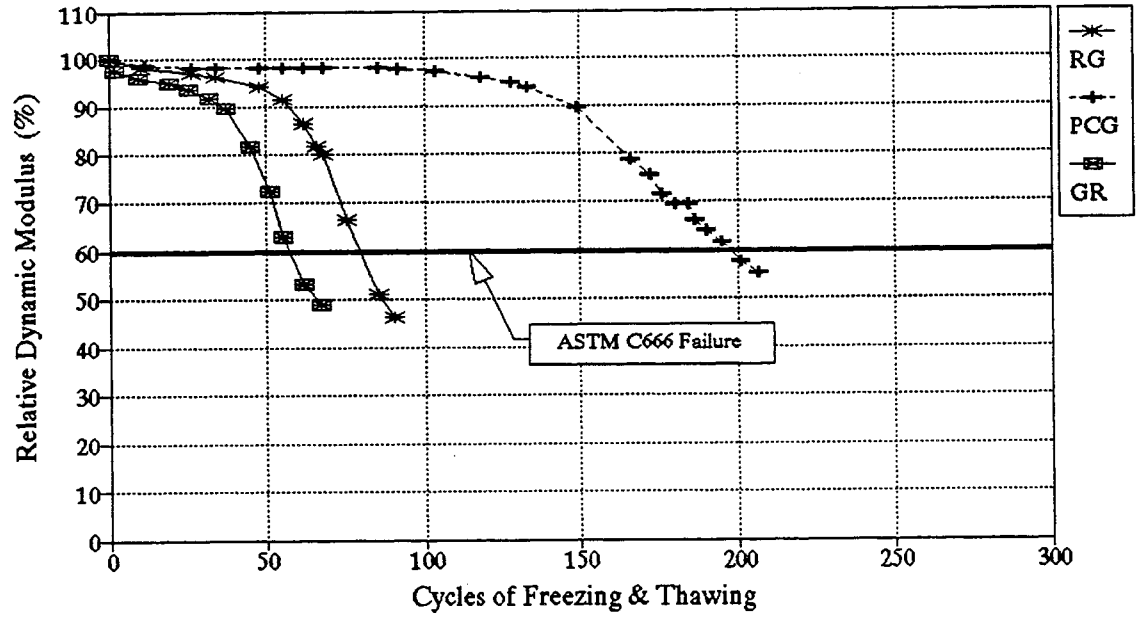

(b) moist-cured 20% fly ash mixes

Figure 4.15 Relative Dynamic Modulus vs. cycles of freezing and thawing

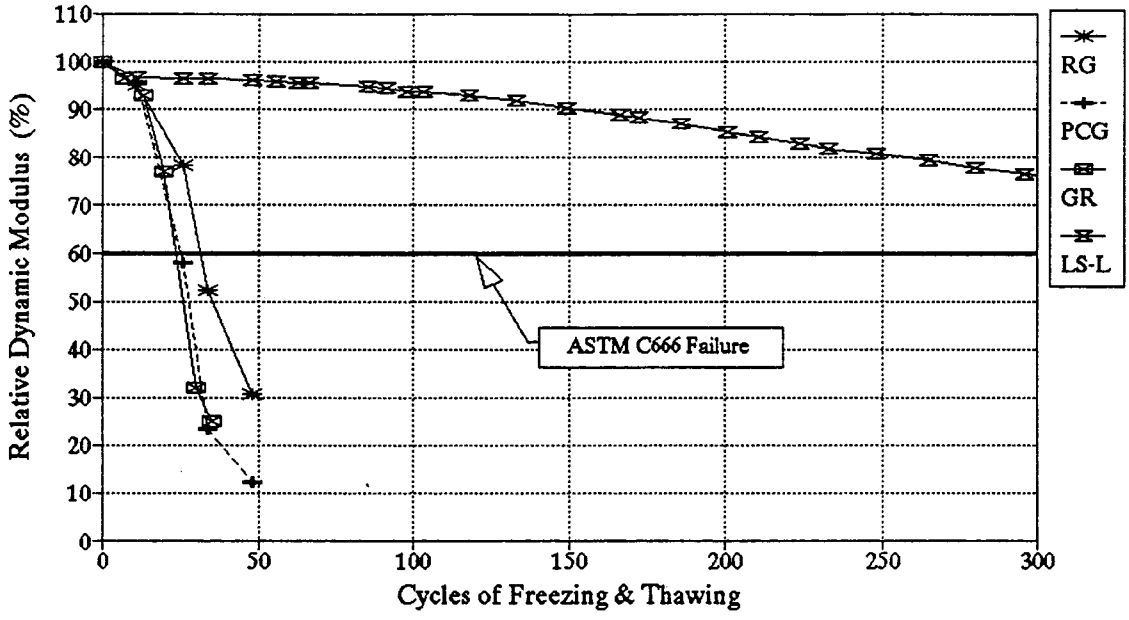

(a) heat-cured 7.5% silica fume mixes

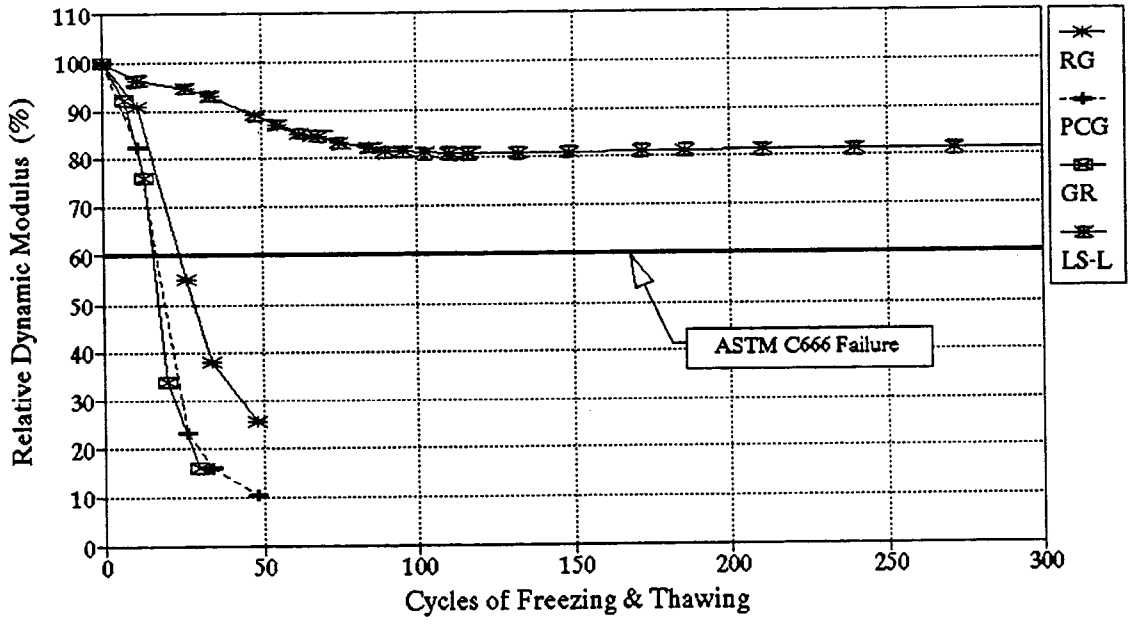

(b) moist-cured 7.5% silica fume mixes

Figure 4.16 Relative Dynamic Modulus vs. cycles of freezing and thawing

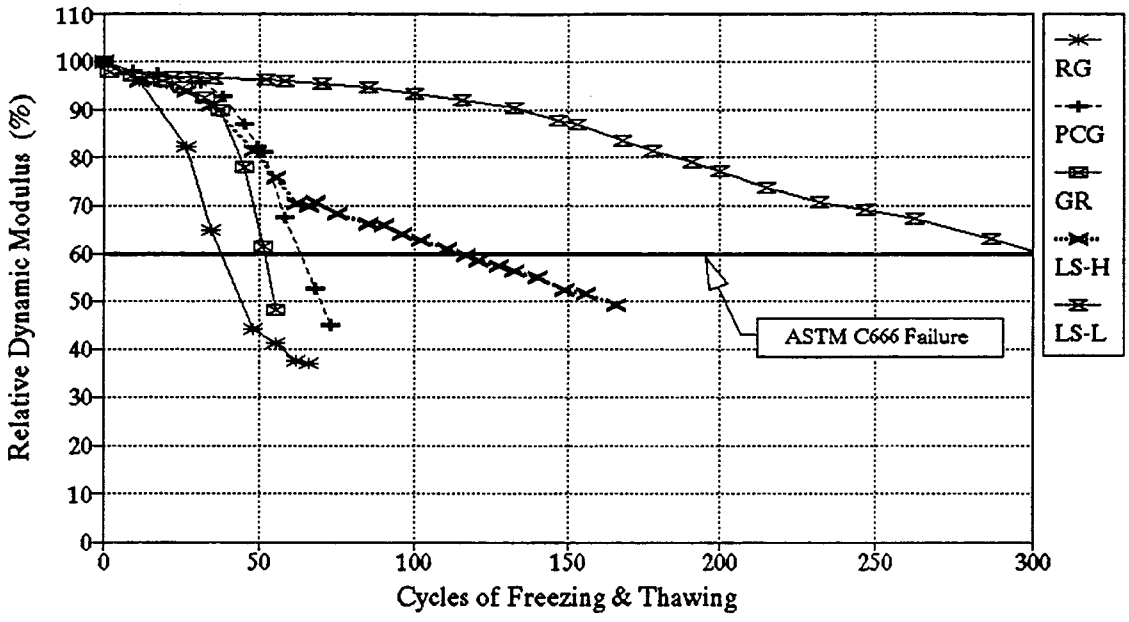

(a) heat-cured 20% fly ash with 7.5% silica fume mixes

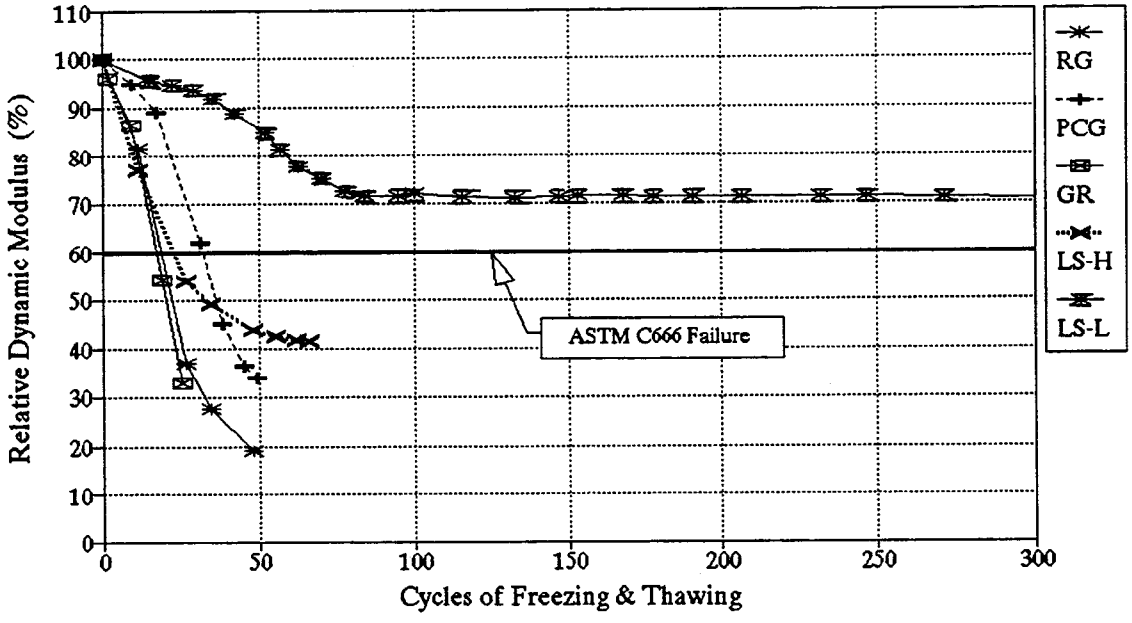

(b) moist-cured 20% fly ash with 7.5% silica fume mixes

Figure 4.17 Relative Dynamic Modulus vs. cycles of freezing and thawing

in excess of 90. The heat-cured limestone reference mixes also generally exhibited satisfactory performance.

For both heat- and moist-cured specimens of the low-absorption limestone, the good performance of the reference mixes was followed by the performances of 7.5 percent silica fume and combination of 20 percent fly ash with 7.5 percent silica fume mixes. Similar results were seen in the heat- and moist-cured high-absorption limestone mixes in which the reference mix exhibited better durability than the 20 percent fly ash with 7.5 percent silica fume combination mix (the 7.5 percent silica fume mix was not investigated for the high-absorption limestone).

For the remaining three aggregates (RG, PCG, GR), the effect of variations in cementitious material composition correlated with curing condition. All of the heat-cured specimens exhibited poor durability (DF=3 to 12). When moist-curing was used, the reference and fly ash mixes performed much better than the mixes containing silica fume, especially for the partially-crushed gravel concrete mixes.

Figures presenting the Relative Dynamic Modulus versus the number of cycles of freezing and thawing are provided to further aid in evaluating the effect of cementitious material composition. Figures 4.18(a) through 4.22(b) show the results of all of the heat- and moist-cured Phase I concrete mixes containing round gravel, partially-crushed gravel, granite, and high- and low-absorption limestone, respectively. In each of these five figures, the benefits of moist-curing are clear for the reference and fly ash concrete specimens, whereas moist-curing did not improve the performance of the concrete specimens containing silica fume.

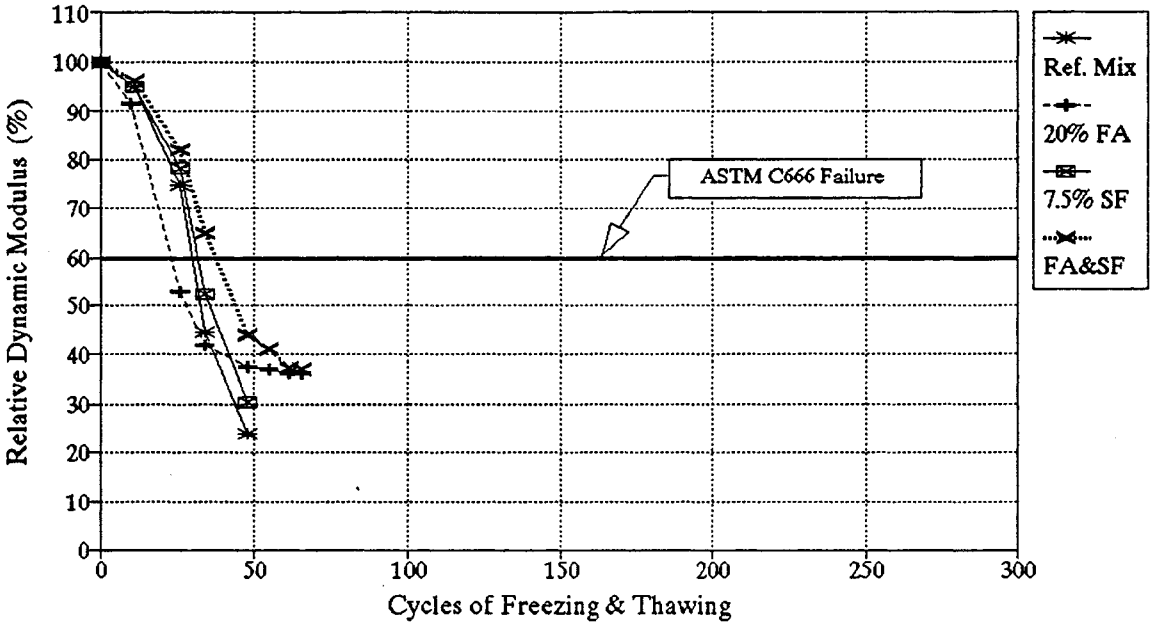

(a) heat-cured round gravel mixes

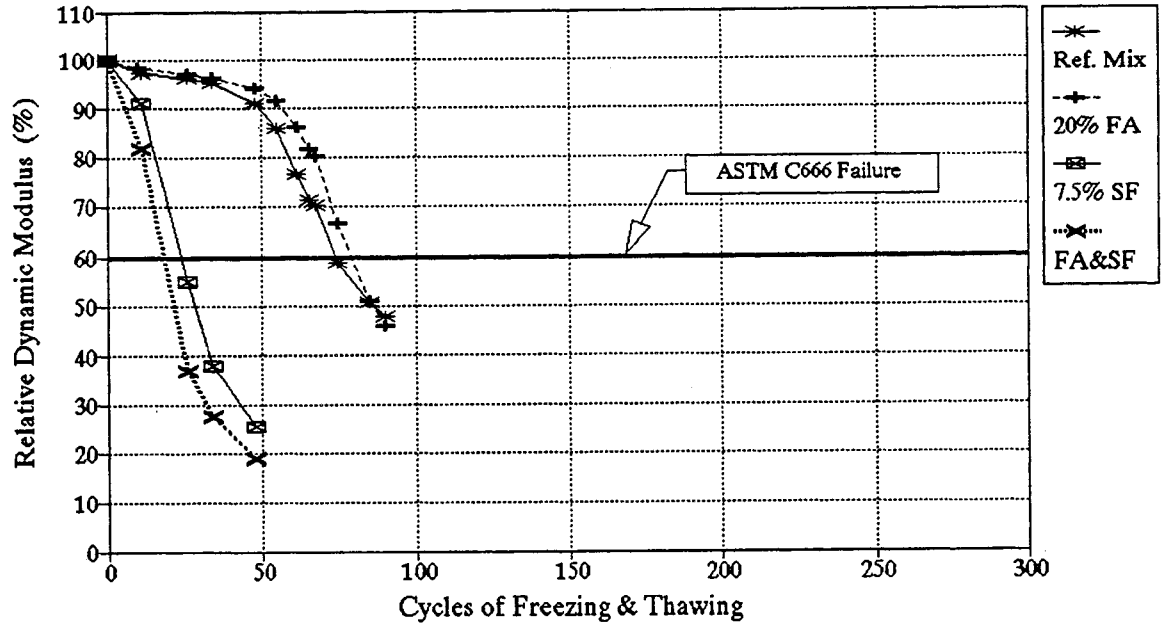

(b) moist-cured round gravel mixes

Figure 4.18 Relative Dynamic Modulus vs. cycles of freezing and thawing

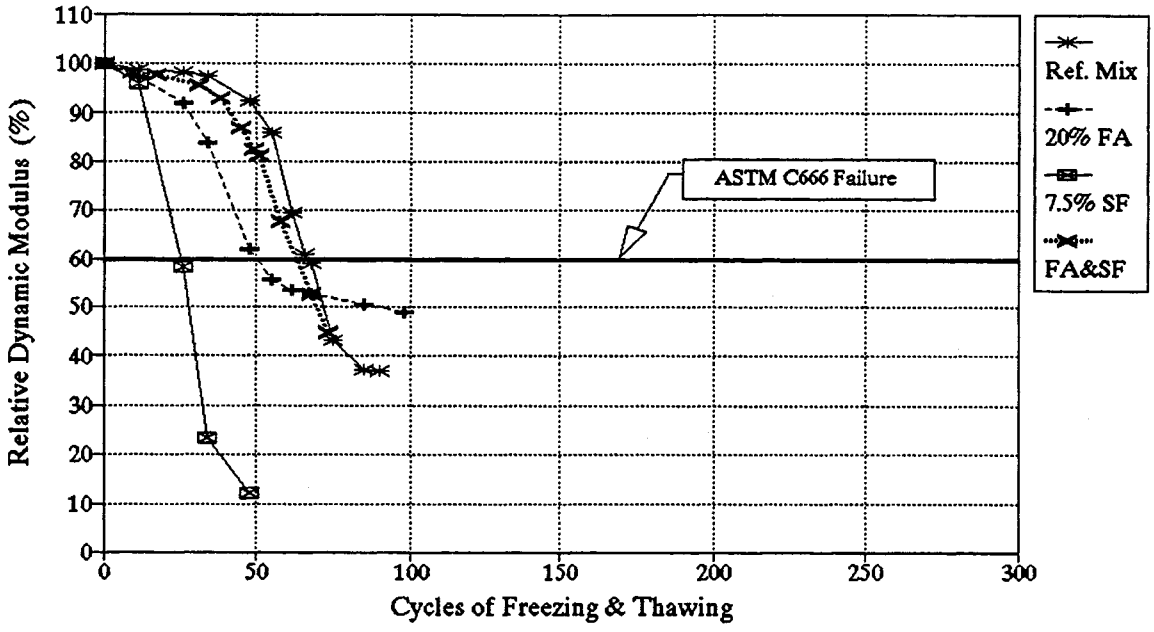

(a) heat-cured partially-crushed gravel mixes

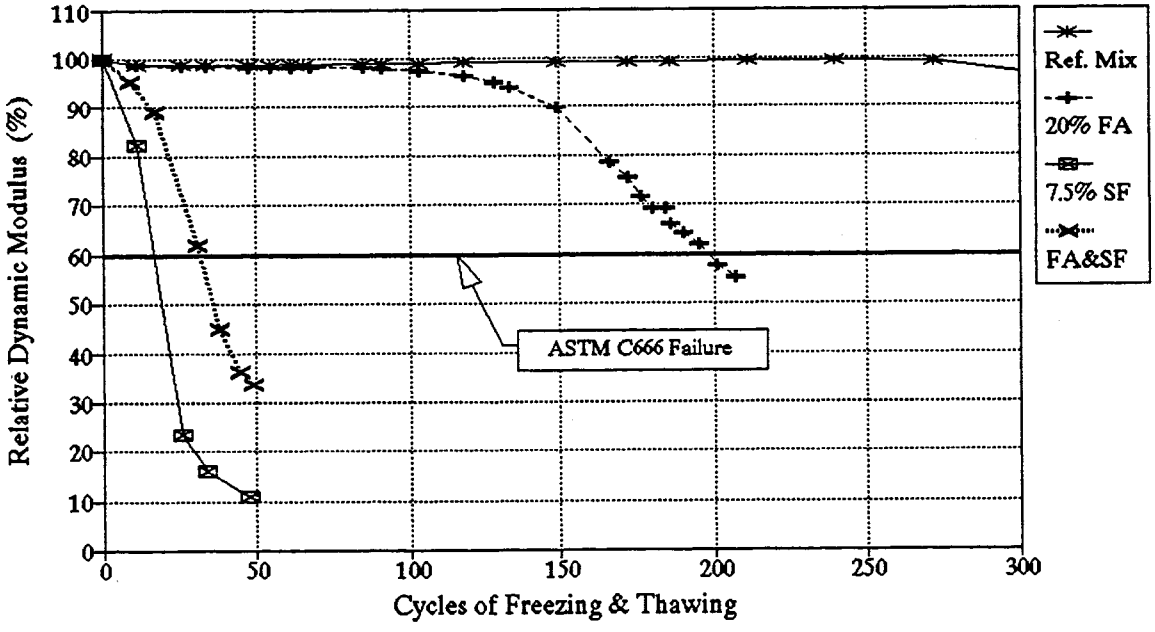

(b) moist-cured partially-crushed gravel mixes

Figure 4.19 Relative Dynamic Modulus vs. cycles of freezing and thawing

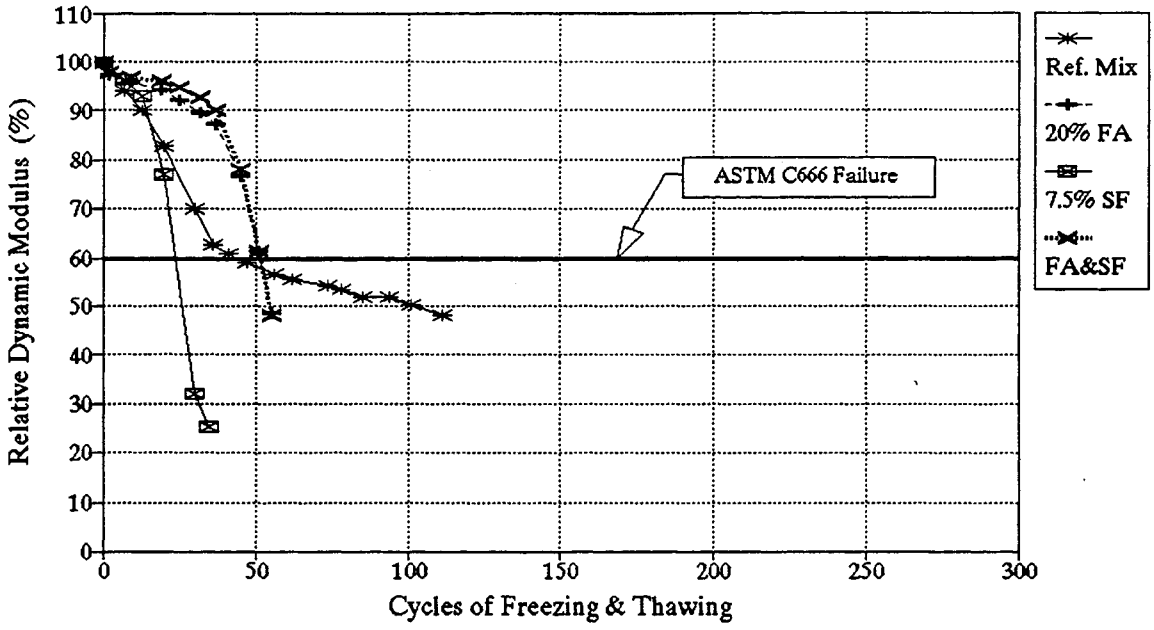

(a) heat-cured granite mixes

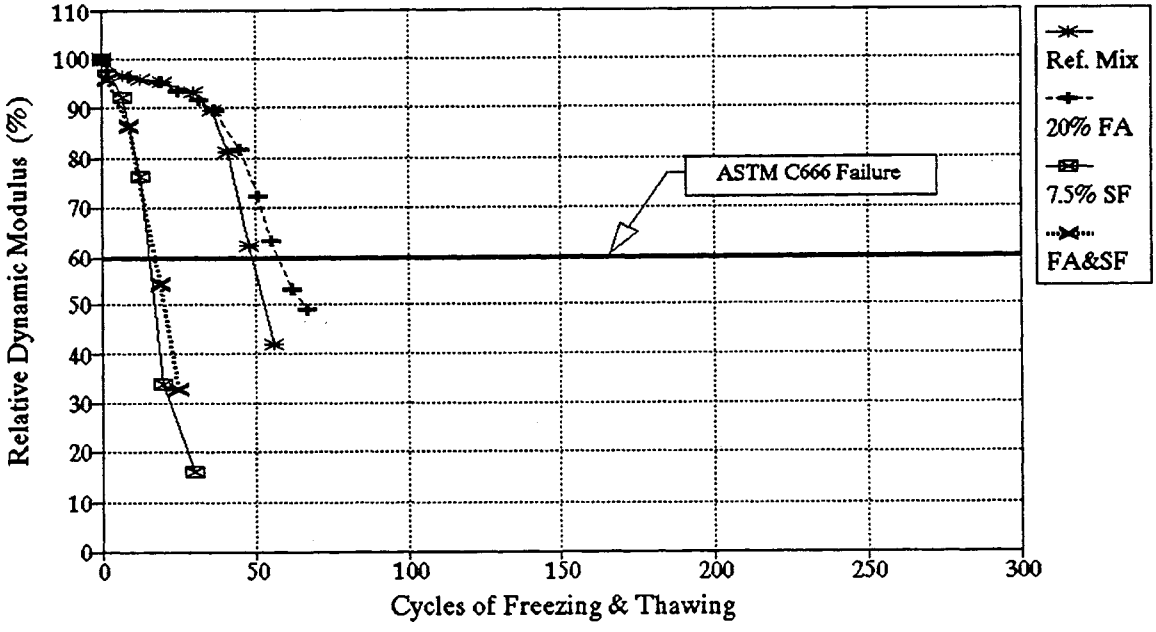

(b) moist-cured granite mixes

Figure 4.20 Relative Dynamic Modulus vs. cycles of freezing and thawing

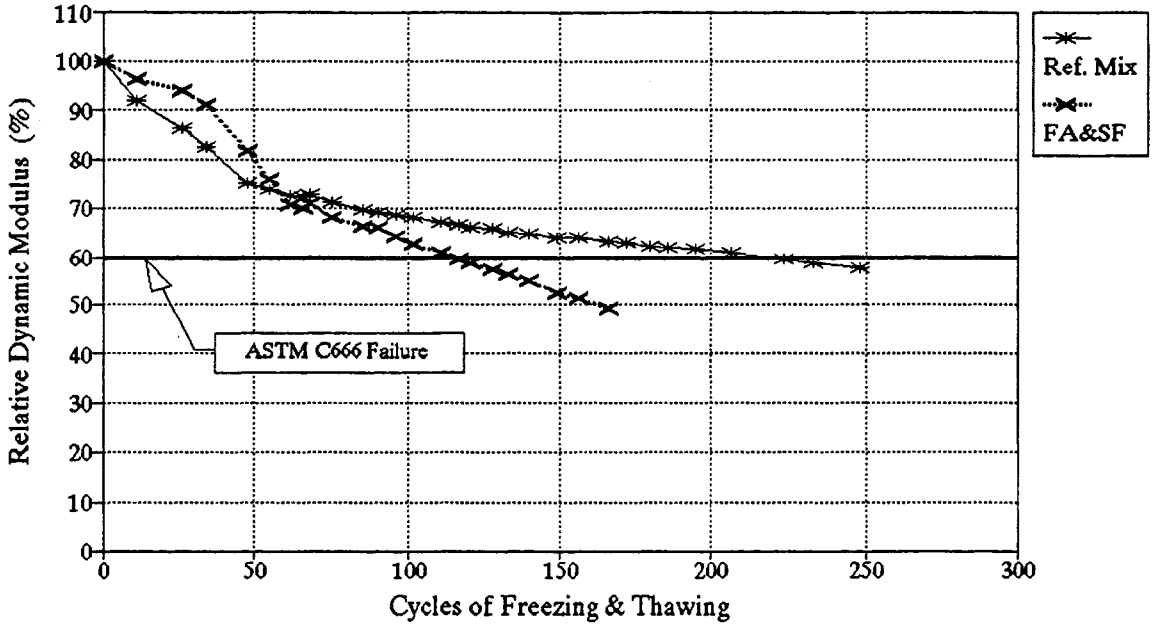

(a) heat-cured high-absorption limestone mixes

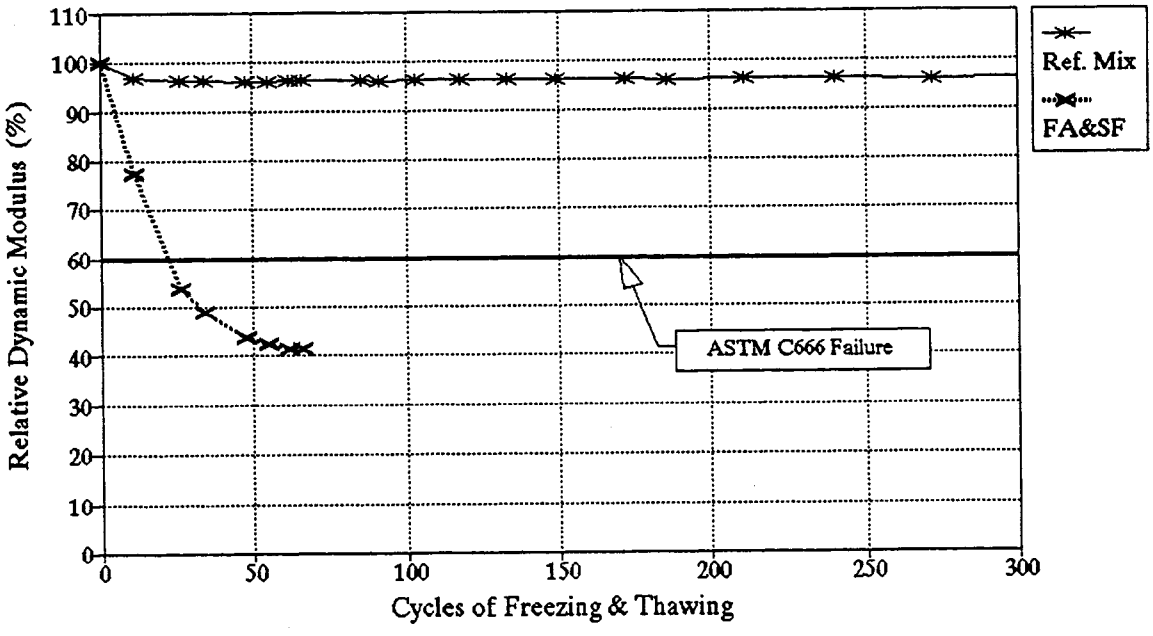

(b) moist-cured high-absorption limestone mixes

Figure 4.21 Relative Dynamic Modulus vs. cycles of freezing and thawing

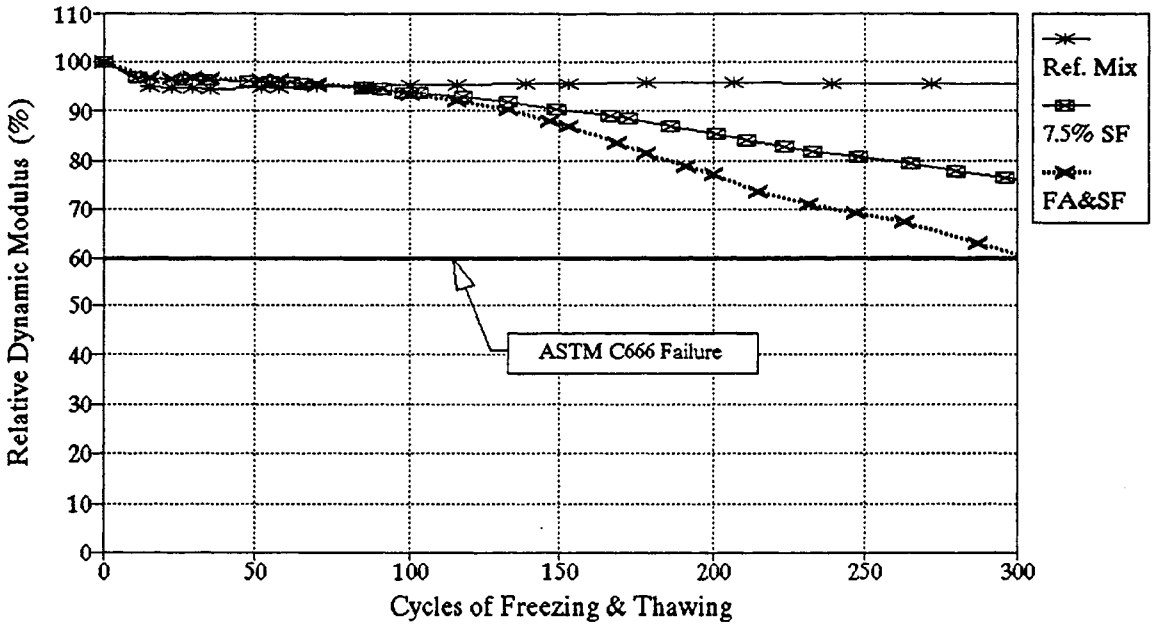

(a) heat-cured low-absorption limestone mixes

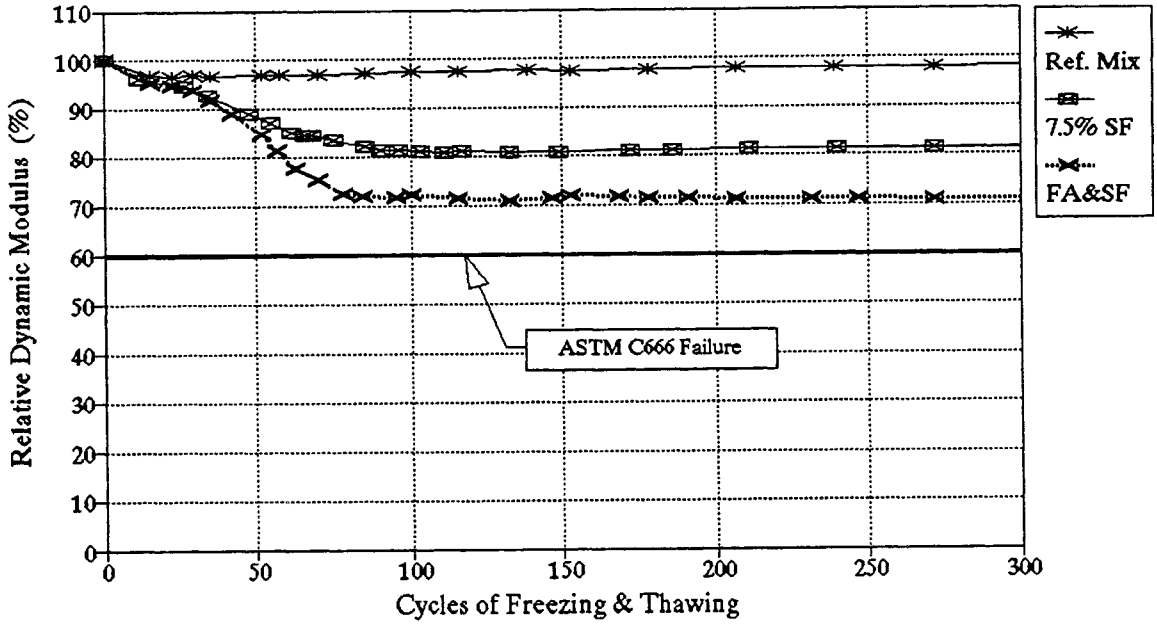

(b) moist-cured low-absorption limestone mixes

Figure 4.22 Relative Dynamic Modulus vs. cycles of freezing and thawing

The concrete absorption tests showed that the concrete specimens containing fly ash typically absorbed the most water, followed by the reference mix specimens. The silica fume specimens absorbed the least water, with the silica fume and fly ash with silica fume combination specimens exhibiting similar performance (with a slightly higher absorption observed for the specimens containing the combination of fly ash with silica fume). The concrete containing silica fume had experienced the least amount of weight loss while aging, and also the least water absorption potential. A possible explanation for the poor performance of the concrete containing silica fume (when compared with the concrete containing only portland cement and the concrete containing fly ash) may be due to the effect of silica fume in concrete. The ability of silica fume to fill the voids in the paste with additional hydration products and unreacted silica fume may have prevented the saturated aggregate to dry out prior to freeze-thaw testing. Although the concrete containing silica fume was less permeable, as the absorption tests show, the trapped water inside the aggregate may have been unable to escape and may have led to the failure of the concrete. The concrete without silica fume may have had a more open pore structure, which allowed movement of water through the aggregate and the surrounding paste.

Observed Failure Mechanisms

After failing both the Relative Dynamic Modulus and the length expansion criteria or completing over 1500 cycles, the Phase I beam specimens were removed from the freeze-thaw testing machine. Slices of the concrete beam specimens were cut, prepared and examined as described in Chapter 3. The freeze-thaw failure mechanisms were identified for the selected

specimens and are presented in Table 4.9. The failure mechanisms were characterized as: aggregate cracking, deterioration of the aggregate/paste interface, and paste cracking. The observed failure was rated using values of 0 to 3 for negligible to major amount of visible damage.

The Relative Dynamic Modulus test was used to identify failure of the concrete beam specimens; the visual observations provide an idea of how the concrete specimen failed. Examining a single slice of one beam provides insight into obvious failure mechanisms, but does not suggest certainty of failure mechanism. For example, examining a cross section of the PCG w/FA&SF concrete beam provided no insight as to why the concrete failed (rated '0' for all types). With an RDM < 46, the concrete beam had failed. The '0' ratings only indicate that in this particular cross section of the beam, none of the identified failure mechanisms were seen.

Included in the table are the Relative Dynamic Modulus values of the concrete specimens at the time the sample was cut for visual observation. The RDM value provides an indication of the degree of deterioration of the concrete and can be used to aid in comparison of the different concrete mix samples. Because the samples were taken after specimen failure or after completing the 1500 (Phase I) freeze-thaw cycles, the level of damage obtained from the visual observations corresponded with a wide variation in number of freeze-thaw cycle exposures and degree of deterioration. For example, looking at the ratings of the two heat-cured, partially-crushed gravel mixes, one with fly ash and one with silica fume, the failure rating for the aggregate/paste interface was 2 and 3, respectively. However, instead of concluding that silica fume had a more negative effect on this failure, it should be noted that the concrete mix sample

Table 4.9: Observed Failure Mechanisms: Phase I mixes

Mix	Cure	Cycle specimen was removed	RDM of sample at time specimen taken	Failure Mechanism*		
				cracks in aggregate	aggr/paste interface	microcracks in paste
PHASE I MIXES						
RG Ref	heat	48	24	1	3	1
	moist	98	<46	1	3	0
RG w/FA	heat	66	35	0	3	0
	moist	98	<46	1	2	0
RG w/SF	heat	55	29	0	1	0
RG w/FA&SF	heat	66	36	1	3	0
PCG Ref	heat	98	<38	1	2	0
	moist	1507	101	0	0	0
PCG w/FA	heat	98	49	0	2	0
	moist	240	50	1	1	0
PCG w/SF	heat	48	12	1	3	0
PCG w/FA&SF	heat	81	<46	0	0	0
GR Ref	heat	111	48	3	3	0
	moist	56	42	2	2	0
GR w/FA	heat	62	39	2	1	0
GR w/SF	heat	43	<26	3	3	0
GR w/FA&SF	heat	55	43	3	3	0
	moist	32	<32	2	2	0
LS-H Ref	heat	248	48	1	1	0
	moist	1507	87	1	0	0
LS-H w/FA&SF	heat	166	47	0	0	0
	moist	66	40	1	0	0
LS-L Ref	heat	1520	87	0	0	0
	moist	1520	101	0	0	0
LS-L w/SF	heat	895	48	1	1	0
	moist	1511	79	1	0	1
LS-L w/FA&SF	heat	387	47	1	0	0
	moist	1520	52	0	0	3

* Failure rating: 0 = negligible; 1 = minor; 2 = moderate; 3 = major amount of damage observed.

containing silica fume had a RDM value of only 12 at the time the specimen slice was cut, whereas the concrete sample containing fly ash had a RDM value of 49. This provides a reason for the worse rating of the silica fume mix sample; it was taken out of the freeze-thaw testing machine at a much more advanced stage of deterioration.

The visual observations indicated that there were general failure mechanisms associated with each aggregate type. The mixes containing round gravel aggregates tended to deteriorate at the aggregate/paste interface. Figures 4.23 and 4.24 show examples of deterioration at the transition zone in round gravel concrete specimens. The mixes using partially-crushed gravel aggregates suffered similar damage (Figure 4.25), but not to the extent of the round gravel aggregate mixes. The slightly better performance may be attributed to the surface texture and angularity of the aggregate. Angular, rough-surfaced aggregates generally develop a better bond with the cement paste, strengthening the transition zone between the paste and aggregate. A weak transition zone could result in microcracking around the aggregates. This theory is supported by the durability factors of the partially-crushed gravel and round gravel concrete specimens. When mix composition is held constant, the specimens containing partially-crushed gravel (with the more angular, rough-surfaced particles) generally exhibited better freeze-thaw durability (see Table 4.7). For example, reference concrete mixes made with partially-crushed gravel and round gravel resulted in durability factors of 12 and 5 respectively.

The granite concrete specimen failures tended to be dominated by cracks in the aggregate and deterioration of the aggregate/paste interface (which may have resulted from the aggregate

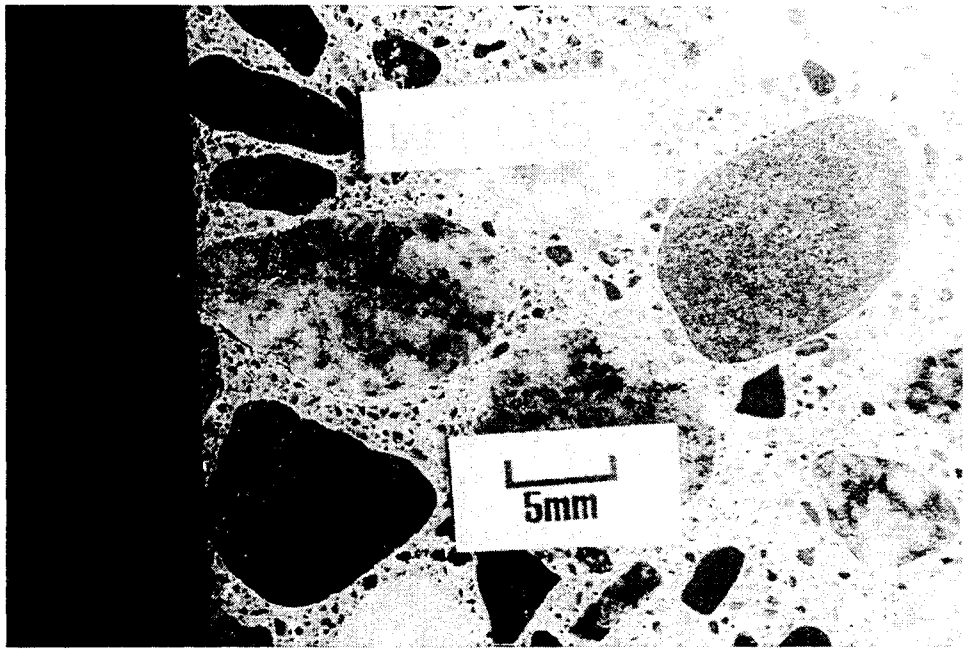

Figure 4.23 Moist-cured round gravel reference mix specimen: failure at aggregate/paste interface (RDM < 46)

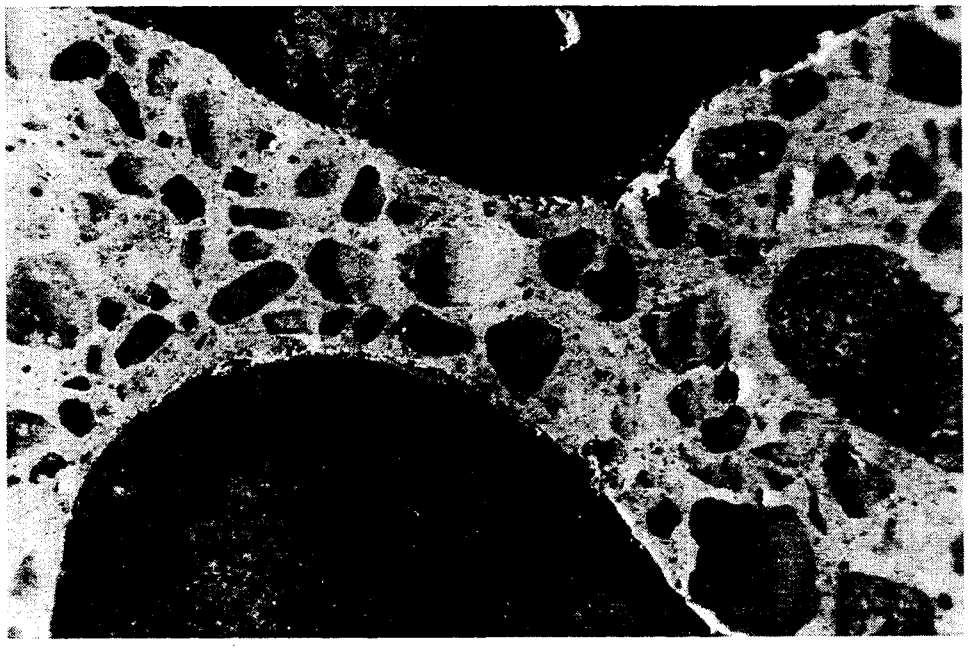

Figure 4.24 Moist-cured round gravel with fly ash mix specimen: failure at aggregate/paste interface (RDM < 46)

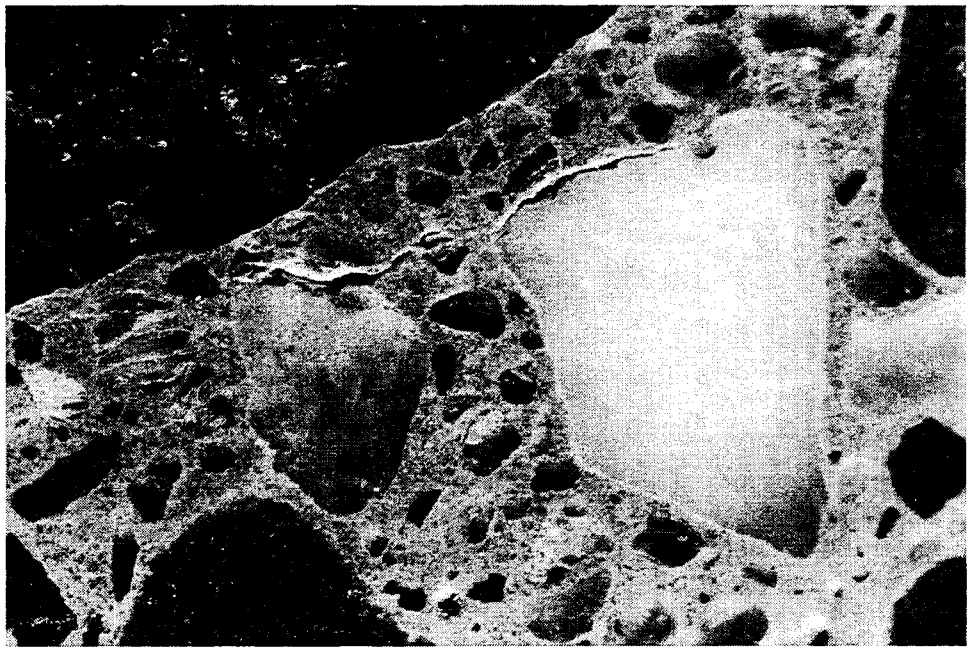

Figure 4.25 Heat cured partially-crushed gravel with silica fume mix specimen: failure at aggregate/paste interface (RDM = 12)

deterioration). Figures 4.26 through 4.29 provide examples of the deterioration seen in the granite concrete specimens. As noted above, the durability of the granite concrete mixes was very poor (DF < 10).

The concrete specimens fabricated with limestone aggregate were subjected to numbers of freeze-thaw cycles that were orders of magnitude greater than the other specimens, but there was little visual evidence of deterioration, even in the specimens which failed the dilation criterion. Under microscopic view, the structure of some of the limestone aggregates appeared quite similar to that of the surrounding paste (Figures 4.30 and 4.31). As suggested earlier, the structure of the limestone concrete (especially the reference mix) may consist of pore sizes that allow water flow through the concrete.

As reported in Table 4.9, most of the limestone concrete specimens experienced a minor amount of damage to the aggregate. In most cases this deterioration was in the form of radial cracks coming from the aggregate and extending into the cement paste, as shown in Figure 4.32. With the large dilations measured in most of the limestone concrete freeze-thaw test beams, some cracking is expected. Radial cracks from the limestone aggregates provide evidence of the high strength of the bond between the limestone aggregate particles and the cement paste (i.e. the limestone aggregate itself was the weak component; in most cases, there was no failure in the transition zone).

Two of the limestone concrete specimens did experience a minor amount of damage in the aggregate/paste interface (see Table 4.9). Figure 4.33 shows a limestone specimen that

Figure 4.26 Heat-cured granite reference mix specimen: aggregate failure (RDM = 48)

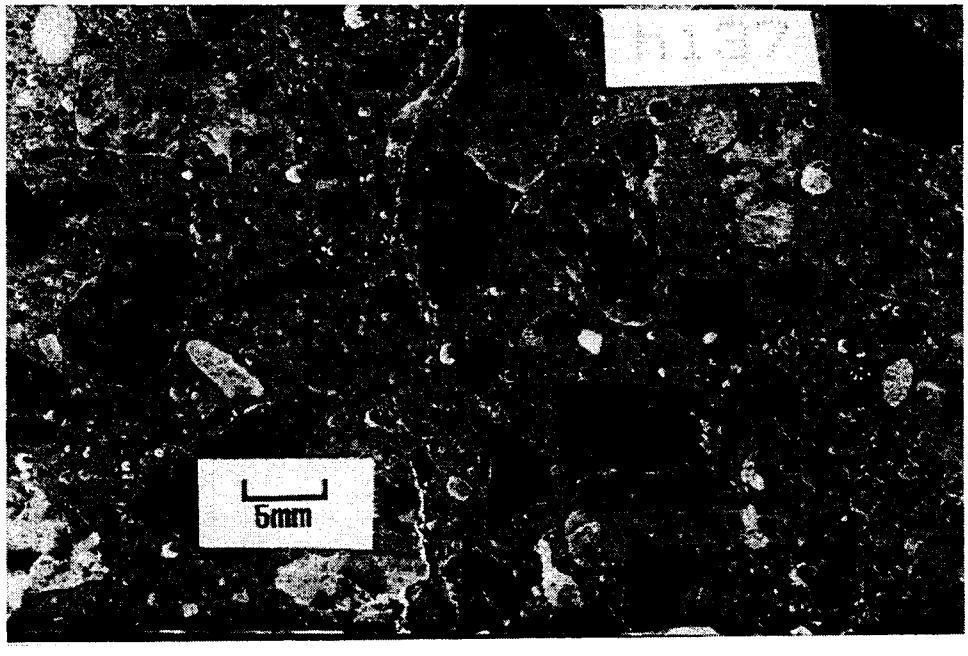

Figure 4.27 Heat-cured granite with silica fume mix specimen: aggregate failure (RDM < 26)

Figure 4.28 Heat-cured granite with silica fume mix specimen: failure at transition zone & agg. cracking (RDM < 26)

Figure 4.29 Moist-cured granite with fly ash & silica fume mix specimen: aggregate failure (RDM < 25)

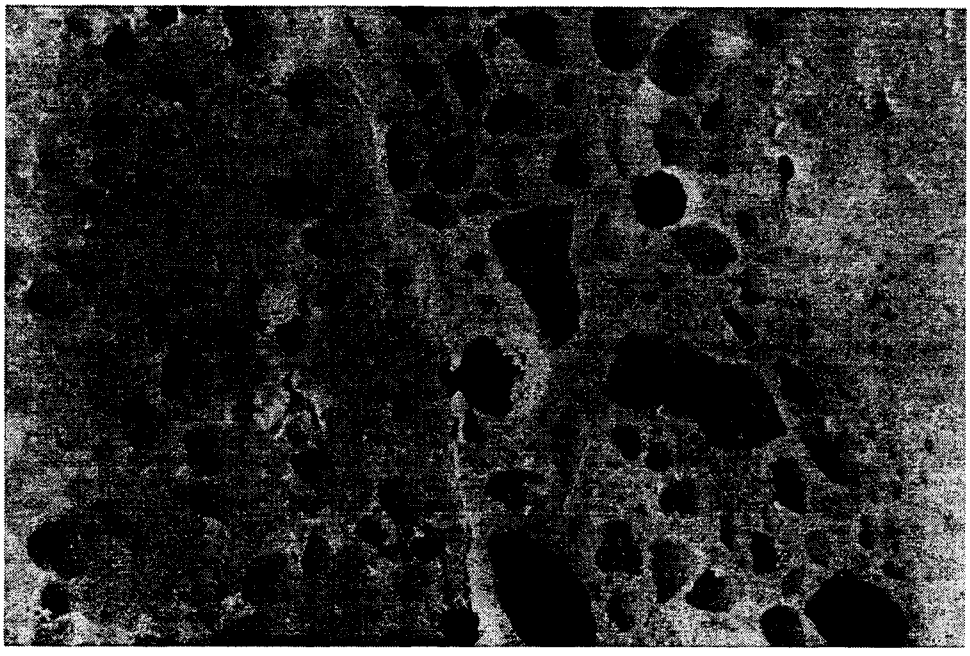

Figure 4.30 Limestone concrete specimen

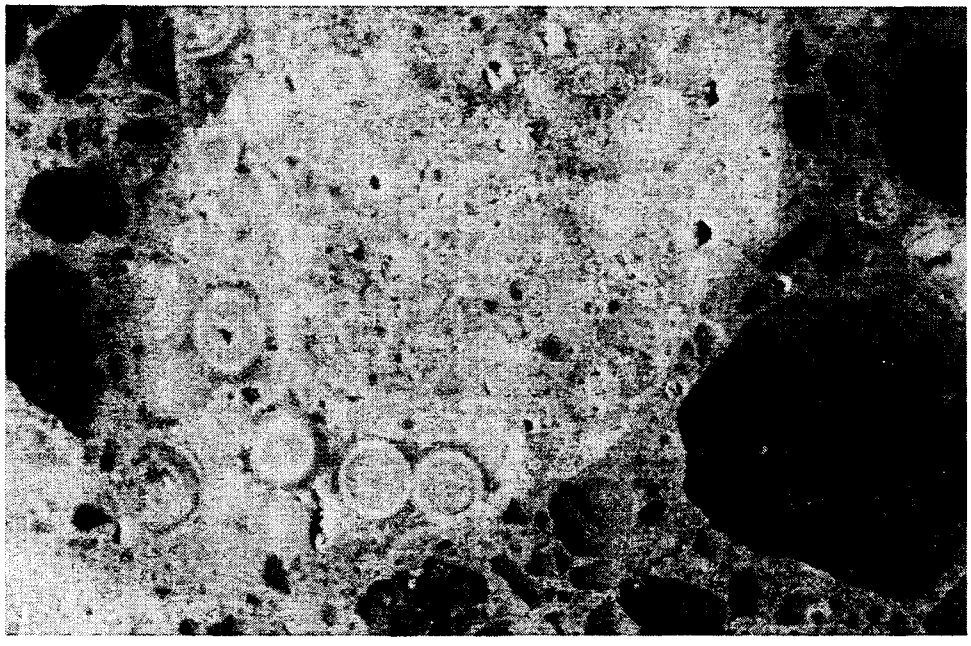

Figure 4.31 Limestone concrete specimen

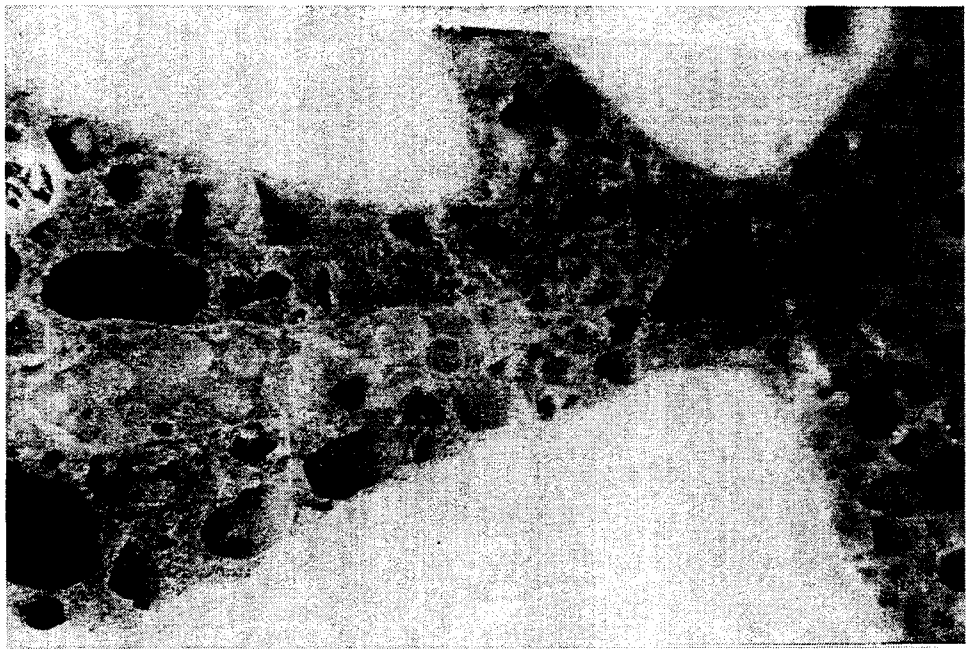

Figure 4.32 Limestone concrete specimen: radial cracks extending from limestone aggregate

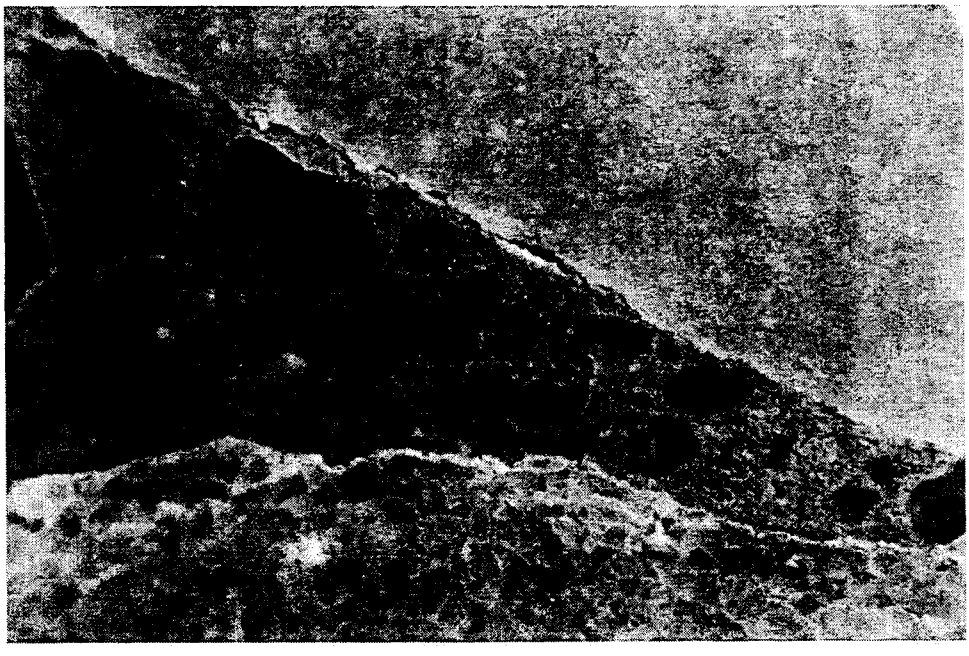

Figure 4.33 Heat-cured high-absorption limestone ref. mix specimen: minor damage at the agg./paste interface (RDM = 48)

COMPRESSIVE STRENGTHS

The compressive strengths of all Phase I laboratory mixes were tested as part of the mechanical properties of high-strength concrete portion of the study [3]. The results are given in Table 4.10. Compressive strengths are listed for 6x12-in (150x300-mm) cylinders. As noted in the table, where 4x8-in (100x200-mm) cylinders were tested, the results were converted to 6x12-in (100x200-mm) cylinder strengths using a conversion factor of 1.06 [3].

The 28-day compressive strengths are reported as well as the concrete compressive strength at the approximate time the concrete beam specimens were placed in the freeze-thaw testing machine. To approximate the strength of the concrete beam specimens at the time the freeze-thaw tests were initiated, the 182-day concrete compressive strengths are given. The Phase I concrete beam specimens were aged to 189 days prior to beginning the freeze-thaw testing procedure (immersion in constant temperature bath); their age upon placement in the freeze-thaw testing machine is given in Table 4.7. For the 182-day strength measurement, only the 28-day moist-cured specimens were tested to determine compressive strengths. The moist-cured concrete freeze-thaw specimens were only moist-cured for seven days. However, the 28-day moist-cured specimen compressive strength is given to provide an approximate level of strength of the concrete beam specimens at the time they began freeze-thaw testing.

Plots of the durability factors versus the 28-day compressive strengths of the heat- and moist-cured (7-day) concrete specimens of Phase I and Phase II are shown in Figures 4.34 (a) and (b), respectively. Figures 4.35 (a) and (b) show the durability factors versus the

Table 4.10: Compressive Strengths: Phase I Mixes; 6x12-in (150x300-mm) cylinders [3]

Mix	f'c, 28-day compressive strength psi (MPa)		compressive strength @ approximate time concrete beam specimens placed in freeze-thaw testing machine** psi (MPa)	
	heat-cured	moist-cured for 7 days*	heat-cured*	moist-cured for 28 days*
RG Ref	11270 (77.7)	13393 (92.4)	10769 (72.3)	14098 (97.2)
RG w/FA	9997 (68.9)	12475 (86.0)	10660 (73.5)	14078 (97.1)
RG w/SF	11924 (82.2)	14316 (98.7)	12362 (85.3)	14967 (103.2)
RG w/FA&SF	11007 (75.9)	14057 (96.9)	10672 (73.6)	15068 (103.9)
PCG Ref	12291 (84.8)	15192 (104.8)	12025 (82.9)	15835 (109.2)
PCG w/FA	11694 (80.6)	14182 (97.8)	11759 (81.1)	15286 (105.4)
PCG w/SF	12833 (88.5)	15493 (106.8)	13452 (92.8)	16101 (111.0)
PCG w/FA&SF	12262 (84.6)	15583 (107.5)	12318 (85.0)	16193 (111.7)
GR Ref	11778 (81.2)	13544 (93.4)	11870 (81.9)	14923 (102.9)
GR w/FA	11003 (75.9)	13547 (93.4)	11041 (76.4)	14520 (100.1)
GR w/SF	12826 (88.5)	16364 (112.9)	12942 (89.3)	16846 (116.2)
GR w/FA&SF	12112 (83.5)	14243 (98.2)	12153 (83.8)	16051 (110.7)
LS-H Ref	14789 (102.0)	16164 (111.5)	14277 (98.5)	16727 (115.4)
LS-H w/FA&SF	12630 (87.1)	14905 (102.8)	12905 (89.0)	15702 (108.3)
LS-L Ref	14310 (98.7)	16419 (113.2)	14763 (101.8)	15947 (110.0)
LS-L w/SF	15362 (105.9)	17315 (119.4)	15538 (107.2)	18028 (124.3)
LS-L w/FA&SF	15086 (104.0)	17018 (117.4)	15358 (105.9)	16842 (116.2)

* 4x8-in (100x200-mm) cylinders tested and converted to 6x12-in (150x300-mm) cylinder strength using conversion factor of 1.06 {i.e. [6x12-in (150x300-mm) compressive strength] = [4x8-in (100x200-mm) compressive strength]/1.06}

** 182-day compressive strength given; age concrete beam specimens placed in freeze-thaw testing machine given in Table 4.7.

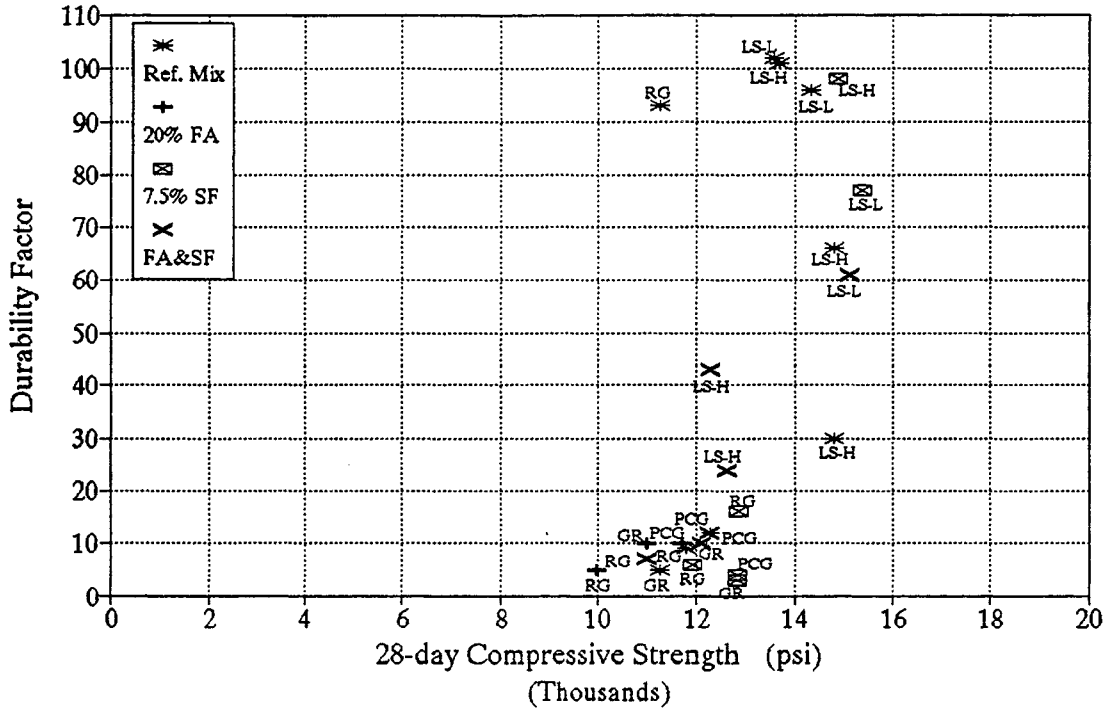

(a) heat-cured concrete specimens

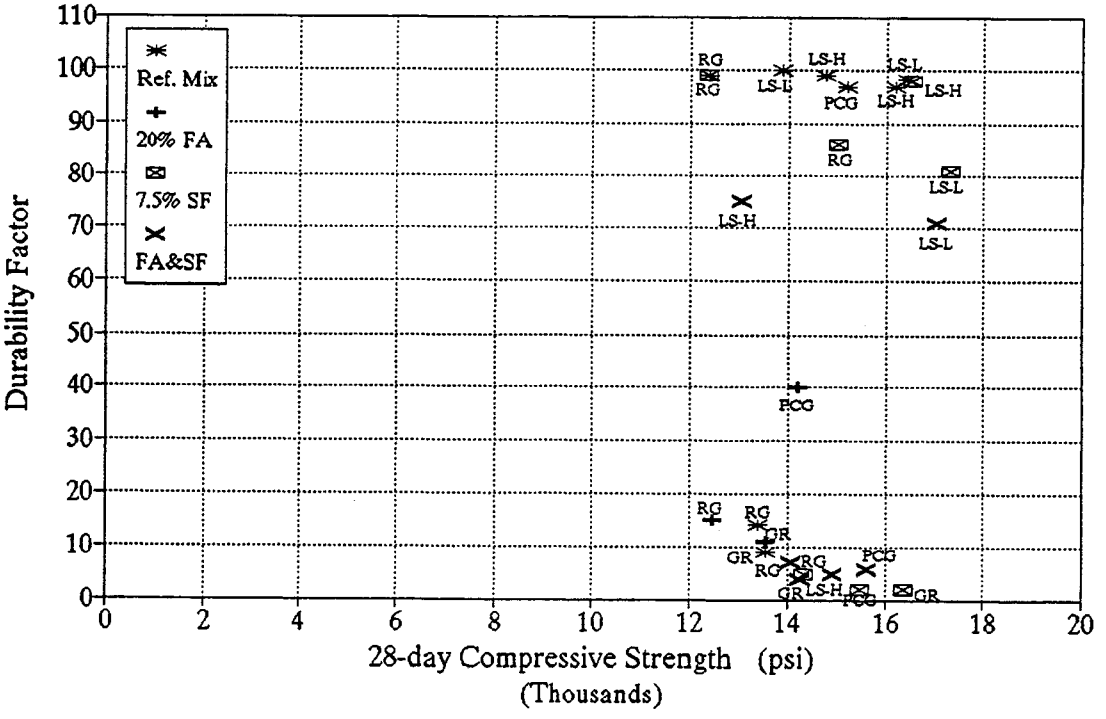

(b) moist-cured concrete specimens

Figure 4.34 Durability Factor vs. 28-day compressive strength (Phase I & II)

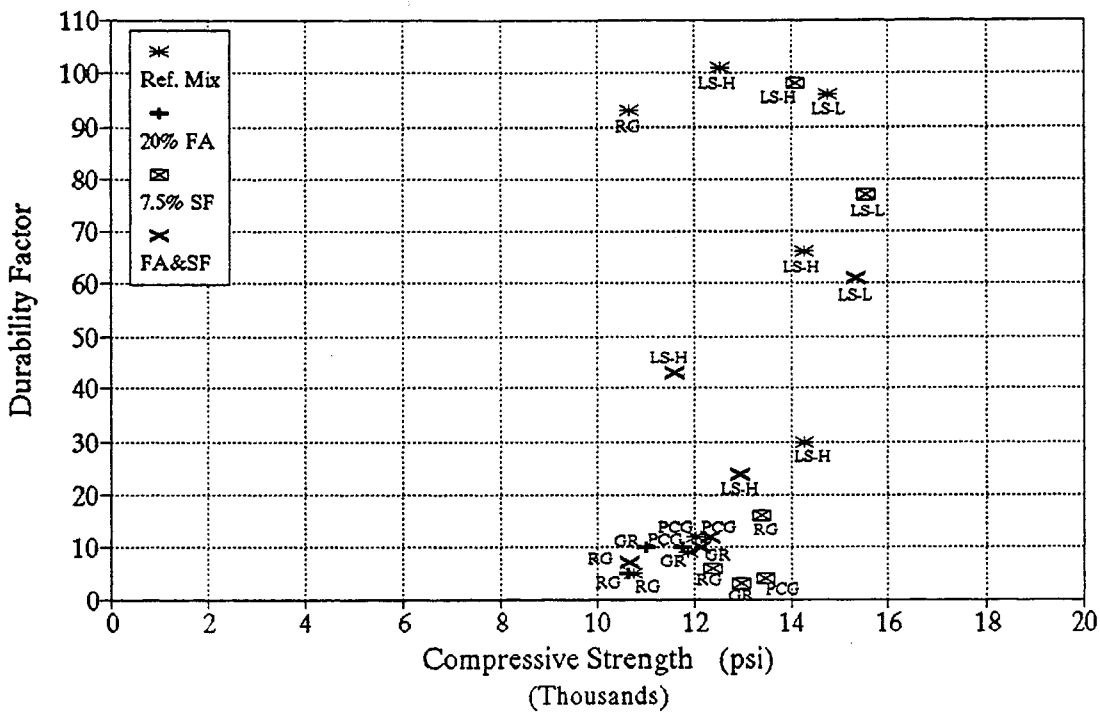

(a) heat-cured concrete specimens

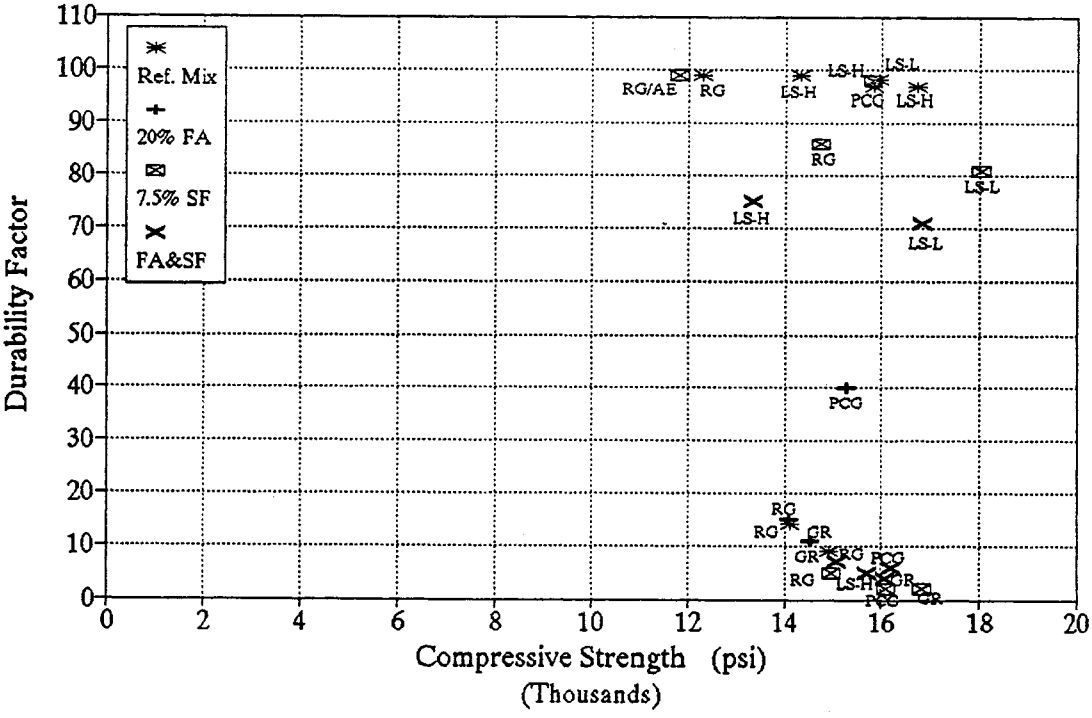

(b) moist-cured concrete specimens

Figure 4.35 Durability Factor vs. compressive strength (Phase I & II)

compressive strength at the approximate time the concrete beam specimens were placed in the freeze-thaw testing machine for the heat- and the moist-cured (28-day) concrete specimens, respectively. Data in these figures indicate that the relationship between compressive strength and durability factor is strongly influenced by aggregate type. For a given aggregate type for which a range of concrete strengths was produced (e.g. for GR, range in f'c of 11,041 to 16,846 psi (76.4 to 116.2 MPa)), little change in freeze-thaw durability was observed.

PHASE II FREEZE-THAW TEST RESULTS

As described previously, ten of the Phase I concrete mixes were repeated in Phase II to further explore reasons for the freeze-thaw behavior exhibited in Phase I. The freeze-thaw test results for the seven Phase II concrete laboratory mixes are given in Table 4.11. Three girder mixes from Phase I were also mixed in the laboratory in Phase II; the results of these repeated freeze-thaw tests are given in Appendix E with the results of the Phase I girder concrete specimens.

Given in Table 4.11 are the average number of cycles after which the failure criteria were met and the corresponding durability factor for each pair of specimens. Measurements of each individual specimen may be found in Appendix H. As with the Phase I test results, the replicate specimen measurements were generally very close to one another. In the cases where the measurements were different, both measurements are given. All of the plots of RDM versus cycles of freezing and thawing are given for each specimen in Appendix D.

Table 4.11: Phase II Freeze-Thaw Test Results

Mix	Age placed in freeze-thaw testing machine* (days)	Cycles to Observed RDM Failure *Length Change Failure*			Durability Factor		
		heat-cured	moist-cured	ASTM-cured	heat-cured	moist-cured	ASTM-cured
(RG Ref)R	49	660+(587) *366*	660+ *660+*	660+ *660+*	93	99	99
(RG w/SF)R	49	94 *94*	610+ *610+(398)*	610+ *610+*	16	86	98
	81	109 *79*	730+(637) *476*	NT	20	85	NT
(RG w/SF)AE	49	500+ *500+*	500+ *500+*	500+ *500+*	99	99	100
(LS-H Ref)R	49	500+ *500+*	500+ *500+*	119 *107*	101	99	23
(LS-H w/SF)	49	610+ *610+*	610+ *610+*	610+ *610+*	98	98	95
(LS-H w/FA&SF)R	49	216 *141*	660+(502) *153*	372(283) *198*	43	75	60
(LS-L Ref)R	49	750+ *750+*	750+ *750+*	405 *287*	102	100	78

* Age = (28 days drying) + (21 days in water bath) + (days frozen prior to testing).
NT Indicates curing condition not tested.
+ Indicates that the specimens had not yet failed the test criterion.
( ) Indicates value for companion specimen if different.

Similar to the Phase I test results, the Phase II limestone aggregate concrete specimens failed the dilation criterion much more quickly than the RDM criterion. However, large dilations were also seen in the round gravel reference concrete specimens. Table 4.12 provides the length change and the weight change of the concrete specimens at the cycle the RDM failure was observed. The dilation of the heat-cured round gravel reference specimens was 0.264 percent at the cycle RDM failure was observed. The complete set of plots of RDM versus length change and RDM versus weight change are given in Appendix D.

Table 4.12: Length and Weight Change at Cycle RDM Failure Observed

Mix	Length Change (%)			Weight Change (%)		
	heat-cured	moist-cured	ASTM-cured	heat-cured	moist-cured	ASTM-cured
PHASE II MIXES						
(RG Ref)R	0.264	0.007 *(100,660)*	0.004 *(100,663)*	0.562	-0.073	-0.057 *(100, 663)*
(RG w/SF)R	0.197*	0.155	0.003 *(99,615)*	0.551	0.280	-0.238* -0.079*
(RG w/SF)AE	0.007 *(101,663)** 0.033 *(96,663)**	0.009 *(100, 663)*	-0.002 *(101,504)*	0.019 *(101,663)** 0.152 *(96,663)**	-0.035 *(100,663)** -0.162 *(100,663)**	-0.193 *(101, 504)*
(LS-H Ref)R	0.026 *(102,663)*	0.009 *(100,663)*	0.140	-0.028 *(102,663)*	-0.099 *(100,663)*	0.492
(LS-H w/SF)R	0.030 *(98,661)*	0.004 *(99,661)*	0.012*	0.127 *(98,661)*	-0.072 *(99, 661)*	-0.105
(LS-H w/FA&SF)R	0.380	0.306* 0.316 *(70, 708)**	0.169	0.739	0.605 *(70, 708)** 0.628*	0.259
(LS-L Ref)R	0.008 *(105,754)*	0.002 *(101,754)*	0.265	-0.116 *(105,754)*	-0.130 *(101, 754)*	0.577

* Indicates measurement for one beam specimen (not an average of two measurements).
(a,b) Indicates measurement on beam specimen that did not fail RDM criterion.
Measurement taken at RDM value = *a* and at cycle = *b*.
NT Indicates curing condition not tested.

Effect of Frozen Period on Test Results

One of the concerns regarding the Phase I results was the effect, if any, of the period of time many of the Phase I concrete specimens were kept frozen at a constant temperature prior to testing. Three Phase II concrete mixes were tested to explore this concern. The round gravel with silica fume concrete mix and the two repeated project girder concrete mixes (described in Appendix E) were mixed in the laboratory for this purpose. The results are presented in Figure 4.36, as well as in Table 4.11. As the figure and table show, the specimens which were frozen

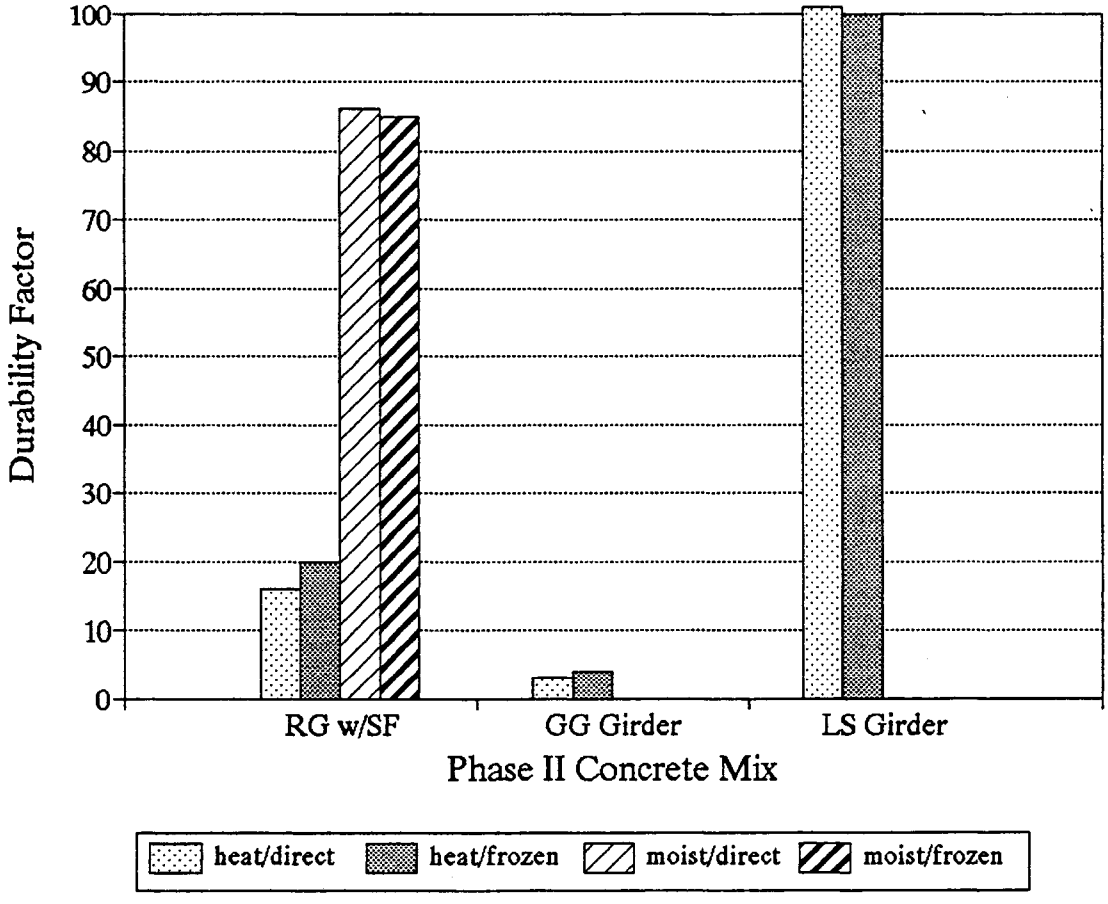

Figure 4.36 Effect of frozen period on freeze-thaw test results

for a period of time (32 and 35 days in this case) before freeze-thaw testing resulted in durability factors very close to those of identical specimens placed directly in the freeze-thaw testing machine after removal from the constant temperature water bath. This finding is consistent with the ASTM C666 procedure recommendation that "when the sequence of freezing-and-thawing cycles must be interrupted, store the specimens in a frozen condition [20]." These results concerning the effect of the frozen period prior to freeze-thaw testing indicate that all freeze-thaw test results may be used for comparison, even if some of the concrete specimens were subjected to an extended frozen period.

Effect of Aggregate Moisture Content

Unlike the Phase I test results, the freeze-thaw behavior of Phase II concrete specimens were not clearly grouped according to aggregate type. Figures 4.37 (a) and (b) provide the results of the heat- and moist-cured Phase II reference mix specimens. The poor performance of the round gravel aggregate concrete in Phase I was not seen in the Phase II concrete mix specimens.

Figure 4.38 shows the durability factors of the Phase I and Phase II concrete specimens for comparison. Each Phase II mix is a replicate of a Phase I concrete mix. For the Phase II concrete mixes, additional aggregate was obtained from the same source as the corresponding Phase I concrete mix. The only variables were the moisture content of the aggregate at the time of mixing, the time period the specimens were aged prior to freeze-thaw testing and the resulting strength of the concrete specimens.

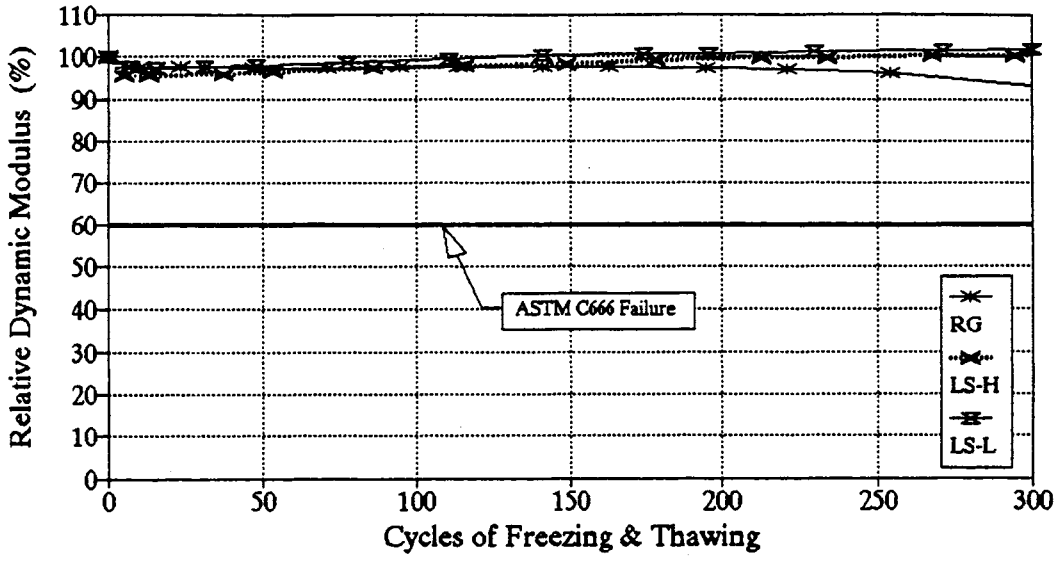

(a) heat-cured concrete specimens

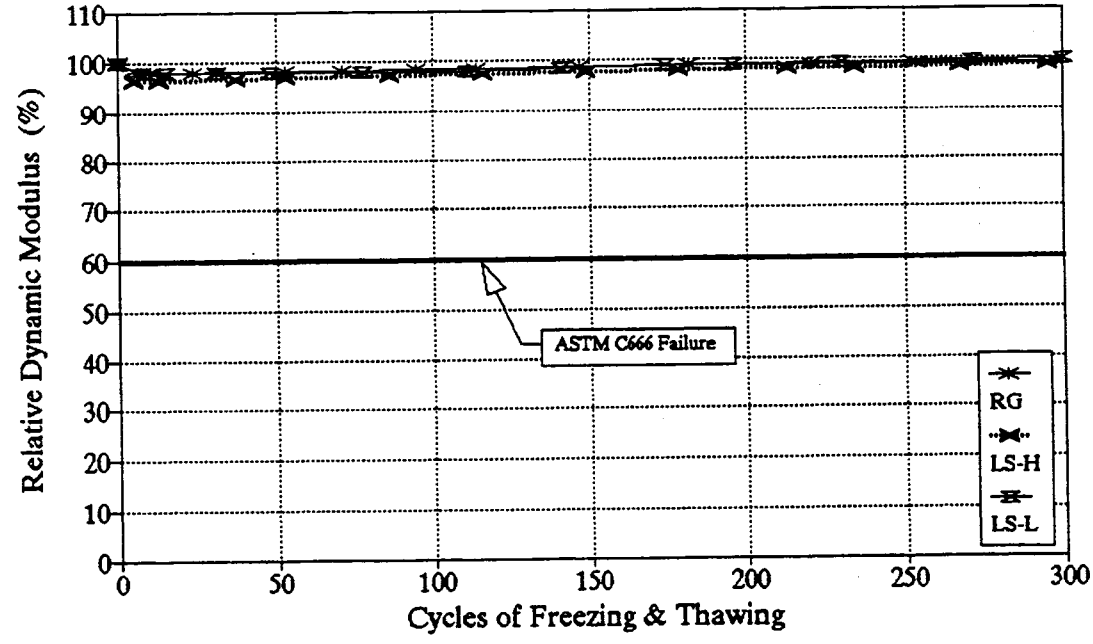

(b) moist-cured concrete specimens

Figure 4.37 Relative Dynamic Modulus vs. cycles of freezing and thawing: Phase II reference concrete specimens

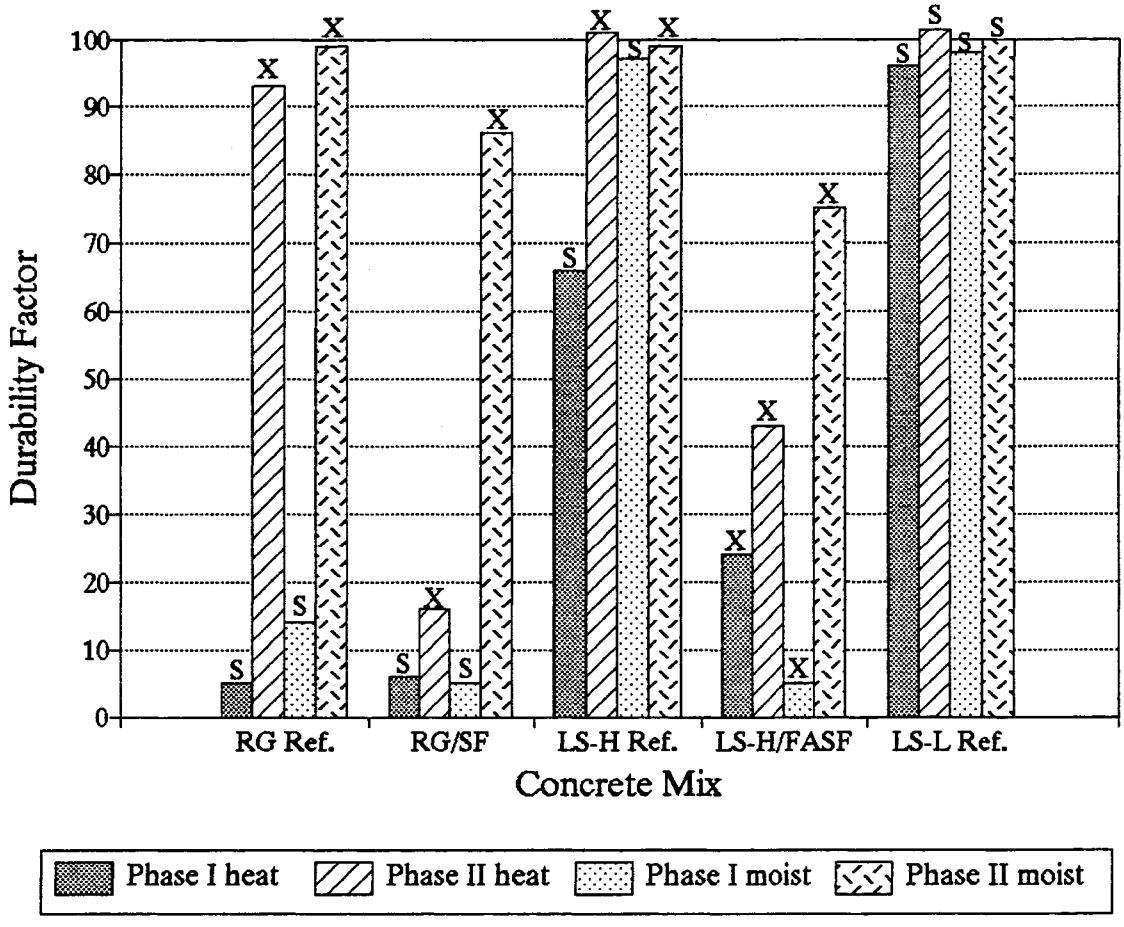

Figure 4.38 Durability Factors: Phase I vs. Phase II concrete mixes

The figure indicates that the round gravel aggregate performance may correlate with its moisture content at the time of mixing. Moisture contents of the aggregate at the time of mixing were given in Table 3.2. The round gravel reference mix performed very poorly when the aggregate was saturated (over 130 percent), but when the aggregate was not saturated (85 percent saturation) good performance was seen. Percent saturation of the aggregates were given in Table 3.2 (as calculated by Eq. 3-1). The low-absorption limestone aggregate concrete specimens exhibited good performance, and the low-absorption limestone coarse aggregate was saturated at the time of mixing for both Phase I and II. Figures 4.39 (a), (b) and (c) provide plots of the durability factor versus the coarse aggregate moisture content at the time of mixing for the heat-, moist- and ASTM-cured concrete specimens from Phases I and II.

The round gravel aggregate and the limestone aggregate may not exhibit the same behavior under saturated conditions. The excess water in an over-saturated round gravel aggregate particle tends to cling to the smooth aggregate surface, and may create a weakened transition zone between the aggregate and the paste. Using round gravel that is not saturated allows some absorption into the aggregate that improves the contact between the cement paste and the aggregate, thus increasing the strength of the bond. In the round gravel with silica fume concrete mix, greatly improved freeze-thaw performance was seen in the moist-cured concrete specimens when using unsaturated aggregate, but no improvement was seen in the heat-cured concrete specimens. With the hydration limited by the amount of mix water in the heat-cured concrete, benefits of the silica fume to strengthen the bond between the aggregate and the cement paste would not be realized. Microcracking may also develop upon drying.

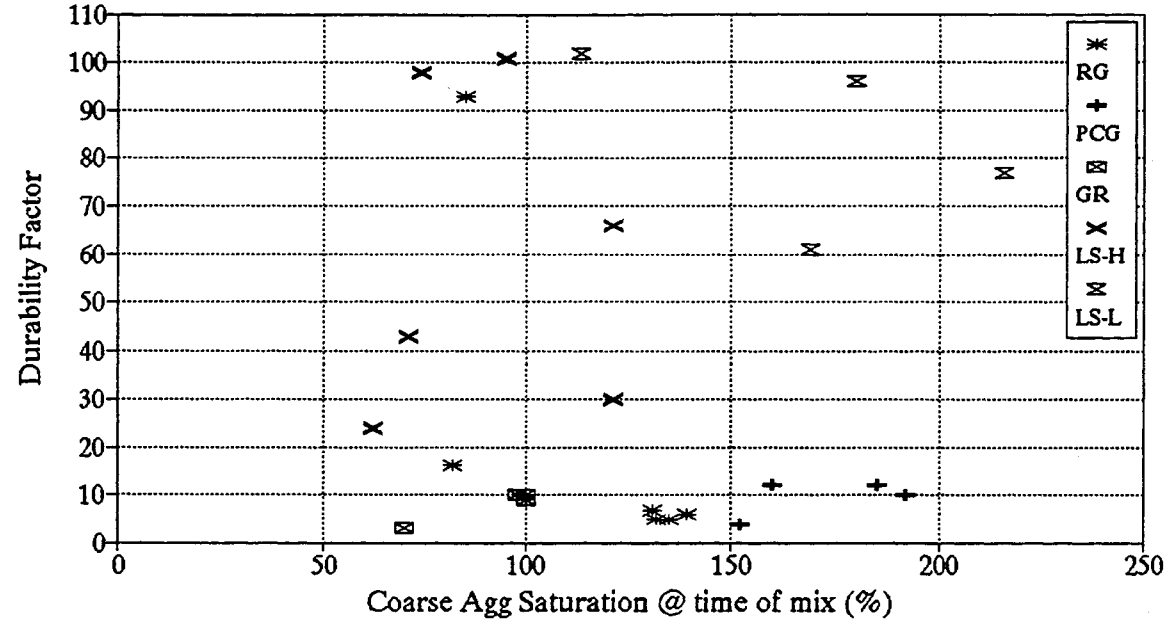

(a) heat-cured concrete specimens

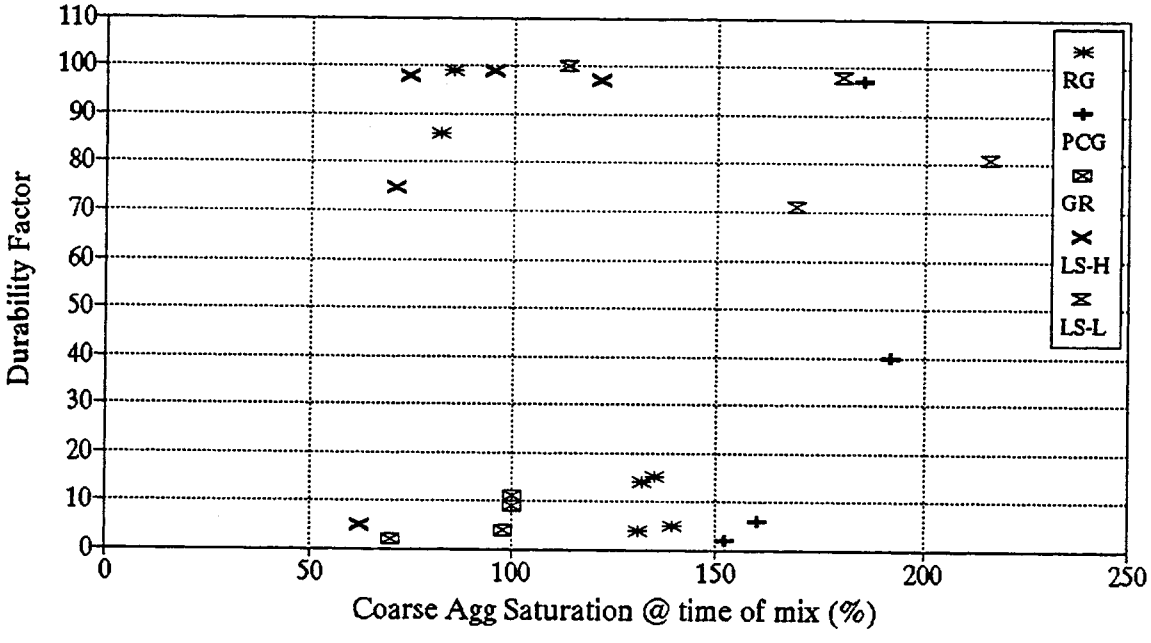

(b) moist-cured concrete specimens

Figure 4.39 Durability Factor vs. coarse aggregate saturation at the time of mix

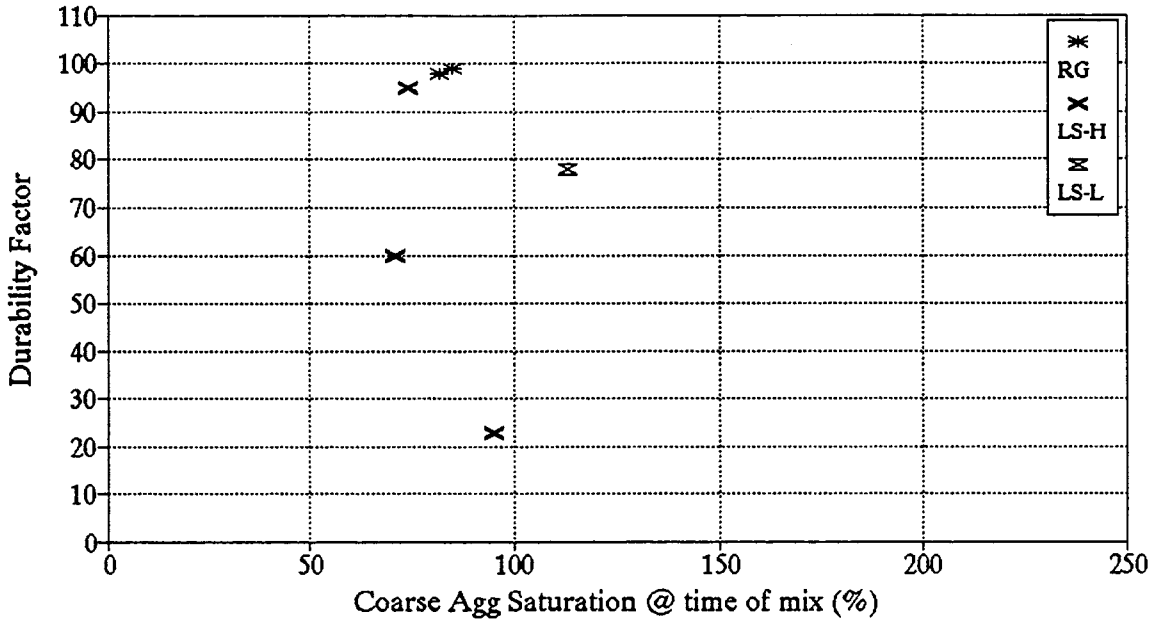

(c) ASTM-cured concrete specimens

Figure 4.39 Durability Factor vs. coarse aggregate saturation at the time of mixing

The moisture content of the limestone aggregate at the time of mixing did not appear to have as great an effect. The crushed limestone aggregate of angular shape and rough surface texture provide a better contact area than the smooth round gravel, whether the limestone aggregate is saturated or not. The high-absorption limestone reference mix performed better when it was not saturated, possibly due to the ability of the aggregate to absorb some cement paste to improve contact and strengthen the bond between the aggregate and the paste. In the high-absorption limestone containing fly ash with silica fume, the limestone aggregate was not saturated in Phase I or Phase II. The Phase II high-absorption aggregate was 71% saturated while the Phase I high-absorption limestone aggregate was 62% saturated at the time of mixing. The Phase II concrete mix may have performed better than the Phase I mix due to the higher saturation of the aggregate at the time of mixing. In this concrete mix containing fly ash and silica fume, the absorbed water in the aggregate could have been drawn out by capillary action and may have reacted with any unhydrated cement or pozzolan material to strengthen the transition zone. The low-absorption limestone reference mix performed very well and it was saturated at the time of mix in both Phase I and Phase II. In this case, the water inside the limestone aggregate could also have been drawn out and used as curing water with any unhydrated cement, providing increased contact between the aggregate and the paste. Furthermore, a transition zone may have been created that consisted of pore sizes that permitted easy flow of water through the concrete, as previously discussed. This theory is supported by the fact that concrete specimens from the low-absorption limestone reference mix experienced no expansion during freeze-thaw testing.

Effect of Curing

Similar to the Phase I mix results, the performance of the Phase II concrete specimens improved when moist-curing (7-day) was used (compared to heat-curing). Phase II concrete beam specimens were also cured according to the ASTM C666 procedure in order to compare the standard 14-day moist-cure with the curing methods used in this study. The results of all ten Phase II concrete mix specimens (including the repeated girder concrete mix specimens) are shown in Figures 4.40 (a) and (b). Results are separated by aggregate type. Figure 4.40 (a) shows the durability factors of the glacial gravel concrete specimens (the round gravel and the glacial gravel girder concrete mixes) and Figure 4.40 (b) gives the durability factors of the limestone concrete specimens (the high- and low-absorption limestone concrete mixes and the limestone girder concrete mix).

Results appear to differ according to aggregate type. In the glacial gravel concrete mixes, the ASTM-cured specimens performed as well or better than the 7-day moist-cured specimens. As discovered in the Phase I concrete specimens, the failure mechanism for the gravel aggregate was in the transition zone between the aggregate and the cement paste. The improved performance of the ASTM-cured specimens may be due to the additional time the specimens were moist-cured (14-day versus 7-day) which allowed additional hydration and strengthening of the transition zone.

In the limestone aggregate concrete mixes, the ASTM-cured specimens consistently performed worse than the 7-day moist-cured specimens. As discussed previously, the moisture

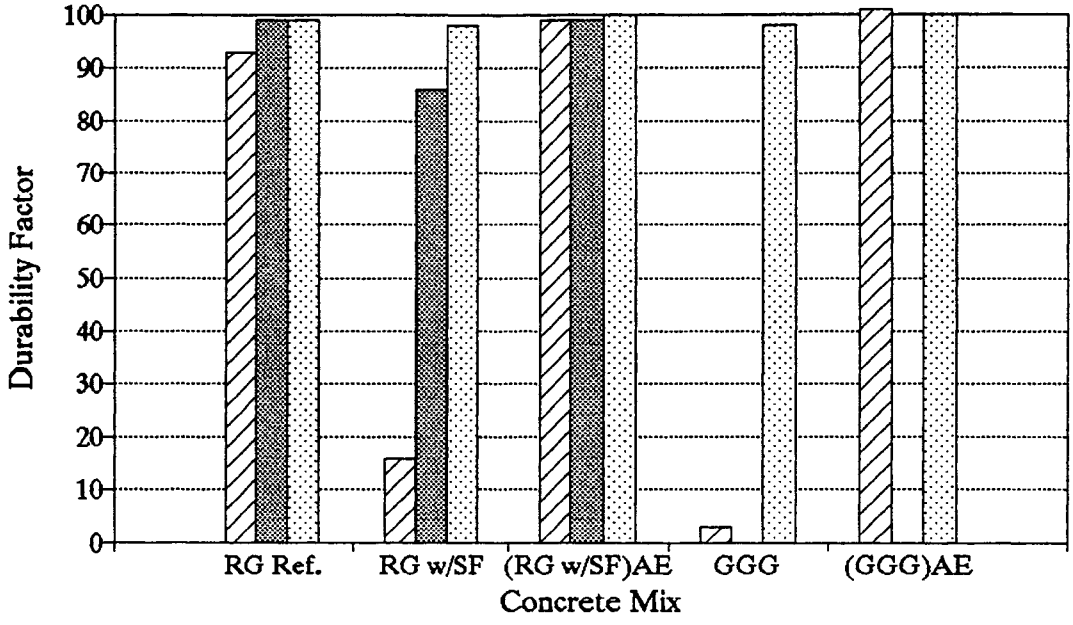

(a) Glacial Gravel concrete specimens

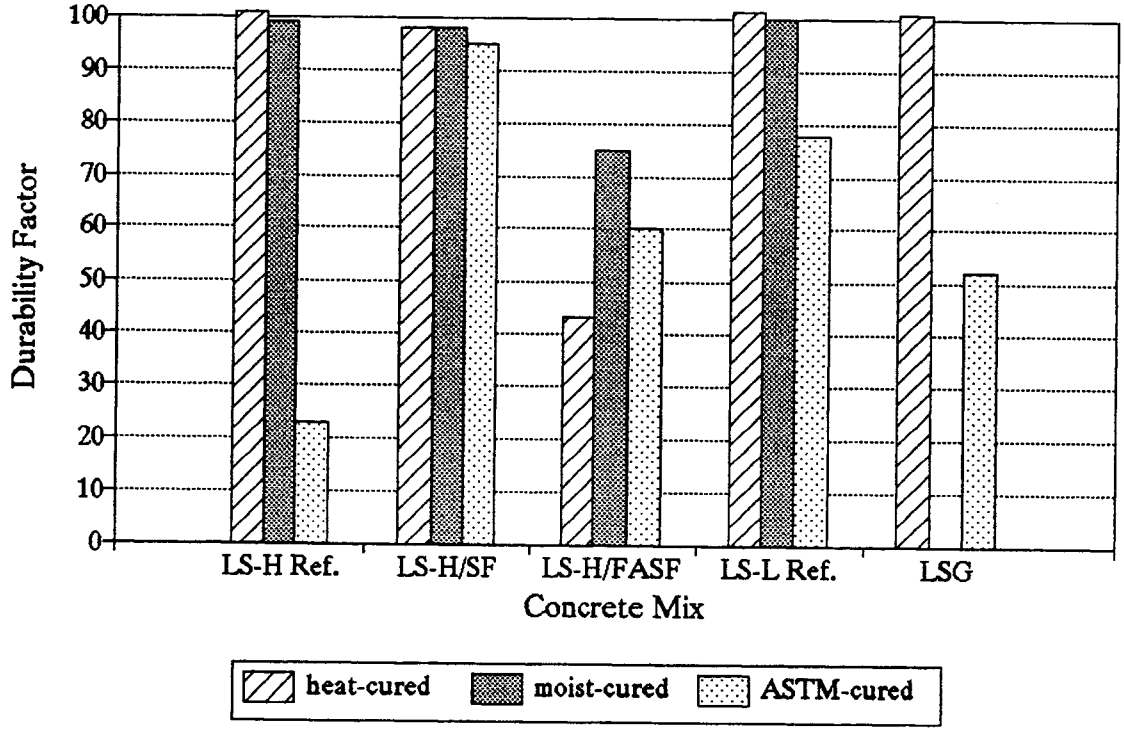

(b) Limestone concrete specimens

Figure 4.40 Effect of curing condition: Phase II concrete mixes

content of the limestone aggregate did not appear to influence the freeze-thaw performance of the concrete. Saturated limestone aggregate performed well in Phase I concrete mixes. The improved performance of the 7-day moist-cured concrete specimens may be due to the time period allowed for the concrete specimen to dry out and the older age at the beginning of testing (higher compressive strength). Although the ASTM-cured specimens had a longer period of moist-curing for continued hydration, the specimens were placed immediately in the freeze-thaw testing machine. Water in the saturated limestone aggregate in the ASTM-cured concrete specimens could not escape prior to freezing and probably caused the concrete beam failure. It is possible that the limestone aggregate needed the time period of drying to perform well in the freeze-thaw test. During the period of drying, water from the saturated limestone aggregate could have been drawn out by capillary action and used as cure water with any unreacted cementitious material to strengthen the transition zone between the aggregate and the cement paste.

The observed failure mechanisms of selected Phase II concrete specimens following freeze-thaw testing are given in Table 4.13. The visual observations of the failed specimens supported the theories presented above. In the round gravel concrete specimens, a moderate amount of damage was observed in the aggregate/paste transition zone in the heat-cured and 7-day moist-cured concrete specimens (Figures 4.41 and 4.42). As the figures show, the deterioration was similar to the damage seen in the Phase I round gravel concrete specimens. However, no damage was observed in the ASTM-cured concrete specimen containing round gravel. Thus, the concrete specimens made with round aggregate may have needed the longer period of moist-curing to strengthen the transition zone between the aggregate and the cement

Table 4.13: Observed Failure Mechanisms: Phase II mixes

Mix	Cure	Cycle specimen was removed	RDM of sample at time specimen taken	Failure Mechanism*		
				cracks in aggregate	aggr/paste interface	microcracks in paste
PHASE II MIXES						
(RG Ref)R	heat	708	59	1	2	0
(RG w/SF)R	heat	100	50	0	0	0
	moist	661	64	0	2	1
	ASTM	615	99	0	0	0
(LS-H Ref)R	heat	663	102	0	0	0
	moist	663	100	0	0	0
	ASTM	149	47	0	1	0
(LS-L Ref)R	heat	754	105	0	0	0
	moist	754	101	0	0	0
	ASTM	471	50	1	2	0

* Failure rating: 0 = negligible; 1 = minor; 2 = moderate; 3 = major amount of damage observed.

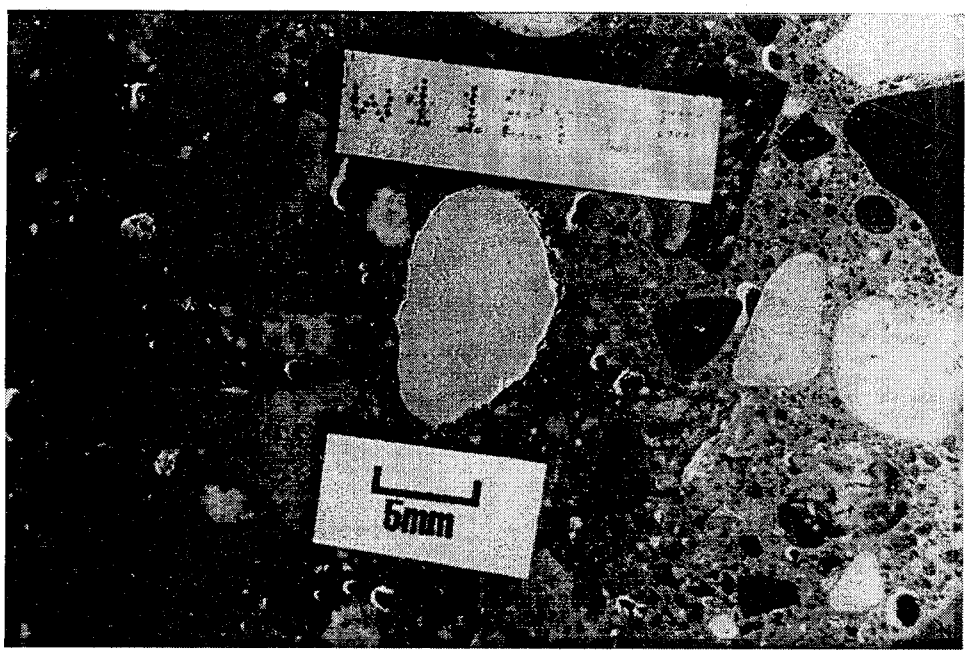

Figure 4.41 Phase II moist-cured round gravel with silica fume mix specimen

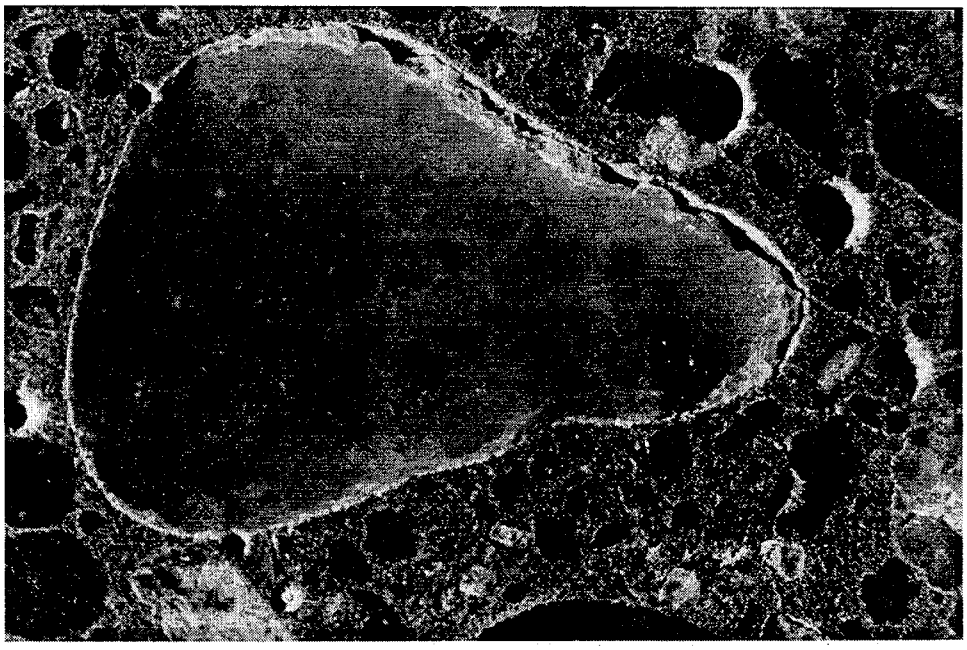

Figure 4.42 Phase II moist-cured round gravel with silica fume mix specimen

paste.

Looking at the failure ratings of the concrete specimens fabricated with limestone aggregate, the failure in the ASTM-cured concrete specimens was in the transition zone and the aggregate itself. This supports the theory that water inside the saturated aggregate caused the failure. Noting that the heat- and 7-day moist-cured concrete specimens made with limestone aggregate showed no damage at the transition zone or in the aggregate, it is probable that the limestone concrete specimens benefitted from the period of drying prior to exposure to freeze-thaw conditions. This period of aging allowed the saturated limestone aggregate to dry out, decreasing (or eliminating) the amount of freezable water in the aggregate and possibly increasing the bond with the cement paste, as previously discussed.

Compressive Strength

Table 4.14 gives the Phase II concrete compressive strengths at 28-days and at the approximate time the concrete beam specimens were placed in the freeze-thaw testing machine. These compressive strengths were tested as a part of this study, and the 6x12- in (150x300-mm) concrete cylinders were handled identical to the concrete beam specimens. The cylinders were cured, aged to 28 days in the environment of relatively constant temperature and humidity (73 °F (23 °C) and 50% RH), and immersed in the constant temperature water bath for 21 days prior to testing for compressive strength. In addition, companion cylinders were moist-cured with the concrete beam specimens following the ASTM C666 curing procedure. These cylinders were

Table 4.14: Compressive Strengths: Phase II Mixes; 6x12-in (150x300-mm) cylinders

Mix	f'c, 28-day compressive strength, psi (MPa)		compressive strength @ approximate time concrete beam specimens placed in freeze-thaw testing machine, psi (MPa)		
	heat-cured	moist-cured for 7 days	heat-cured*	moist-cured for 7 days*	ASTM Procedure+ (moist-cured for 14 days)
(RG Ref)R	11246 (77.6)	12394 (85.5)	10687 (73.3)	12275 (84.7)	11036 (76.1)
(RG w/SF)R	12855 (88.7)	14980 (103.3)	13361** (92.1)	14748** (101.7)	12635 (87.1)
(RG w/SF)AE	10191 (70.3)	12358 (85.2)	9928 (68.5)	11819 (81.5)	10472 (72.2)
(LS-H Ref)R	13683 (94.4)	14745 (101.7)	12541 (86.5)	14315 (98.7)	12349 (85.2)
(LS-H w/SF)R	14873 (102.6)	16540 (114.1)	14077 (97.1)	15812 (109.0)	14477 (99.8)
(LS-H w/FA&SF)R	12281 (84.7)	13039 (89.9)	11627 (80.2)	13311 (91.8)	11323 (78.1)
(LS-L Ref)R	13580 (93.7)	13851 (95.5)	NT	NT	12157 (83.8)

NT Indicates measurement not tested.

* 49-day compressive strength given for 6x12 concrete cylinders handled same as freeze-thaw concrete beam specimens (i.e. cured, aged in same environment to 28 days, and immersed in constant temperature water bath for 21 days).

** For these specimens, 86-day compressive strength given (i.e. after curing, aged to 28 days, immersed in constant temperature water bath for 21 days, frozen at constant temperature for 33 days, and then thawed in water 4 days prior to compressive test).

+ 14-day compressive strength given.

moist-cured for 14 days and tested for compressive strength immediately upon removal from the lime-water curing bath. Thus, the measurements in Table 4.14 provide relatively accurate estimates of the strengths of the Phase II concrete beam specimens at the time they began freeze-thaw cycling.

The relationship between compressive strength and durability factor was shown in Figures 4.34 and 4.35 for all of the heat- and 7-day moist-cured concrete specimens from Phases I and

II of the investigation. Figure 4.43 presents the durability factor versus the compressive strength of the ASTM-cured concrete specimens of Phase II at the time the concrete specimens began the freeze-thaw test. As was seen in the previous figures, there does not appear to be a correlation between durability factor and compressive strength (without considering the other variables involved (i.e., aggregate type)).

Effect of Air Entrainment

As previously discussed, two of the mixes that performed poorly in Phase I were repeated in Phase II with the addition of an air-entraining agent to assess its affect on improving the concrete frost resistance. Air-entraining improves the frost resistance of concrete by providing expansion space in the cement paste for the freezing water. Air-entrainment also modifies the transition zone around the aggregate to permit the expulsion of water from the aggregate pores. This is especially evident in concrete containing silica fume (which tends to fill the paste pores).

Figure 4.44 provides results of the four Phase II mixes cast for this purpose, one mix with and one mix without air-entrainment for each of the two mixes listed. The figure shows the well-known benefits of air-entrainment on the freeze-thaw resistance of concrete. All air-entrained concrete specimens exhibited durability factors approaching 100. Improved performance of the air-entrained concrete specimens was very significant for the heat-cured concrete specimens. The already good performance of the 7-day moist-cured concrete specimens and the ASTM-cured concrete specimens improved slightly with air-entrainment.

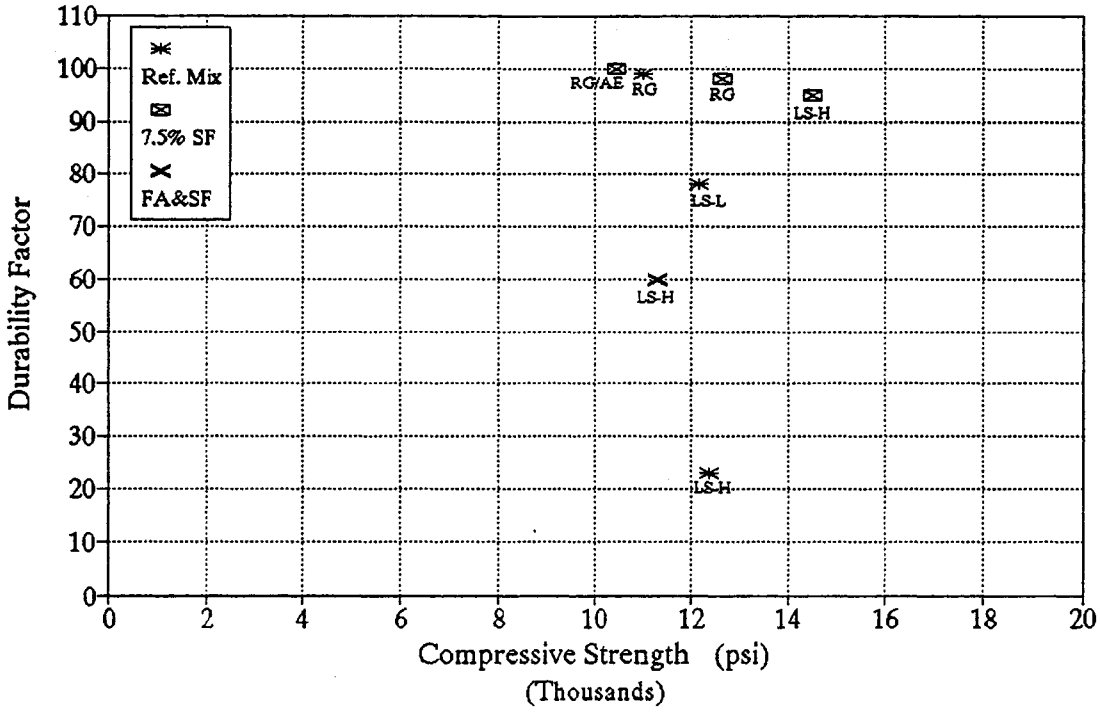

Figure 4.43 Durability Factor vs compressive strength: ASTM-cured specimens

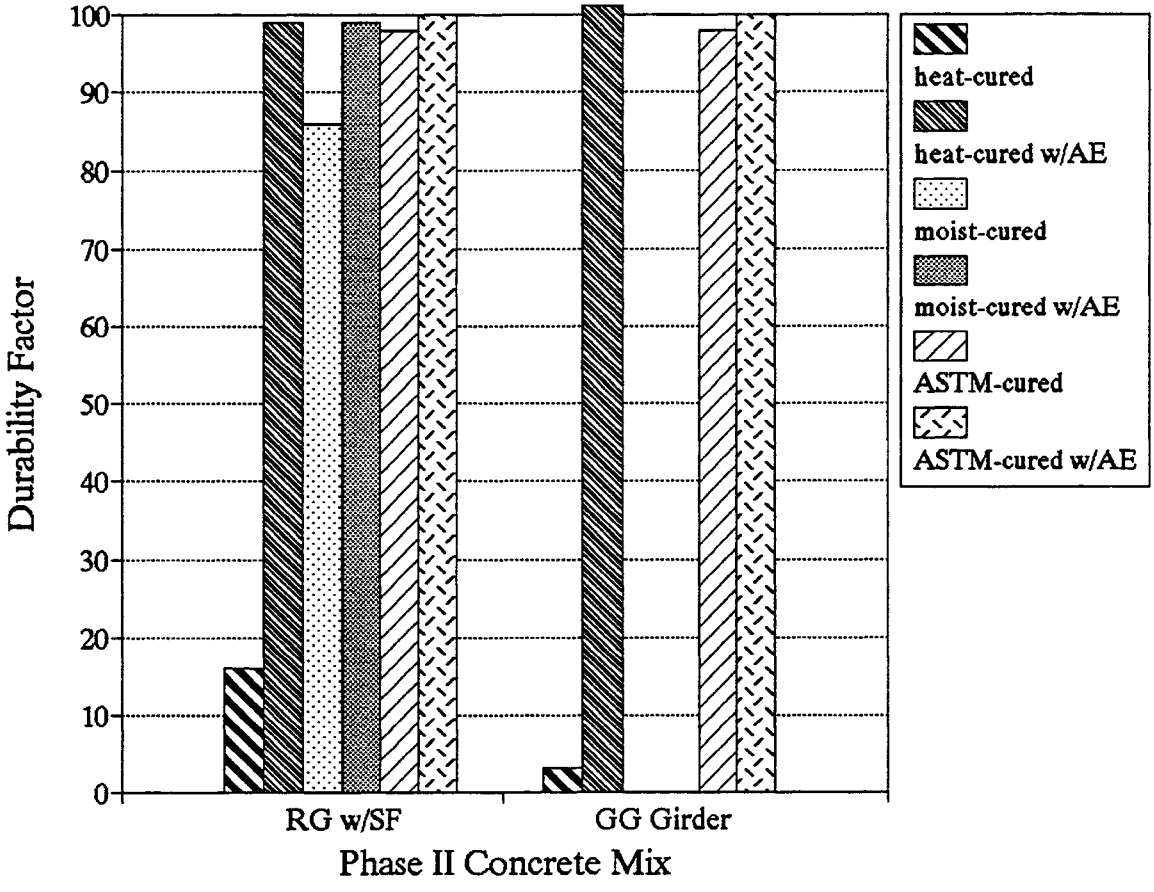

Figure 4.44 Effect of air entrainment on freeze-thaw durability

As reported in Table 4.14, the 28-day compressive strength of the heat-cured, air-entrained round gravel with silica fume concrete was approximately 10,200 psi (70 MPa). This air-entrained concrete mix produced high strength concrete with excellent freeze-thaw durability. However, introducing air entrainment in the production of high-strength concrete for prestressed girders has significant drawbacks. For example, the addition of air-entrainment in concrete is believed to result in increased creep, which leads to loss of prestressing force.

CHAPTER 5

CONCLUSIONS AND RECOMMENDATIONS

SUMMARY

An investigation of the freeze-thaw durability of non-air-entrained high-strength concrete was completed as a portion of an extensive study on the application of high-strength concrete to prestressed bridge girder production. The superior mechanical properties of high-strength concrete offer significant benefits to the prestressed bridge girder industry. Because the prestressed concrete industry experiences some difficulty obtaining the specified high strengths while providing the air contents required for frost resistance, the results of this study are of particular interest.

Twenty-four laboratory concrete mixes were batched (including seven repeated mixes) and over 130 concrete beam specimens were tested for freeze-thaw durability. The effects of curing condition, aggregate type, and cementitious material composition were investigated. Five different types of local coarse aggregates were used: round gravel, partially-crushed gravel, granite, a high-absorption limestone and a low-absorption limestone. Four different cementitious material combinations were used in the concrete mixes: portland cement only (reference mix), 20 percent fly ash, 7.5 percent silica fume and 20 percent fly ash with 7.5 percent silica fume. The pozzolan material was incorporated in each mix as a replacement by weight of the portland cement. In all of the concrete mixes, the total cementitious material content (750 lb/yd^3 (445

kg/m^3)), the water-to-cementitious material ratio (0.30 by weight) and the coarse-to-fine aggregate ratio (1.5 by weight) were held constant. To investigate curing effects, concrete specimens were moist-cured for 7 days or heat-cured to simulate the precasting process. After the prescribed curing, the specimens were aged a period of time prior to testing for freeze-thaw durability in order to simulate the casting and aging of prestressed members prior to exposure to freeze-thaw conditions. Many experts agree with altering the age-at-test and specimen conditioning requirements of ASTM C666 (which specifies freeze-thaw testing after a 14-day moist-cure) to test the frost resistance of specimens under more typical exposures [11].

CONCLUSIONS

Results of this investigation indicate that it is possible to produce portland cement concrete with high strength and freeze-thaw durability without air-entrainment. The frost-resistant high-strength concrete produced in this study had air void spacing factors greater than the 0.008 in (0.20 mm) recommended for durable concrete, providing further evidence of the need for a greater spacing factor limit for frost-resistant high-strength concrete [7, 14, 15].

Specific objectives of this study were to determine the effects of aggregate type, cementitious material composition and curing condition on the freeze-thaw durability of non-air-entrained portland cement concrete. Brief summaries of the findings are presented below.

Effect of Aggregate Type

Of the five aggregate types investigated, the concrete specimens containing limestone aggregates consistently exhibited the best performance in freeze-thaw durability testing. Several of the low-absorption limestone concrete specimens endured more than 1500 freeze-thaw cycles without failing (RDM criterion) before removal from the freeze-thaw testing machine. This good performance of the concrete specimens containing limestone was repeated in Phase II. Microscopic observations of the tested specimens found little evidence of deterioration. The strong bond between the limestone aggregate and the cement paste was determined to be the reason for the exhibited freeze-thaw durability. The lower stiffness of the limestone aggregate or the high strength of each component of the limestone concrete was demonstrated by the large dilations seen in some limestone concrete specimens (without RDM failure). The limestone aggregate, the cement paste, and the transition zone between the aggregate and the cement paste were each able to withstand the tensile forces due to the expansion without evidence of deterioration.

The partially-crushed gravel and the round gravel aggregate were found to be suitable aggregates for use in the production of durable concrete. Each of these aggregates produced some frost-resistant concrete specimens; the cement paste was found to be the critical component in the frost resistance of these concrete mixtures. The reference mix concrete specimens containing partially-crushed gravel aggregate performed very well. The Phase II concrete specimens containing round gravel performed well (with and without air-entrainment). A factor believed to be related to the inconsistent freeze-thaw performance of these aggregates was the

coarse aggregate moisture content at the time of mixing.

The granite aggregate was found to be unsuitable for the production of frost-resistant concrete. All concrete specimens containing granite aggregate performed very poorly. The forensic investigation determined that the failure of the concrete specimens containing granite was due to the failure of the aggregate itself.

The large dilations seen in many of the concrete specimens is a concern that may be related to the type of aggregate used. The inability of some aggregate particles to restrain the dilations of the cement mortar may be critical in some applications. Large dilations were seen only in the limestone aggregate in Phase I testing. However, the round gravel aggregate concrete specimens also experienced large dilations (without failing the RDM criterion) in Phase II testing. The low-absorption (1.5%) limestone reference mix, however, exhibited excellent freeze-thaw durability in terms of both RDM and dilation, withstanding over 1100 cycles without failing. In the reference concrete mix, the concrete structure produced may have consisted of pore sizes that permitted easy flow of water through the concrete.

Effect of Cementitious Material Composition

Research has shown that portland cement concrete containing silica fume can be produced to be frost resistant without air-entrainment. In this study the concrete specimens from the reference mixes performed better than the mixes containing pozzolan material for any given aggregate type. Comparing the freeze-thaw test results of Phases I and II provided insight as

to possible reasons for the poorer performance of the concrete containing pozzolan (fly ash or silica fume) in this study. The performance of the concrete containing silica fume may be related to the moisture content of the aggregate at the time of mixing. In this investigation, the concrete containing silica fume was less permeable, as the weight loss and absorption tests have shown. However, the low permeability of the cement paste may have prevented the saturated aggregate from reducing (or eliminating) its freezable water content prior to freeze-thaw testing. The concrete without pozzolan material may have had a more open pore structure, which allowed movement of water through the aggregate and cement paste.

Effect of Curing Condition

The moist-cured specimens generally exhibited better frost resistance than the heat-cured concrete specimens. Generally, moist-curing allowed continuous hydration of the cementitious materials, strengthening the transition zone between the aggregate and the cement paste.

In Phase II of the investigation, a comparison was made between the curing condition used in this study with the ASTM C666 standard curing procedure. Results were dependent on the type of aggregate used in the concrete production. The freeze-thaw performance of the round gravel concrete specimens improved when cured according to the ASTM C666 procedure, possibly due to the additional moist-curing and strengthening of the transition zone between the aggregate and the cement mortar. The limestone concrete specimens, however, exhibited the opposite behavior. The limestone ASTM-cured concrete specimens performed worse than the aged specimens that were heat- or moist-cured according to the curing procedures used in this

study. The limestone aggregate, saturated at the time of mixing, may have needed the time period of drying prior to exposure to freeze-thaw conditions to reduce its freezable water content. In Phase I, during the aging period of the low water-to-cementitious material ratio concrete, water from the saturated limestone aggregate could have been drawn out by capillary action and used as cure water with any unhydrated cement to strengthen the transition zone between the aggregate and the cement paste. Water in the saturated limestone aggregate in the ASTM-cured concrete specimens could not escape prior to freezing (since the concrete beam was kept continuously wet) and probably caused the failure.

RECOMMENDATIONS

The results of this investigation are limited to the particular materials (aggregate, portland cement, fly ash, silica fume, etc.) and methods used in this study. Results indicate that the aggregate type had a critical effect on the frost resistance of the concrete. For this reason, if a non-air-entrained concrete is to be used, it is recommended that freeze-thaw studies be conducted on concrete specimens fabricated with the particular aggregate to be used before application of the concrete in a freeze-thaw environment.

As discussed above, the moisture content of the coarse aggregate seemed to have a great effect on the freeze-thaw durability of the concrete. Therefore, caution should be used with regard to the degree of saturation of the coarse aggregate at the time of mixing. The large length dilations, observed in many of the concrete specimens, should also be considered in terms of the adverse effects this behavior may have in particular applications of non-air-entrained high-

strength concrete.

REFERENCES

1. Ahlborn, T. M., "Tests of Two Long-Span High-Strength Prestressed Bridge Girders," Ph. D. Dissertation, Department of Civil Engineering, University of Minnesota, Minneapolis, MN, in progress, 1998.

2. Kielb, J. A., "Instrumentation and Fabrication of Two High-Strength Concrete Prestressed Bridge Girders," Master of Science Thesis, Department of Civil Engineering, University of Minnesota, Minneapolis, MN, 1995.

3. Mokhtarzadeh, A., "Mechanical Properties of High-Strength Concrete," Ph. D. Dissertation, Department of Civil Engineering, University of Minnesota, Minneapolis, MN, 1998.

4. Perenchio, W. F. and Klieger, P., "Some Physical Properties of High-Strength Concrete," PCA Research and Development Bulletin RD056.01T, 1978.

5. Bjegovic, D., Mikulic, D. and Ukraincik, V., "Theoretical Aspect and Methods of Testing Concrete Resistance to Freezing and Deicing Chemicals," Concrete Durability - Katherine and Bryant Mather International Conference, ACI Special Publication 100, 1987, pp. 947-971.

6. Powers, T. C., "Freezing Effects in Concrete," Durability of Concrete, ACI Special Publication 47, 1975, pp. 1-11.

7. Detwiler, R. J., Dalgleish, B. J. and Williamson, R. B., "Assessing the Durability of Concrete in Freezing and Thawing," ACI Materials Journal, January-February 1989, pp. 29-35.

8. American Concrete Institute Committee 201, "Guide to Durable Concrete", ACI 201.2-92, 1992, 41 pp.

9. Fidjestohn, P., Discussion of "Non-Air-Entrained High-Strength Concrete - Is it Frost Resistant?" ACI Materials Journal, Vol. 90, No. 3, May-June 1993, pp. 295-296.

10. Mehta, P. K. and Aitcin, P. C., "Microstructural Basis of Selection of Materials and Mix Proportions for High-Strength Concrete," High-Strength Concrete: Second International Symposium, ACI Special Publication 121, 1990, pp. 265-286.

11. Philleo, R. E., "Frost Susceptibility of High-Strength Concrete," Concrete Durability - Katherine and Bryant Mather International Conference, ACI Special Publication 100,

1987, pp. 819-842.

12. Philleo, R. E., "Freezing and Thawing Resistance of High-Strength Concrete," NCHRP Synthesis of Highway Practice 129, Transportation Research Board, National Research Council, Washington, D. C., 1986, 31 pp.

13. Mehta, P. K., "Durability of High Strength Concrete," Paul Klieger Symposium on Performance of Concrete, ACI Special Publication 122, 1990, pp. 19-27.

14. Foy, C., Pigeon, M. and Banthia, N., "Freeze-Thaw Durability and Deicer Salt Scaling Resistance of a 0.25 Water-Cement Ratio Concrete," Cement and Concrete Research, Vol. 18, No. 4, 1988, pp. 604-614.

15. Attiogbe, E. K., Nmai, C. K. and Gay, F. T., "Air-Void System Parameters and Freeze-Thaw Durability of Concrete Containing Superplasticizers," Concrete International, Vol. 14, No. 7, July 1992, pp. 57-61.

16. Robson, G., "Durability of High-Strength Concrete Containing a High Range Water Reducer," Concrete Durability - Katherine and Bryant Mather International Conference, ACI Special Publication 100, 1987, pp. 765-780.

17. Dhir, R., Tham, K. and Dransfield, J., "Durability of Concrete with a Superplasticizing Admixture," Concrete Durability - Katherine and Bryant Mather International Conference, ACI Special Publication 100, 1987, pp. 741-764.

18. Ellis, W. E., Jr., "For Durable Concrete, Fly Ash Does Not 'Replace' Cement," Concrete International, July, 1992, pp. 47-51.

19. Tuthill, L. H., "Long Service Life of Concrete," Paul Klieger Symposium on Performance of Concrete, ACI Special Publication 122, 1990, pp. 173-179.

20. American Society for Testing and Materials (ASTM), Annual Book of ASTM Standards, Philadelphia, PA, 1993.

21. Johnston, C. D., "Effects of Microsilica and Class C Fly Ash on Resistance of Concrete to Rapid Freezing and Thawing and Scaling in the Presence of Deicing Agents," Concrete Durability - Katherine and Bryant Mather International Conference, ACI Special Publication 100, 1987, pp. 1183-1204.

22. Goldman, A. and Bentur, A. "Effects of Pozzolanic and Non-Reactive Microfillers on the Transition Zone in High Strength Concrete," Interfaces in Cementitious Composites, Proceedings of the RILEM International Conference, October, 1992, pp. 53-61.

23. Johnston, C. D., "Durability of High Early Strength Silica Fume Concretes Subjected to Accelerated and Normal Curing," Fly Ash, Silica Fume, Slag, and Natural Pozzolans

in Concrete, Proceedings Fourth International Conference, ACI Special Publication 132, Vol. II, 1992, pp. 1167-1187.

24. Virtanen, J., "Freeze-Thaw Resistance of Concrete Containing Blast-Furnace Slag, Fly Ash or Condensed Silica Fume," Fly Ash, Silica Fume, Slag, and Other Mineral By-Products in Concrete, Vol. II, ACI Special Publication 79, 1983, pp. 923-942.

25. Galeota, D., Giammatteo, M. M., Marino, R. and Volta, V., "Freezing and Thawing Resistance of Non Air-Entrained and Air-Entrained Concretes Containing a High Percentage of Condensed Silica Fume," Durability of Concrete, ACI Special Publication 126, 1991, pp. 249-261.

26. Pigeon, M., Gagne, R., Aitcin, P. C., and Banthia, N., "Freezing and Thawing Tests of High-Strength Concretes," Cement and Concrete Research, Vol. 21, No. 5, 1991, pp. 844-852.

27. Cohen, M. D., Zhou, Y. and Dolch, W. L., "Non-Air-Entrained High-Strength Concrete - Is it Frost Resistant?," ACI Materials Journal, Vol. 89, No. 2, July-August, 1992, pp. 406-415.

28. Burg, R. G. and Ost, B. W., "Engineering Properties of Commercially Available High-Strength Concretes," PCA Research and Development Bulletin RD104T, 1992, 55 pp.

29. Hooton, R. D., "Influence of Silica Fume Replacement of Cement on Physical Properties and Resistance to Sulfate Attack, Freezing and Thawing, and Alkali-Silica Reactivity," ACI Materials Journal, Vol. 90, March-April, 1993, pp. 143-151.

30. Tachibana, D., Imai, M., Yamazaki, N., Kawai, T. and Inada, Y., "High-Strength Concrete Incorporating Several Admixtures," High-Strength Concrete: Second International Symposium, ACI Special Publication 121, 1990, pp. 309-330.

31. Hammer, T. A. and Sellevold, E. J., "Frost Resistance of High-Strength Concrete," High-Strength Concrete: Second International Symposium, ACI Special Publication 121, 1990, pp. 457-487.

32. Washa, G. W. and Witing, N. H., "Strength and Durability of Concrete Containing Chicago Fly Ash," Journal of the American Concrete Institute, Vol. 24, No. 8, April, 1953, pp. 701-712.

33. Klieger, P. and Gebler, S., "Fly Ash and Concrete Durability," Concrete Durability - Katherine and Bryant Mather International Conference, ACI Special Publication 100, 1987, pp. 1043-1069.

34. Carrasquillo, P., "Durability of Concrete Containing Fly Ash for Use in Highway Applications," Concrete Durability - Katherine and Bryant Mather International Conference, ACI Special Publication 100, 1987, pp. 843-861.

35. Nasser, K. W. and Lai, P. S. H., "Resistance of Fly Ash Concrete to Freezing and Thawing," Fly Ash, Silica Fume, Slag, and Natural Pozzolans in Concrete, Proceedings of the Fourth International Conference, ACI Special Publication 132, Vol. I, 1992, pp. 205-226.

36. Mather, B., "How to Make Concrete that will be Immune to the Effects of Freezing and Thawing," Paul Klieger Symposium on Performance of Concrete, ACI Special Publication 122, 19 , pp. 1-18.

37. Whiting, D., "Durability of High-Strength Concrete," Concrete Durability - Katherine and Bryant Mather International Conference, ACI Special Publication 100, 1987, pp. 169-186.

38. Bayasi, Z., "Effects of Fly Ash on the Properties of Silica-Fume Concrete," Concrete International, April 1992, pp. 52-54.

39. Marzouk, H. "Durability of High-Strength Concrete Containing Fly Ash and Silica Fume," Serviceability and Durability of Construction Materials, Proceedings of the First Materials Engineering Congress, Vol. 2, August, 1990, pp. 1026-1038.

40. Waugh, W. R., "Selection and Use of Aggregates for Concrete," Journal of the American Concrete Institute, Vol. 58, No. 5, November, 1961, pp. 513-542.

41. Sawan, J., "Cracking Due to Frost Action in Portland Cement Concrete Pavements - A Literature Survey," Concrete Durability - Katherine and Bryant Mather International Conference, ACI Special Publication 100, 1987, pp. 781-803.

42. Chatterji, S. and Jensen, A. D., "Formation and Development of Interfacial Zones Between Aggregates and Portland Cement Pastes in Cement-Based Materials," Interfaces in Cementitious Composites, Proceedings of the RILEM International Conference, October, 1992, pp. 3-12.

43. Rhoades, "Petrography of Concrete Aggregates," Journal of the American Concrete Institute, Vol. 17, No. 6, June, 1946, pp. 581-600.

44. Minnesota Department of Transportation, Standard Specifications for Construction, 1988 Edition, St. Paul, MN, 1988.

45. Walker, R. D. and Hsieh, T., "Relationship Between Aggregate Pore Characteristics and Durability of Concrete Exposed to Freezing and Thawing," Highway Research Record

226, 1968, pp. 41-49.

46. Lane, D. and Meininger, R., "Laboratory Evaluation of the Freezing and Thawing Durability of Marine Limestone Coarse Aggregate in Concrete," Concrete Durability - Katherine and Bryant Mather International Conference, ACI Special Publication 100, 1987, pp. 1311-1323.

47. Fiorato, A. E., "PCA Research on High-Strength Concrete," Portland Cement Association Research and Development Bulletin RD093TC, 1989, 7 pp.

48. Kukko, H. and Matala, S., "Effect of Composition and Aging on the Frost Resistance of High-Strength Concrete," Durability of Concrete, ACI Special Publication 126, 1991, pp. 229-248.

49. Neville, A. M., Properties of Concrete, Pitman Publishing Ltd., London, UK, 1981.